Mechanistic Understanding of the NOB Suppression by Free Ammonia Inhibition in Continuous Flow Aerobic Granulation Bioreactors

Timothy R. Kent

Thesis Submitted to the faculty of the Virginia Polytechnic Institute and State University in partial fulfillment of the requirements for the degree of

Master of Science
In
Civil Engineering

Zhiwu Wang, Chair
Charles Bott
Zhen He

December 10, 2018
Manassas, VA

Keywords: Free ammonia inhibition, granule size, AOB:NOB ratio, partial nitritation-anammox

Mechanistic Understanding of the NOB Suppression by Free Ammonia Inhibition in Continuous Flow Aerobic Granulation Bioreactors

Timothy R. Kent

Abstract

A partial nitritation-anammox continuous flow reactor (CFR) was operated for eight months demonstrating that a mixture of large anammox-supported aerobic granules (ASAGs) and small conventional aerobic granules (CAGs) can be maintained stably for extended periods of time. The influent NH_4^+ was kept at 50 to 60 mg N L^{-1} to verify that the upper range of total ammonia nitrogen (TAN) for domestic wastewater can supply an inhibitory level of free ammonia (FA) for nitrite oxidizing bacteria (NOB) suppression in CFRs at pH around 7.8. The ammonia oxidizing bacteria (AOB):NOB activity ratio was determined for a series of granule sizes to understand the impact of mass diffusion limitation on the FA inhibition of NOB. When dissolved oxygen (DO) limitation is the only mechanism for NOB suppression, the AOB:NOB ratio was usually found in previous studies to increase with the granule size. However, the trend is reversed when FA has an inhibitory effect on NOB, as was observed in this study. The decrease in AOB:NOB ratio indicates that the resistance to the diffusion of FA along the granule radius limited its ability to inhibit NOB. This means smaller granules, e.g. diameter < 150 μm, are preferred for nitrite accumulation when high FA is present, e.g. in the partial nitritation-anammox process. The trend was further verified by observing the increase in the apparent inhibition coefficient, $K_{I,FAapp}$, as granule size increased. This study for the first time quantified the effect of diffusion limitation on the $K_{I,FAapp}$ of NOB in granules and biofilms. A mathematical model was then utilized to interpret the observed suppression of NOB. The model predicted that NOB suppression was only complete at the granule surface. The NOB that did survive in larger granules was forced to dwell within the granule interior, where the FA concentration was lower than that in the bulk solution. This means FA inhibition can be taken advantage of as an effective means for NOB suppression in small granules and thin biofilms. Further, FA and DO were found to be both required for the stratification of AOB and NOB in partial nitritation-anammox CFRs. The structural stratification commonly observed in granules is then concluded to be a consequence but not a cause of the NOB suppression.

Mechanistic Understanding of the NOB Suppression by Free Ammonia Inhibition in Continuous Flow Aerobic Granulation Bioreactors

Timothy R. Kent

General Audience Abstract

A partial nitritation-anammox continuous flow reactor (CFR) was operated for eight months demonstrating that granular sludge can be maintained stably for extended periods of time. In this approach, NH_3 is only partially converted to NO_2^- (partial nitritation), and the conversion to NO_3^- is prevented by the suppression of nitrite oxidizing bacteria (NOB). NH_3 and NO_2^- are then utilized by anammox bacteria to create N_2 gas. The influent NH_4^+ fed to the reactor was kept at 50 to 60 mg N L^{-1} to verify that the upper range of total ammonia nitrogen (TAN) for domestic wastewater can supply a sufficiently high level of free ammonia (FA) to inhibit NOB growth in CFRs at a pH around 7.8. It is expected that the penetration of a substrate into granule sludge will experience diffusional resistance as it moves from water to denser solid material and is consumed by bacteria. The ammonia oxidizing bacteria (AOB):NOB activity ratio was determined for a series of granule sizes to understand the impact of mass diffusion limitation on the FA inhibition of NOB. When dissolved oxygen (DO) limitation is the only mechanism for NOB suppression, the AOB:NOB ratio was usually found in previous studies to increase with the granule size. However, the trend is reversed when FA has an inhibitory effect on NOB, as was observed in this study. The decrease in AOB:NOB ratio indicates that the resistance to the diffusion of FA, which increases with increasing granule size, along the granule radius limited its ability to inhibit NOB. This means smaller granules, e.g. diameter < 150 µm, are preferred for NO_2^- accumulation when high FA is present. The trend was further verified by observing the increase in the apparent inhibition coefficient, $K_{I,FAapp}$, as granule size increased. This coefficient quantifies the effectiveness of an inhibitor, with larger values indicating weaker inhibition. This study for the first time quantified the effect of diffusion limitation on the $K_{I,FAapp}$ of NOB in granules and biofilms. A mathematical model was then utilized to interpret the observed suppression of NOB. The model predicted that NOB suppression was only complete at the granule surface. The NOB that did survive in larger granules was forced to dwell within the granule interior, where the FA concentration was lower than that in the bulk solution. This means FA inhibition can be taken advantage of as an effective means for NOB suppression in small granules and thin biofilms. Further, FA and DO were found to be both required for the stratification of a layer of AOB at the surface over a layer of NOB in partial nitritation-anammox CFRs. The structural stratification commonly observed in granules is then concluded to be a consequence but not a cause of the NOB suppression.

Acknowledgements

I would first like to thank my advisor, Dr. Zhiwu Wang, for his guidance in completing my research and thesis. His commitment to my success was clearly displayed in his assistance in my experimental design and analysis. He gave me the opportunity to publish my first ever paper in the well-respected journal, Biotechnology Advances, and often used his weekends to provided his expertise in review of my work. I further appreciate his patience as I strove to complete my thesis writeup while I work full-time. I would further like to thank Dr. Charles Bott and Dr. Zhen He for their willingness to serve on my committee and for the helpful feedback they provided. Dr. Bott and HRSD have my deepest gratitude for covering tuition and providing funding as I completed my graduate coursework and thesis research. Besides this financial support, HRSD provided the granular sludge used to seed my reactor, without which none of my research would have been possible. I would like to thank Dr. Bott, finally, for introducing me to Dr. Beverly Stinson, which led to my current employment with AECOM.

I would next like to thank my fellow graduate students who assisted me in completing my thesis. Yewei Sun was instrumental in the development of the Matlab model used to predict the biomass and nitrogen profiles along the radius of the aerobic granules used in my study. Zhaohui An's assistance with reactor operation and granule imaging allowed me to complete my experimental work in a timely manner. Further, I would like to thank Parita Shah for her help in selecting and learning the Hach methods for determination of NH_4^+, NO_2^-, and NO_3^-.

I would like to thank the staff of OWML for their part in my success as a graduate research assistant. Mrs. Marilyn Stull and Mrs. Alicia Tingen were a great help in the process for orders and returns on lab equipment and materials. Mr. Curt Eskridge, Ms. Joan Wirt, and Mr. Alex Clare were also always more than willing to assist me in learning how to use equipment in the lab and resolve issues I encountered.

Finally, I would like to thank my family and friends who supported me during my time in graduate school. I would not have gained the knowledge and success I have enjoyed without their love and encouragement.

Table of Contents

List of Figures

Figure 10. Morphology of aerobic granular sludge in CFRs: (a-c) formation of granules from activated sludge in an upflow reactor (Xin et al., 2017); (d-f) formation of granules from biofilm biomass (Yang et al., 2014); (i-k) disintegration of seeded granules to form irregular, fluffy granules (Li et al., 2016c); (l) seed sludge and (m) large, loose aggregates formed without sufficient settling- or size-based selection pressure (Chen et al., 2015b). (*Permission for reproduction of copyrighted material in this figure has been obtained*)

Figure 11. Continuous bubble columns with internal solid/liquid separators: (a) a bubble column with a long baffle (Xin et al., 2017), (b) a bubble column with a short baffle on the top (Tsuneda et al., 2003), (c) a bubble column with a three-phase separator on the top (Chen et al., 2009), (d) SBR/MBR in series with intermittent sludge exchange (Sajjad et al., 2016) *(blue – Reactor and membrane; red – water flow; green – air bubbles; small black circle – floc biomass; large black circle - granules)*

Figure 12. Other configurations of CFRs implementing settling velocity-based selection pressure: (a) a modified oxidation ditch with inclined plate settlers (Li et al., 2014), (b) phosphorous removal system (anaerobic, aerobic, settling tanks) with adjustable effluent port height (L) (Li et al., 2016e), (c) an upflow reactor with multiple internal settling tanks (Bumbac et al., 2015). *(blue – Reactor and membrane; red – water flow; green – air bubbles; yellow – stirring device; small black circle – floc biomass; large black circle - granule; purple – variable effluent port depth)*

Figure 13. Continuous ALR configurations: (a) an ALR with a three-phase separator on the top (Ramos et al., 2016), (b) an ALR with baffled settling zones (Qian et al., 2017), (c) a hybrid ALR/bubble column (Liu et al., 2015) *(blue – Reactor and membrane; red – water flow; green – air bubbles; small black circle – floc biomass; large black circle - granules)*

Figure 14. CFRs implementing particle size-based selection pressure: (a) an ALR and a settling tank in series with an MBR and an external settling tank equipped with a sieve screen (Liu et al., 2012), (b) a bubble column and an external selection tank equipped with a sieve screen (Liu et al., 2014), (c) a bubble column with an internal screen (Wang and Peng, 2008). *(blue – Reactor and membrane; red – water flow; green – air bubbles; small black circle – floc biomass; large black circle - granule)*

Figure 15. Extent of granulation of total biomass and SVI in an SBR with settling velocity selection and a CFR with granule size selection using a sieve (Liu et al., 2014)

Figure 16. SOURs in SBRs and CFRs over an 85-day cultivation period (Wan et al., 2014a)

Figure 17. Separation technology for full-scale operations: (a) a schematic of hydrocyclone separating biomass particles based on density and size, (b) a photo of hydrocyclones installed at HRSD, (c) a photo of a rotating sieve drum used in Strass, Austria treatment plants

List of Tables

Chapter 1 – Introduction

Traditional nitrogen removal in wastewater treatment plants (WWTPs) has been carried out through the mechanism illustrated in **Figure 1a**. Ammonia (NH_3) is converted to nitrite by ammonia oxidizing bacteria (AOB) and subsequently oxidized to nitrate (NO_2^-) via nitrite oxidizing bacteria (NOB). Denitrifying heterotrophic organism (DHO) use this nitrate (NO_3^-) as an electron acceptor to first reduce NO_3^- back to NO_2^- and then further reduce NO_2^- to nitrogen gas by using chemical oxygen demand (COD) as an electron donor. However, this process is energy intensive, given the need for extensive aeration, and frequently requires the addition of supplemental COD for denitrification. Significant savings in energy and chemical costs can be achieved by shortcut nitrogen removal processes, where NO_2^- is accumulated by the suppression of NOB. This accumulated NO_2^- may be converted directly to N_2 gas by DHO, i.e. nitrite shunt (Nogaj et al., 2014) (**Figure 1b**), or, in the presence of excess NH_4^+, by anaerobic ammonia oxidizing bacteria, namely anammox (AMX), i.e. deammonification (Xu et al., 2015) (**Figure 1c**). Both of these processes require the suppression of NOB. Several strategies have been suggested, including SRT control, dissolved oxygen (DO) limitation, and bioaugmentation of AOB (Xu et al., 2015). One method of note for NOB suppression is free ammonia (FA) inhibition. At sufficiently high levels, FA has been shown to selectively inhibit NOB over AOB. Implementation of such a strategy has been successful in sidestream treatment of reject wastewater (Cao et al., 2017; Gu et al., 2007). It is unclear, however, if FA inhibition may be used effectively under mainstream conditions.

Another trend is the rising interest in granular sludge for wastewater treatment (Kent et al., 2018). Aerobic granulation has been observed in sequential batch reactors (SBRs) for many years and research is now being focused on continuous flow reactors (CFRs). Granular sludge provides the benefits of improved sludge retention and settleability, as well as allowing for the development of a stratified structure with different microbial communities inhabiting different layers. This phenomenon of different functional groups arranging in coherent layers is largely explained by the profiles of DO and substrate, as they diffuse toward the granule interior. This property is especially important because if DO is depleted in the granule core, anoxic bacteria, e.g. AMX, will be able to grow underneath the upper aerobic strata. Aerobic granules, therefore, are specially adapted to allow for total nitrogen removal, i.e. conversion of NH_3 to N_2 gas, in a single reactor. Stratification has also been linked to NOB suppression in granules, although a comprehensive explanation for the spatial separation of AOB and NOB has not yet been proposed (Picioreanu et al., 2016). While DO limitation has been identified as a requirement for stratification of AOB and NOB, it cannot explain the phenomenon on its own. It would be advantageous to apply aerobic granulation technology to mainstream wastewater treatment and to more fully understand the mechanisms of stratification.

Granular sludge exists in a broad spectrum of different particle sizes. While the individual trends of AOB, NOB, and AMX activity in different granule sizes have been documented, little research has been devoted to the relevance of their ratios to the nitrogen removal pathway. Indeed, it is

actually the ratio of AOB-to-NOB activity that is important to nitrite accumulation, rather than their individual abundances. The previous studies presented in **Table 3** are not sufficient to explain the mechanistic effect of granule size on AOB:NOB activity ratio, but the results from the studies by Vlaeminck et al., 2010 and Luo et al., 2017 in particular give reason to believe that increasing particle size from small values has a substantial impact on the aforementioned ratios.

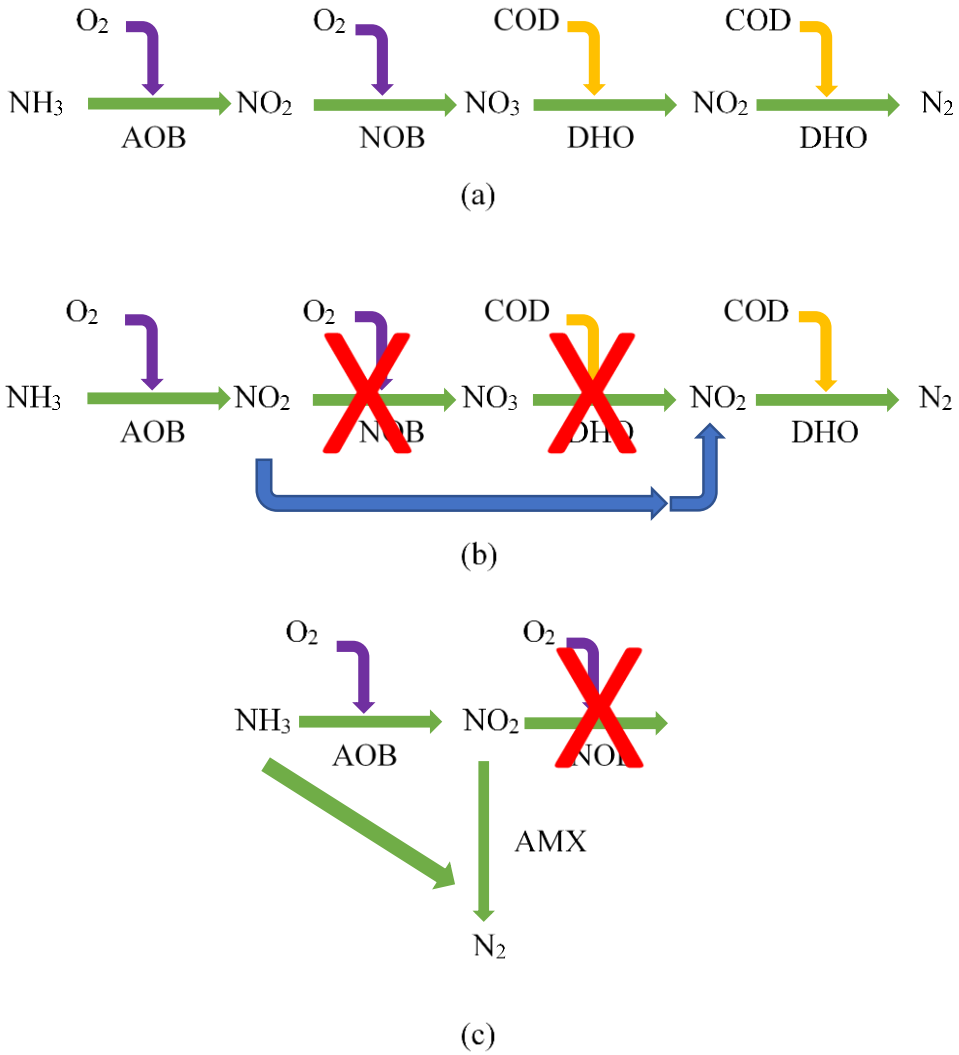

Figure 1. Nitrogen removal pathways: (a) traditional nitrification and denitrification processes; (b) nitrite shunt; and (c) partial nitritation-anammox

This study looks at the possibility of leveraging FA as a mechanism for particle size-dependent NOB suppression in granules and its potential role in determining the mechanism of granule stratification. It is possible to explain the separation of AOB and NOB into separate layers if FA

inhibits NOB at the granule surface, but falls below inhibitory levels as it penetrates along the granule radius. This would allow NOB to survive in the granule interior while AOB dominates at the surface. This hypothesis was tested in this study by evaluating the impact of granule size, i.e. diffusion resistance, on the relative ratios of activity and abundance for AOB and NOB, and comparing the results with that of a mathematical model prediction. The apparent inhibition coefficient of FA, namely $K_{I,FAapp}$ as defined in Eq. (12), in aerobic granular sludge was also quantified and evaluated with regards to the particle size effect on the NOB abundance.

Chapter 2 – Literature Review

[Sections 2.1 to 2.8 were published by me as Biotechnology Advances 36 (2018) 1139–1166]

2.1 Rising interest in the application of aerobic granulation to continuous flow reactors

Researchers during the past two decades have shown a great interest in treating domestic and industrial wastewater with aerobic granular sludge (**Figure 2**). Aerobic granules, as opposed to anaerobic granules, are operated under aerated conditions and essential for treating high organic loads, as well as performing nitrogen and phosphorus removal. Aerobic granulation allows for a higher biomass retention, as well as improved settleability and resistance to shock loading and toxic compounds, compared to activated sludge. The layered structure of aerobic granules also allows for multiple biological processes, e.g. nitrification and denitrification, to occur in a single tank (Gao et al., 2011). In fact, ammonia oxidation in granules has been reported to be significantly faster than in conventional activated sludge systems due to the higher biomass concentration maintained in granular systems (Hasebe et al., 2017). Until recently, aerobic granulation has been performed mostly in sequential batch reactors (SBRs). SBRs are a well understood bioprocess and can provide conditions known to promote sludge taking a granular form (Gao et al., 2011; Liu et al., 2005). However, CFRs provide several advantages over SBRs, as summarized below:

(1) *Ease of operation and control*. SBRs utilize a cyclic operation of filling, reaction, settling, and draining. Such a process is complicated, requiring separate control of each step. The filling and draining steps are especially problematic as they must be performed in a short period of time, necessitating large pumping systems and radical hydraulic condition changes. This is still a technical hurdle for the latest Nereda® technology that simplifies the SBR operation by integrating the fill and draw phases into a simultaneous process. After all, the significantly shorter fill/draw time over the cycle time (e.g. 15%) is an intrinsic operational disadvantage of SBR (Pronk et al., 2015). In contrast, CFRs provide advantages over SBRs in terms of simpler operation and control of treatment processes (Chen et al., 2017; Corsino et al., 2016; Juang et al., 2010; Li et al., 2016e; Qian et al., 2017).

(2) *Flow Mode*. Batch reactors are also limited in that they can only handle small portions at a time, possibly requiring storage of large amounts of wastewater as it waits for treatment. Although this may be addressed by operating multiple SBRs in sequence or installing an equalization tank, doing those requires a large footprint, high capital cost, and even more complicated operating procedures. In fact, full-scale SBRs are usually limited to low flow systems. Only very few large SBRs exist in the world, such as a 3.8×10^4 m^3 day^{-1} (10 million gallon per day (MGD)) wastewater treatment system in the United Arab Emirates (US EPA, 1999) and a 9.6×10^5 m^3 day^{-1} (250 MGD) Ringsend plant in Dublin, Ireland

(Celtic Anglian Water, n.d.). In the United States, all full-scale SBRs operate at even lower flow rates, with the largest reaching only 7.6×10^3 m^3 day^{-1} (2 MGD) (US EPA, 1999). In contrast, plants at large cities must handle substantial flow, e.g. 1.1 x 10^6 m^3 day^{-1} (300 MGD) at Blue Plains WWTP (Washington D.C., U.S.) (DC Water, n.d.) and 2.6 x 10^6 m^3 day^{-1} (700 MGD) at Stickney Water Reclamation Plant (Chicago, U.S.) (MWRD, n.d.). Nereda® is an emerging technology that allows for continuous fill and draw, reducing the time needed for reactor volume exchange. However, Nereda® is still a SBR that needs to stop inflow during the aeration and settling phases, consisting of 85% of the cycle time. Therefore, the need for an equalization tank or several SBRs run in sequence remains (Pronk et al., 2015). It is clear that CFRs are the only practical option for treating such large quantities of wastewater flow.

(3) *Current Infrastructure*. Most, if not all, of current large-scale wastewater operations are using continuous flow systems. It will be much simpler to directly implement aerobic granular sludge in existing infrastructure than to convert current operations to batch mode. Further, the higher biomass retention of granular systems will allow CFRs to improve performance with no need of expanding the existing infrastructure.

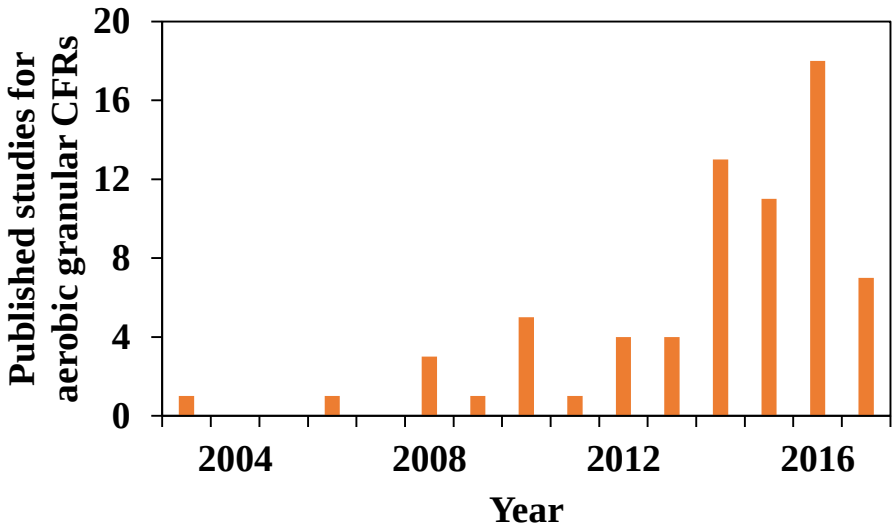

Figure 2. Number of journal publications on the topic of aerobic granulation in CFRs since 2003. The record for 2017 is current as of July 2017.

Nonetheless, only when aerobic granules can be stably maintained in a CFR will they be feasible for widespread, mainstream application. In other words, the advantages of granules described above, e.g. improved sludge settleability, have yet to be applied to mainstream wastewater treatment. Despite its advantages over batch operations, application of continuous flow to aerobic granulation is a new endeavor since the CFR conditions have been believed to make granulation unfavorable and unstable (Lee et al., 2010). **Figure 2** surveyed the number of papers published on

the topic of CFR aerobic granulation since 2003, showing a clear rising trend in the focus on this important topic over the past few years. The only published review mentioning aerobic granular sludge in CFR was written prior to the boom of CFR granulation research beginning in 2013 (Lee et al., 2010); its focus is more on SBR granulation, and only briefly touched on continuous flow systems. Therefore, there is a need for a timely and comprehensive review of the state of the art of technology development as it relates to granular sludge in CFRs. This paper meets that need by evaluating the current state of continuous flow as used in aerobic granular sludge technology, identifying the technological gaps, and recommending future research directions based on the experience and lessons learned from both CFR and SBR aerobic granulation studies.

2.2 Definition and classification of aerobic granules

An aerobic granule must be defined in order to properly understand the aerobic granulation process. For purposes of this review, three types of granular sludge will be distinguished. The most common form of aerobic granule, as defined herein, is an aggregate of microbial cells formed by cell-to-cell aggregation. They should possess a fast settling velocity, compact structure, and clear, round shape, as well as be biologically active. A 2006 workshop has suggested a minimum size of 0.2 mm, but this is not meant to exclude smaller aggregates that may meet the other aspects of granular sludge (de Kreuk et al., 2007). To our knowledge there is no general consensus on a cutoff SVI for distinguishing between flocs and granules. Although aerobic granules actually belong to the family of biofilms in that they can be viewed as one cell using another cell's surface as a carrier to attach, excluded from this description are granule-shaped biofilms which are formed over an abiotic carrier. This definition is in line with other definitions used in the literature (Gao et al., 2011; Liu and Tay, 2002). This does not exclude the possibility of inorganic cores, however, as metals may facilitate bonding with EPSs (Zhou et al., 2013b) or precipitate after granule formation (Juang et al., 2010). Such granules, the formation of which is dependent on an applied selection pressure, are the most commonly encountered in wastewater treatment studies. This type of granules will be referred to as conventional aerobic granules (CAGs) and is the primary focus of this review (**Figure 3**). Unless otherwise specified, "aerobic granules" are to be understood as CAGs.

However, two other forms of aerobic granules were also reported in the CFR literature (**Figure 3**). One form is anammox-supported aerobic granules (ASAGs) comprising layer(s) of aerobic biomass over an AMX core. The aerobic biomass present in ASAGs are typically nitrifiers, and these granules are used primarily for completely autotrophic nitrogen removal over nitrite (CANON) processes. The other form is filamentous aerobic granules (FAGs) which are granule-like pellets formed by the entanglement of filamentous bacteria (Section 2.6.1). The formation of these filamentous pellets usually does not need a settling velocity-based selection pressure, nor do they possess the same settling properties as CAGs. For example, FAGs cultivated in CFRs by Chen et al., 2017 maintained an SVI over 100 mL g^{-1} for the majority of the experimental period.

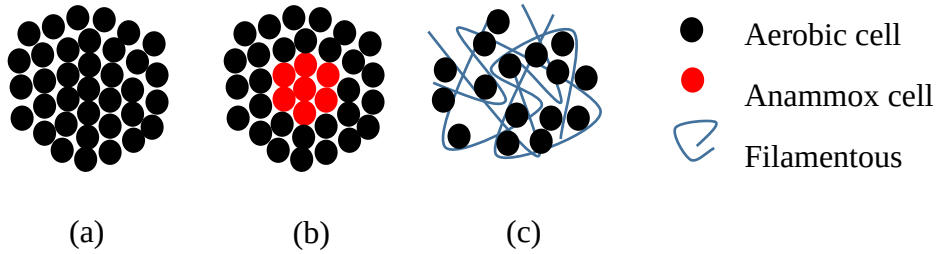

Figure 3. Three types of aerobic granules: (a) conventional aerobic granules, (b) anammox-supported granules, and (c) filamentous aerobic granules.

2.3 Formation mechanism for aerobic granules in SBRs

It has been established from SBR studies that a settling velocity-based selection pressure drives aerobic granulation of activated sludge, while alternation of feast-famine conditions and shear force play supplemental roles (Liu et al., 2005). A "selection pressure", as defined herein, is a stress that induces a change in the behavior of a microbial population. In this respect, both settling velocity and feast/famine are selection pressures. Extracellular polymeric substances (EPSs) and filamentous bacteria also have important functions in the formation and stability of granules. Knowledge of these cultivation conditions and mechanisms present in SBRs holds promise to provide a better understanding of similar processes at work in CFRs.

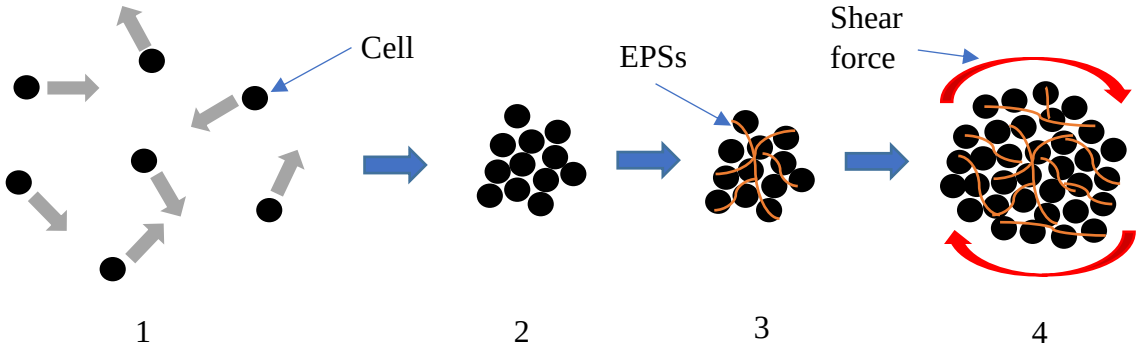

Figure 4. Formation of aerobic granules through: (1) movement and collision of cells, (2) initial reversible attraction and beginning of aggregation, (3) further irreversible aggregation and growth (*orange – EPS*), and (4) round, compact structure shaped by shear force.

Mechanisms for the formation of stable granules have mainly been studied in SBRs. The general process of biomass aggregation constitutes four steps (**Figure 4**): (1) random movement and collision of cells; (2) initial reversible cohesion through cell surface hydrophobicity increase; (3)

further irreversible aggregation and growth within the network connection of EPSs; and (4) morphology shaping by shear force (Liu and Tay, 2002).

2.3.1 Settling velocity-based selection pressure

In an SBR, the influent is firstly fed to fill up the reactor, and then the aerated reaction is allowed to proceed. At the end of a reaction cycle, biomass is only allowed to settle for a short time before the effluent needs to be swiftly drained from the reactor (Liu et al., 2005). This process is modified in some full-scale SBRs utilizing the Nereda® process, where influent is fed and effluent is withdrawn simultaneously (Pronk et al., 2015). Because heavier and larger bioparticles will settle faster than those that are less dense, the short settling time and quick discharge create a selection pressure that only allows the retention of biomass with good settling properties, i.e. biomass having a settling velocity less than a minimum value, namely $(v_s)_{min}$ in Eq. (1), will be washed out (**Figure 5**). This phenomenon will be referred to herein as "settling velocity-based selection pressure." This selection pressure depends not only on the settling time, but also on the settling distance [Eq. (1)]. Besides selecting for biomass with better settling properties, cell surface hydrophobicity and EPS production are promoted, as well (Gao et al., 2011). In fact, settling time and exchange ratio (fraction of reactor volume withdrawn after the settling phase) are identified as determining factors for promoting successful aerobic granule formation as demonstrated previously (Liu et al., 2005; Wang et al., 2006b). It is noteworthy that conventional SBRs with longer settling times, e.g. 0.5 hours (Liu et al., 2005), have been used without observing aerobic granule formation. Such a trend suggests that selection pressure based on settling velocity is indeed the ultimate driving force for aerobic granulation in SBRs. The settling depth, however, is equally as important as the settling time [Eq. (1)], which explains how some specialized processes utilizing deep tanks, e.g. Nereda® (Pronk et al., 2015), allow for longer settling times.

$$(v_s)_{min} = \frac{L}{t_s} \tag{1}$$

in which L stands for liquid height above effluent port, t_s for the settling time, and $(v_s)_{min}$ for the minimum settling velocity of particles that can settle fast enough to be retained in the SBR.

2.3.2 Feast/famine conditions

The cyclic operation of a SBR starts with a feast period and ends with a famine period in which substrate and nutrients are limiting. If the influent is fed from the bottom of the reactor, as in the Nereda® process (Pronk et al., 2015), the "famine" effect will be enhanced as a substrate gradient develops along the height of the sludge bed. It is believed that the shortage of substrate and nutrients during the famine period induces microbes to aggregate to improve survival. For example, the alternation of feast and famine has been found to enhance the hydrophobic nature of the microbial cells for their better co-aggregation (Liu et al., 2005). The starvation period may also

help induce enhanced EPS production (Gao et al., 2011), which is believed to promote granulation. Although this cyclic feast/famine condition is essential to the granulation process, it is not a sufficient driving force for successful aerobic granulation. In other words, settling velocity-based selection is also necessary. This is clearly seen in the fact that conventional SBRs combining feast/famine and relatively long settling times, e.g. 0.5 hours, have not reported aerobic granular sludge formation (Liu et al., 2005). It is important to note, however, that the Nereda® system, a specialized SBR, has achieved granulation with a 30-minute settling time (Pronk et al., 2015), as discussed in Section 2.3.1.

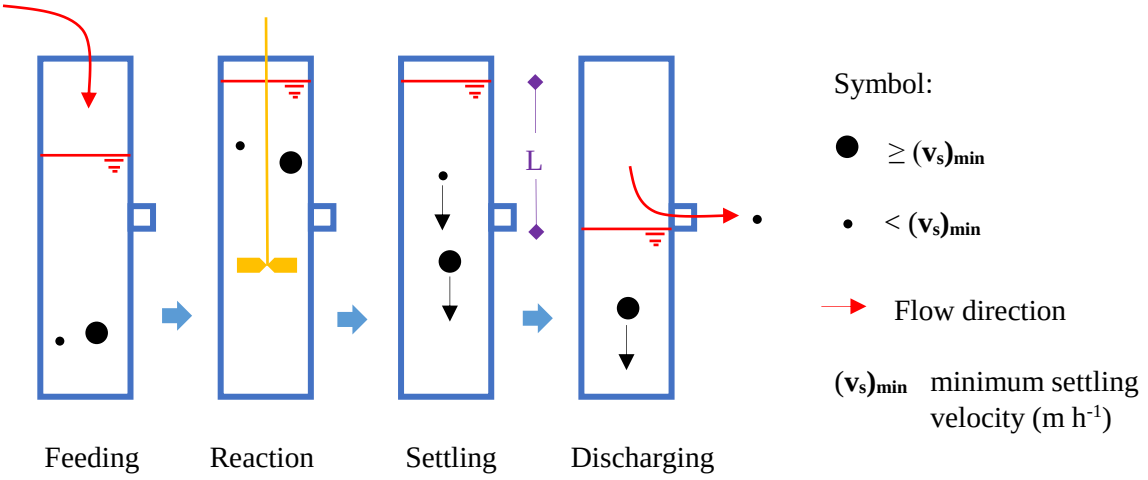

Figure 5. Operation of SBRs with selection of biomass by minimum settling velocity, i.e. biomass with settling velocity below the minimum value $(v_s)_{min}$ will be washed out.

2.3.3 Hydraulics and shear force

Hydraulics and shear forces, although not as essential as selection pressure in the form of settling velocity, are important factors in the granulation process. In the initial stages of granulation**,** hydraulic flows facilitate the collision of microbial cells for aggregation. Shear forces acting on biomass in aerobic SBRs result from these flows (water flow and aeration), as well as from collisions between solids (Liu and Tay, 2002). Shear force induces the secretion of EPSs, enhances cell surface hydrophobicity (Gao et al., 2011), and increases the granule density (Liu et al., 2005). It is also largely responsible for determining the shape and size of granular sludge as it strips the outer cells off the surfaces of the mature granules. This fact suggests that shear force plays an important role in the balance of fast- and slow-growing bacteria at the granule surface. For instance, the shearing off of biomass removes fast-growing filamentous bacteria that may accumulate on the granule surfaces (Lee et al., 2010, Devlin et al., 2017). A large column height-to-diameter ratio in laboratory reactors induces the water to follow a circular flow pattern which shears aerobic granules into a regular, spherical shape (Liu et al., 2005).

The hydraulics within an SBR are largely influenced by the configuration of the reactor. Most laboratory SBRs are bubble columns, i.e. air is bubbled up from the bottom of the reactor. An airlift reactor (ALR) is a special version of the bubble column, in which a suspended baffle induces higher rates of water circulation. ALRs take many forms, but it is common to see the baffle comprised of a cylindrical tube called a riser. Although bubble columns are simpler, ALRs require significantly less air flow to induce the same shear upon biomass (Zhou et al., 2013c). SBRs using airlift technology have been reported for aerobic granulation (Nguyen et al., 2016), but it is expected that they are not widely used since floc biomass in the riser tube can be trapped during the settling phase without being washed out.

2.3.4 Organic loading rate

In view of the fact that aerobic granulation can occur under a wide range of organic loading rates (OLRs), e.g. 2.5 – 15 g COD L^{-1} d^{-1} (Gao et al., 2011), it is clear that OLR is not a decisive selection pressure for successful granulation (Liu et al., 2005). However, OLR has been found to affect the structure and time required for granulation. A high OLR tends to cultivate granules with large size and loose structure, while the opposite is true for granules cultivated under low OLRs in SBRs (Gao et al., 2011).

2.3.5 Influent composition

Aerobic granulation is known to occur in SBRs fed with a variety of different wastewaters (Gao et al., 2011; Liu et al., 2005), suggesting that the type of wastewater is not a primary consideration in the formation mechanism. Aerobic granules are better at degrading less degradable substrates, such as phenol (Liu and Tay, 2004), than flocculent sludge and have been shown to grow even in the presence of particulate organic matter (Schwarzenbeck et al., 2004a; Wagner et al., 2015). However, aerobic granulation has been shown to be hindered when fed with influent containing mainly insoluble, particulate COD (Wagner et al., 2015). The same study demonstrated that first exposing the influent to an anaerobic phase will help solubilize the particulates, allowing easier degradation by aerobic granules.

The composition of the influent may impact the structure of aerobic granules cultivated in SBRs. For example, it is known that acetate promotes the formation of compact aggregates (Liu and Tay, 2004) while glucose and other readily-biodegradable COD sources enable filamentous bacteria to grow (Liu and Liu, 2006; Liu and Tay, 2004). As previously noted, insoluble COD promotes the growth of granules with filamentous organisms (Wagner et al., 2015). In fact, although the formation mechanism is not discussed in depth, Schwarzenbeck et al., 2004a may have developed FAGs in their SBR fed with partially-particulate COD. Such a feed may also increase the diversity of the system by supporting protozoa, which are able to degrade the particulate matter (Schwarzenbeck et al., 2004a).

2.3.6 Dissolved oxygen

DO concentration is not a major factor in granulating aerobic sludge in SBRs. Indeed, DO has ranged from 0.7 – 6 mg L^{-1} in successful granulation experiments (Liu et al., 2005). However, DO may influence granule stability, e.g. low DO environments generally favor filamentous growth and anaerobic core formation (Gao et al., 2011; Rossetti et al., 2005). Cycling through anoxic/anaerobic and aerobic phases (such as in systems with an anoxic or anaerobic selector), however, is known to suppress filamentous organisms since they are inferior to non-filamentous organisms in NO_2^- and NO_3^- reduction (Metcalf and Eddy, 2014).

2.3.7 Other factors

Solids retention time (SRT) is an important parameter in wastewater treatment. However, SRT has not been identified as a controlling factor in SBR aerobic granulation (Liu et al., 2005). Li et al., 2008 confirmed this conclusion after testing SRTs of 3 to 40 days. In this study, SRT was controlled by removing sludge during the aeration phase. They concluded that rather than SRT, selection pressure based on settling velocity was the driving force of aerobic granulation. Another factor that may play a role in granulation is quorum sensing. Quorum sensing is the phenomena where bacterial cells release "signal molecules" which, at sufficiently high concentrations, induce the activation of certain genes. One such signal molecule, c-di-GMP, is believed to regulate EPS production (Wang et al., 2017). Still other theories propose that filamentous bacteria (Wang et al., 2017) or fungi (Liu et al., 2017a) serve as the initial framework upon which biomass may aggregate.

2.4 Structural stability of granular sludge in SBRs

The availability of methods to maintain the structural stability of aerobic granules is actually as important as the development of the technique to promote their formation. As a matter of fact, how to maintain the granule stability has been an intriguing research topic since the introduction of aerobic granulation. Lee et al., 2010 identified some of the primary factors related to granule stability such as filamentous bacteria growth, breakdown of the anaerobic core, and EPS properties. This list shows a clear connection between the mechanisms for granule formation and their structural stability.

2.4.1 Roles of EPSs

Lee et al., 2010 and Gao et al., 2011 both summarize the role of EPSs in aerobic granule formation and stability in SBRs. The majority of EPSs are metabolic products comprising proteins, polysaccharides, lipids, and various acids secreted by bacteria (Lee et al., 2010). EPSs are believed

to be the cementing materials adhering bacterial cells together as they form aggregates. The protein content of the EPSs reduces surface charge repulsion and increases hydrophobicity, while polysaccharides assist in "bridging" of small aggregates into larger entities (Gao et al., 2011). While some EPSs can be consumed by bacteria, stability is provided by a non-biodegradable portion of the EPSs in the outer layer of granules (Gao et al., 2011; Wang et al., 2006a; Wang et al., 2007).

2.4.2 Impact of filamentous bacteria

Filamentous bacteria may serve as the scaffold upon which granular sludge can form as shown in **Figure 3** (Gao et al., 2011). However, uncontrolled growth of filaments can be catastrophic to aerobic granule stability. The excessive presence of these bacteria caused a loose granule structure, which is vulnerable to collapse (Lee et al., 2010). Zheng et al., 2006 determined that both granule density and hydrophobicity decreased as filamentous bacteria became dominant. Filamentous granules also suffered from a diminished SVI and can be easily washed out of the reactor.

Having high specific surface area, filamentous bacteria compete well at low DO and lean substrate conditions. Aerobic granules, which are characterized by concentration gradients of substrate and DO, are inherently susceptible to filamentous growth. As the biomass accumulates in an SBR after multiple cycles, the bulk concentration of substrate and DO in the famine phase may eventually become low enough for filamentous bacteria to proliferate (Liu and Liu, 2006). Zheng et al., 2006 confirmed that low food-to-microbe (F/M) ratios at later cycles in an SBR led to filamentous overgrowth. In addition, the long SRT of the microbial community present in granules allowed filaments to multiply rather than be washed out of the reactor (Liu and Liu, 2006).

2.4.3 Impact of anaerobic cores

Large granules may experience diffusion limitations that promote gradients within the granular structure. Such a DO gradient allows for the formation of an anaerobic core (Zheng et al., 2006). The gases formed as byproducts of anaerobic fermentation can compromise granule stability (Tay et al., 2002). It stands to reason that these gases, if not released in a timely manner, may either be retained, causing flotation, or build up, possibly damaging the granule.

2.4.4 Impact of organic loading

Although the occurrence of granule formation in a SBR is not dependent on OLRs for the most part, the morphology of the granule will be affected. Specifically, a large OLR results in a loose structure, while low OLRs tend to cultivate compact granules (Gao et al., 2011). Granule stability is also dependent on loading rates. For example, Val del Rio et al., 2013 reported that large granules collapsed under an OLR of 4.4 g L^{-1} d^{-1}.

2.5 Challenges of aerobic granulation in CFRs

The configuration of CFRs exposes aerobic granules to a cultivation environment very different from that of SBRs. As a result, settling velocity-based selection pressure and alternation of feast/famine are more difficult to apply in CFRs. Additional difficulties include damage to granules in sludge return equipment.

2.5.1 Application of selection pressure

Selectively retaining faster settling particles has been identified as an ultimate driving force for conventional aerobic granulation in SBRs. However, this kind of selection pressure is easy to apply in column SBRs with short settling times (**Figure 5**), but very difficult to implement in CFRs. Full-scale secondary clarifiers are typically designed with significantly longer settling times to achieve a clear effluent. Even when CFRs are designed with a settling time comparable to an SBR, granules will not settle as well due to the additional disturbance of continuously flowing water (Li et al., 2016e). Therefore, the selection of better settling biomass requires a CFR to be equipped with an effective mechanism for continuously separating faster settling solids from the treated water and retaining them within the reactor. Many attempts have been made to incorporate such a mechanism into CFRs for retaining solids. However, most of them either have an overly complicated structure (Liu et al., 2015; Zhou et al., 2013c) or are difficult to adjust for settling velocity optimization (Li et al., 2014). Simple and effective means for introducing a settling velocity-based selection pressure into CFRs is highly desired.

2.5.2 Granule recirculation pumps

In CFR processes, it is common to perform solids-liquid separation in a gravity sedimentation tank or clarifier. If such an external device is used for solids separation, faster settling bioparticles must be returned to the reaction tank. However, traditional pumping systems may crush and damage returned aggregates (Li et al., 2015; Li et al., 2014).

2.5.3 Provision of feast/famine

It is challenging to provide feast/famine conditions in CFRs. Most of the CFRs used in laboratory studies are completely mixed, such that the effluent concentration is supposed to be identical to the concentration within the reactor. Since substrate is being constantly consumed by the biomass, this means the substrate concentration will be maintained at a constant, low level. WWTPs are comprised, for the most part, of long, rectangular basins. Conditions approach plug flow in these reactors, but feast-famine is still difficult to achieve.

Lower substrate concentrations lead to limited penetration of substrate into the granule structure such that organics, DO, and other nutrients cannot access the core of large granules. Consequently, large granules may develop a loose structure and collapse. This problem has been observed when CFRs were seeded with granules cultivated in SBRs (Corsino et al., 2016; Li et al., 2016e; Liu et al., 2012). In addition, flocculent bacteria are able to outcompete granular biomass at low concentrations, and may begin to become dominant in the reactor (Liu et al., 2015). Therefore, the provision of feast/famine conditions in CFRs is another important consideration in CFR aerobic granulation.

2.6 The state of the art of aerobic granulation in CFRs

Attempts have been made over the past several years to develop strategies to better understand the mechanism of aerobic granulation in CFRs and overcome the challenges previously discussed (**Figure 2**). While some studies have attempted to reproduce the conditions that favor granulation in SBRs (settling velocity-based selection pressure and feast/famine cycles) in CFRs, other creative methods have been tested as well. It is also important to understand how operating conditions and reactor configuration will affect CFR granule formation and stability.

2.6.1 Selection pressure in CFRs

Analysis of the published literature clearly demonstrates that CFRs must implement selection pressure as a necessary driving force for granulation. Multiple approaches have indeed been used successfully to maintain a significant portion of biomass in CFRs. Selection pressure itself may take several forms, discriminating between biomass based on settling velocity, particle size, or some combination, and may be implemented under a variety of reactor configurations. Some authors claimed to develop stable granules without the aid of selection pressure, but a careful examination of their experimental setup and results led to alternative explanations.

The necessity of a settling velocity-based selection pressure is evident from the study by Hou et al., 2017. The effect of hydraulic retention time (HRT), influent pyridine concentration, and DO were determined in a reactor system comprising an ALR, an internal settling tank, and a membrane bioreactor (MBR) in series (**Figure 6a**). The settling tank provided the ALR with selection pressure, as poor settling biomass was washed into the MBR and fast settling bioparticles settled and recirculated back to the ALR. The MBR provided essentially complete biomass retention and, therefore, was deprived of any means of selection. Granulation was observed in the ALR, but the authors did not report such an observation in the MBR. **Figure 7** further shows the SVI over time for sludge in both reactors, confirming that SVI never fell below 60 mL g^{-1} in the MBR without selection pressure, an example baseline for granular sludge (Martin et al., 2016). In contrast, sludge in the ALR with selection pressure demonstrated excellent settling properties. Granules seeded into a MBR (**Figure 8a**) by Corsino et al., 2016 disintegrated during a 42-day operation of

continuous inflow and outflow, resulting in an extent of granulation (granular biomass-to-total biomass ratio) of approximately 40%. By switching to intermittent feeding while effluent removal still remained continuous, the operation was alternated between feast and famine. The extent of granulation stabilized for approximately 30 days, but without a settling velocity-based selection pressure further granulation did not occur (**Figure 9**). Further studies presented in this review also confirmed that providing this selection pressure is a key requirement for aerobic granulation under continuous flow mode.

Although some studies reported the formation of granules with no need of settling velocity–based selection pressure (Chen et al., 2015b; Yulianto et al., 2017), examination of the data suggests this may not be the case. A study by Yulianto et al., 2017 compared SVI and morphology of aggregates formed in a SBR and a continuous ALR. There is no indication that the ALR included a phase separator to provide selection pressure, and the results indicated poor granulation. Photos showing morphology suggest large, loose flocs formed, rather than granules. The SVI of that sludge was 80 to 90 (greater than 60) mL g^{-1}, again indicating failed granulation without an applied selection mechanism.

Similar results were obtained by Chen et al., 2015b. In their study, a completely mixed activated sludge (CMAS) system (**Figure 6b**) achieved granulation with settling time of 2 hours in an external clarifier. Although the author claimed that short settling time was not required for granulation, it is again not clear from the reported morphology that granules actually formed (Chen et al., 2015b). Inspection of the photographs (**Figure 10k**) provided in the study indicates large flocs-like aggregates with SVI ranging from 50 to 90 mL g^{-1} were formed instead. The proposed mechanism of aggregation was entanglement of biomass by filamentous bacteria, but a Gram and Neisser staining process indicated the absence of further growth of filaments within the aggregate. The lack of further filamentous entanglement suggests the aggregates should not be classified as FAGs.

A series of CFR studies from the same research team claimed successful aerobic granulation with no need of a settling velocity-based selection pressure (Zhou et al., 2013a; Zhou et al., 2013b; Zhou et al., 2013c; Zhou et al., 2014). Shear force, according to the study, was regarded as the driving force of granulation. However, it is important to note that all experiments were carried out in ALRs equipped with three-phase separators which is known to be capable of providing selection pressure driving biogranule formation. Hence, selection pressure based on settling velocity was likely at work in the granulation processes. In light of this analysis, it is very likely that settling velocity-based selection through three-phase separators may be a better explanation for the formation of granules than shear force.

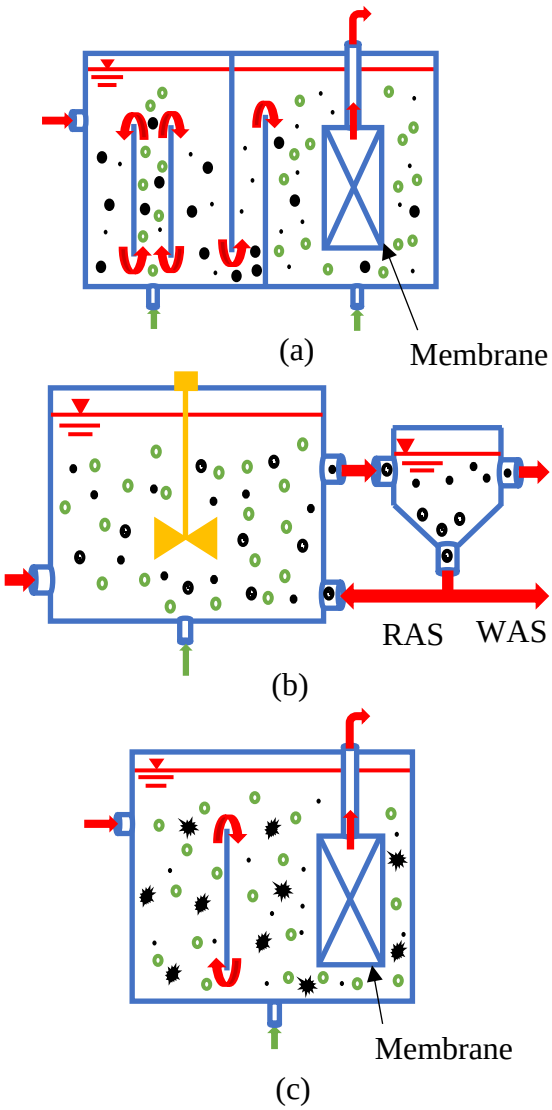

Figure 6. CFR configurations lacking sufficient settling velocity-based selection pressure to promote granulation: (a) system comprising an ALR, a settling tank, and MBR in series (Hou et al., 2017), (b) a CMAS system with 2-hour settling time (RAS: return activated sludge; WAS: waste activated sludge) (Chen et al., 2015b), (c) a MBR with internal circulation (Chen et al., 2017) *(blue – Reactor and membrane; red – water flow; green – air bubbles; yellow – stirring device; small black circle – floc biomass; large black circle - granules; patterned black circle – large floc biomass; jagged black ovals – filamentous aerobic granules)*

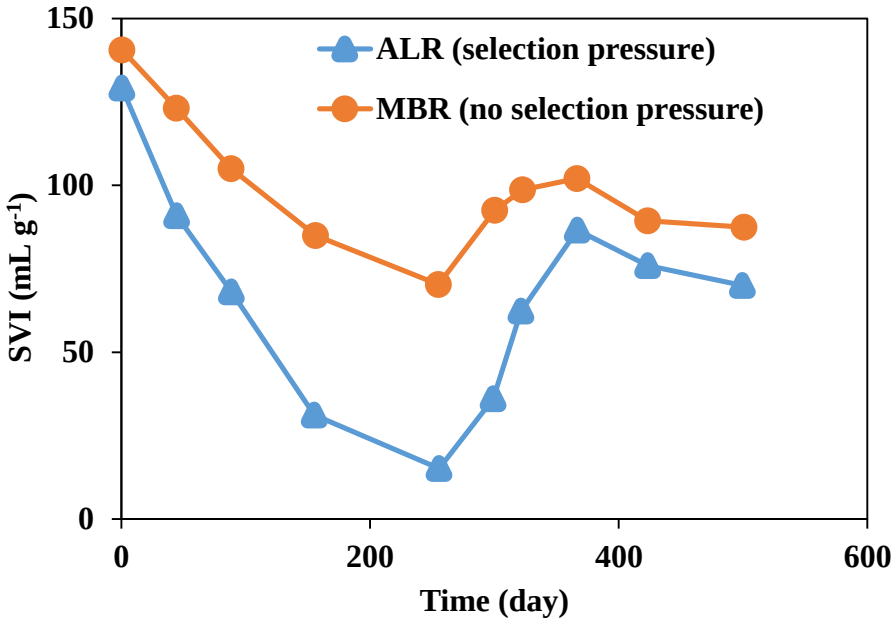

Figure 7. SVI for sludge in a system comprising an ALR (with settling velocity-based selection pressure) and MBR (without selection pressure) in series as shown in **Figure 6a** (Hou et al., 2017). An increase in loading from 3.5 to 4.5 mg L^{-1} d^{-1} on day 250 led to sharp increase in SVI.

Biomass in CFRs may be selected by means of differences either in settling velocity or particle size. Settling velocity-based selection pressure is commonly used in SBRs and achieved in CFRs by means of internal or external solid-liquid separators. Internal separators, commonly used in upflow reactors, typically comprise a baffle which separates an aerated reaction zone from an unaerated settling zone within the same reactor vessel (**Figures 11a,b** and **12c)** (Deng and Zhang, 2012; Xin et al., 2017). A good example is what is commonly known as a three-phase separator (Wan et al., 2014a; Wan et al., 2014c; Yang et al., 2014; Zhou et al., 2013c). A three-phase separator, as used herein, refers to a special baffle located in the top section of an upflow reactor (**Figure 11c**). A portion of the liquid flows up through the middle of the device, where liquid-gas separation occurs. The remaining slurry is directed toward the sides of the reactor, where solids settle out of the unaerated water. Although this design was firstly used in upflow anaerobic sludge blanket (UASB) reactors, it has also been widely used in recent laboratory-scale aerobic, upflow CFRs. ALRs may be used in conjunction with either a three-phase separator (**Figure 13a**) or more conventional baffled settling zones (**Figure 13b**). External separators simply separate the reaction and settling zones by placing them in separate vessels. This was done by Long et al., 2015b who utilized an upflow reactor connected to an external, baffled settling tank by means of an inclined tube (**Figure 8d-e).** Zou et al., 2018 utilized a baffled external settling tank with two settling zones. Heavier biomass settled in the first zone and was returned to the reactor, whereas lighter biomass washed into the second zone.

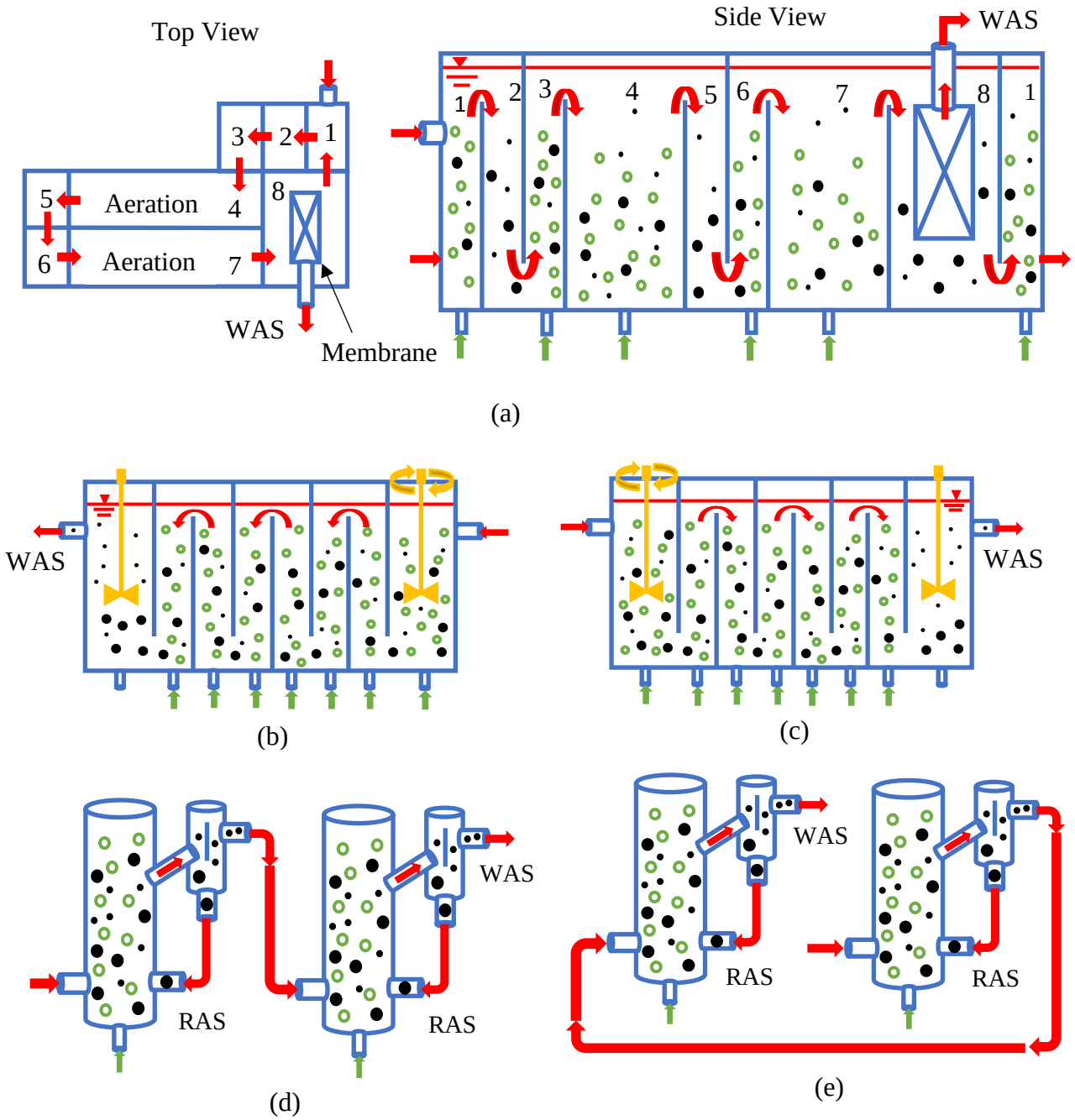

Figure 8. CFRs implementing feast/famine conditions: (a) a baffled MBR (no selection pressure) with alternating aerobic/anaerobic zones (Corsino et al., 2016), (b-c) a baffled CFR in forward- and reverse-flow modes (Li et al., 2015), (d-e) a bubble column with an inclined tube leading to an external, baffled settling tank in forward- and reverse-flow modes (Long et al., 2015b) *(blue – Reactor and membrane; red – water flow; green – air bubbles; yellow – stirring device; small black circle – floc biomass; large black circle - granule)*

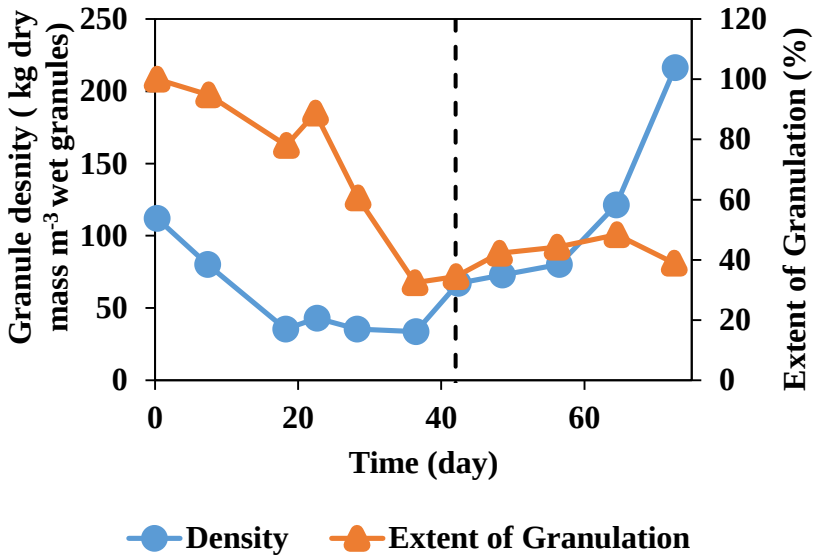

Figure 9. Granule density and extent of granulation for a CFR: Phase I - continuous feeding (prior to day 42), Phase II - intermittent feeding (after day 42) (Corsino et al., 2016)

Some studies have implemented these separation techniques in more complicated configurations. For example, Liu et al., 2015 developed a hybrid reactor in which the bottom portion operated as an ALR and the upper portion as a bubble column (**Figure 13c**). In other words, the enhanced liquid circulation induced by the baffles in the lower portion of the reactor was absent in the upper portion. This baffle-induced circular flow retained granular sludge in the lower airlift portion of the reactor. Li et al., 2014 achieved granulation in a modified oxidation ditch with a unique internal settling zone (**Figure 12a**). This settling zone comprised a movable baffle, which allowed the control of settling time, with inclined plates to facilitate granule settling. Li et al., 2016e also controlled settling time, but used an external settling tank with multiple outlet locations (**Figure 12b**). Allowing flow through a higher port limits the settling time as compared to lower ports. Sajjad et al., 2016 operated an SBR as a seeding reactor next to a MBR (**Figure 11d**). This MBR, unlike others designs in **Figures 6** and **14**, contained an internal settling zone, which allowed for application of selection pressure. The aggregate size in the MBR only reached 0.2 mm, while granules grew to 0.8 mm in the SBR. The smaller diameter achieved in the CFR was attributed to the constant aeration providing high shear forces, although the lower substrate concentrations in well mixed systems likely contributed as well. It is likely the aggregates in the CFR were not actually granules since photographs showed loose, irregular structures and SVI always exceeded 125 mL g^{-1}. In order to maintain uniformity of the granular sludge in the two reactors, a portion of the sludge was periodically exchanged (Section 2.6.5). This allowed for a common granular diameter of 0.63 mm.

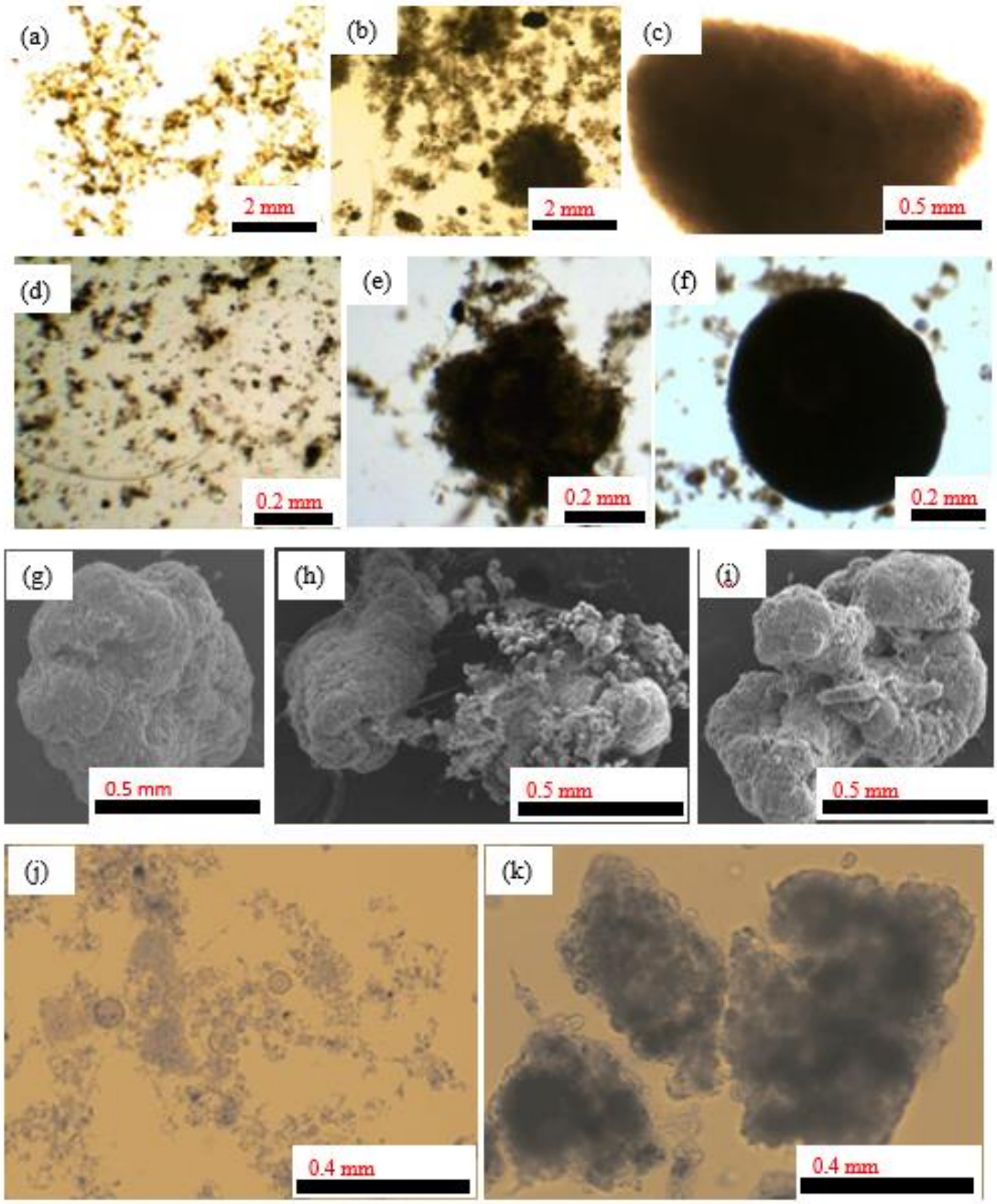

Figure 10. Morphology of aerobic granular sludge in CFRs: (a-c) formation of granules from activated sludge in an upflow reactor (Xin et al., 2017); (d-f) formation of granules from biofilm biomass (Yang et al., 2014); (i-k) disintegration of seeded granules to form irregular, fluffy granules (Li et al., 2016c); (l) seed sludge and (m) large, loose aggregates formed without sufficient settling- or size-based selection pressure (Chen et al., 2015b). (*Permission for reproduction of copyrighted material in this figure has been obtained*)

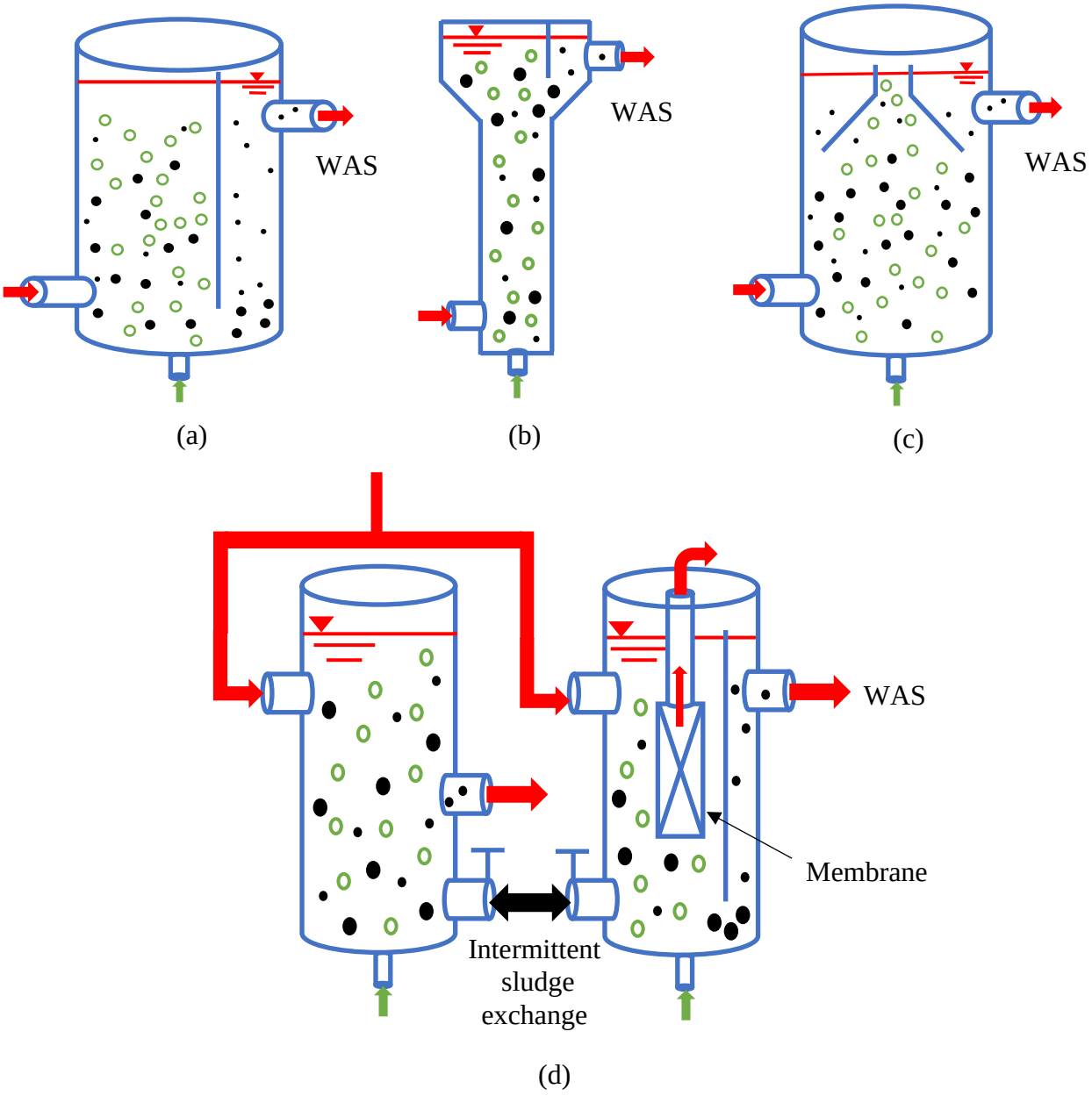

Figure 11. Continuous bubble columns with internal solid/liquid separators: (a) a bubble column with a long baffle (Xin et al., 2017), (b) a bubble column with a short baffle on the top (Tsuneda et al., 2003), (c) a bubble column with a three-phase separator on the top (Chen et al., 2009), (d) SBR/MBR in series with intermittent sludge exchange (Sajjad et al., 2016) *(blue – Reactor and membrane; red – water flow; green – air bubbles; small black circle – floc biomass; large black circle - granules)*

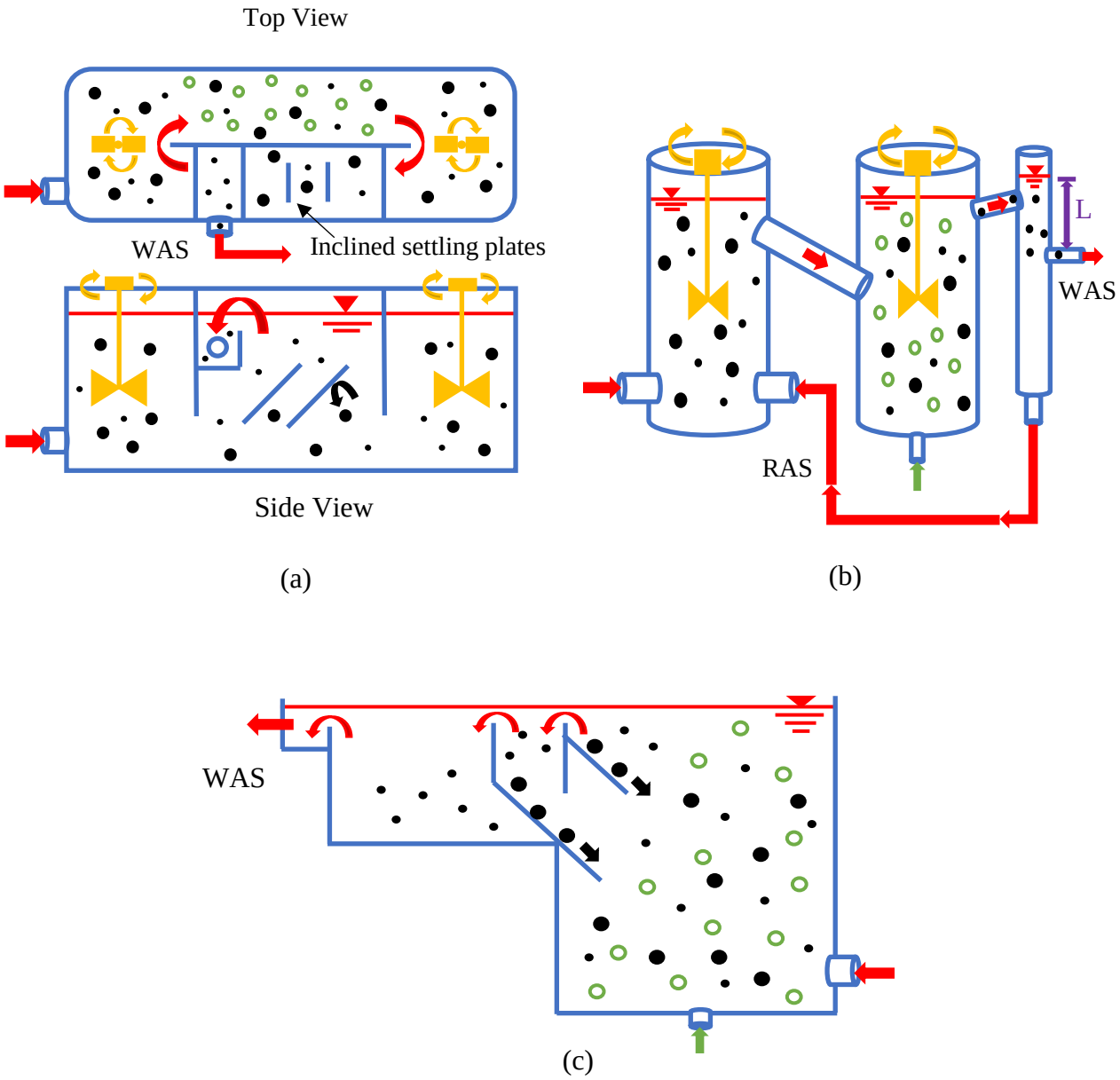

Figure 12. Other configurations of CFRs implementing settling velocity-based selection pressure: (a) a modified oxidation ditch with inclined plate settlers (Li et al., 2014), (b) phosphorous removal system (anaerobic, aerobic, settling tanks) with adjustable effluent port height (L) (Li et al., 2016e), (c) an upflow reactor with multiple internal settling tanks (Bumbac et al., 2015). *(blue – Reactor and membrane; red – water flow; green – air bubbles; yellow – stirring device; small black circle – floc biomass; large black circle - granule; purple – variable effluent port depth)*

Settling time applied in CFRs may also have a significant impact on the startup time required for granulation. When Li et al., 2015 compared operation of a continuous reverse-flow baffled reactor (RFBR) and a SBR, granules formed in the SBR more rapidly than the CFR, which had a longer settling time (**Table 2**). In another study, Li et al., 2014 observed granules formation within 4 days

in an SBR (settling time of 20 minutes) and 13 days in a continuous, modified oxidation ditch (settling time of 60 minutes). Moreover, rapid startup of a CFR was achieved within 16 days by gradually decreasing the settling time from 9 to 3 minutes by means of an adjustable effluent height (**Figure 12b**) (Li et al., 2016d).

Size-based selection pressure, in which a sieve allows only small flocs to pass through, is a possible alternative to settling velocity that has been tested. Liu et al., 2012 used an ALR/MBR system (**Figure 14a**) in which a settling tank provided selection pressure for the ALR, and a sieve screen was placed downstream of the MBR. The screen allowed biomass with size less than 0.1 mm to pass through and be wasted, while larger biomass was returned to the MBR. However, while water flowed through the reactor continuously, sludge was only partially discharged to the sieve once a day. This, along with a constant feed of flocculent biomass from the ALR, seems to have limited the effectiveness of the selection pressure. Liu et al., 2014 analyzed the effectiveness of such a strategy by running three reactors, the first with settling velocity selection, the second with granule size selection (**Figure 14b**), and the third with a combination of both selection pressures. Moreover, the first reactor was run as a SBR and the other two as CFRs. **Figure 15**, which presents the data for the first and second reactors, demonstrates that the extent of granulation and SVI approached the same values between the SBR and the CFR within approximately 20 to 25 days of operation. Notably, the CFR achieved the ultimate extent of granulation more rapidly probably by virtue of its continuous selection. Since the sieve allowed washout of small granules, as well as the flocculent biomass, size-based selection strategy allowed large granules to dominate. The size-based selection pressure also meant that poorly settling biomass, if large, still remained in the reactor; however, it also removed the dead cells of collapsed granules that would settle well in the SBR. This was reflected by a better chemical oxygen demand (COD) consumption rate in the CFR equipped with size-based selection, i.e. 2.3 versus 1.4 kg COD kg^{-1} MLSS d^{-1} in the CFR and SBR, respectively. The two studies just discussed achieved selection pressure by incorporating external sieves. The other option is an internal screen (**Figure 14c**) as used by Wang and Peng, 2008. This paper credited the fast formation of large granules (2 to 3 mm) to a high organic loading rate (OLR). Although not discussed, the size-based selection provided by the screen may have also contributed to the cultivation of the large granules.

Since ASAG formation actually depends on the formation of AMX granules under anoxic conditions, it is necessary to briefly discuss how AMX granules are formed. The formation mechanism of AMX granules is not understood as well as that of aerobic granules. However, it is believed that AMX granulation is not dependent on settling-velocity based selection pressure, as evidenced by the fact that those granules can be maintained in MBRs for extended periods of time (e.g. 375 days) (Trigo et al., 2006). Since MBRs fully retain biomass, no settling velocity-based selection pressure was applied, nor indeed was needed. It is also noteworthy that hydrocyclones are commonly used in conjunction with SBRs in the DEMON (DEaMmOnificaN) process in which flocculent AOB and granular AMX coexist in the same reactor for nitrogen removal through the partial nitritation-anammox process (Lackner et al., 2014). The hydrocyclone provides a vortex selection pressure (Section 2.8.5) which retains slow growing AMX and washes out flocculent

biomass mainly consisting of AOB (Gonzalez-Martinez et al., 2015). The effect of hydrocyclones on microbial makeup of partial nitritation-anammox reactors was investigated by Shi et al., 2016, who compared the sludge of conventional SBRs with and without a hydrocyclone. The presence of granules in the SBR without a hydrocyclone again verified that selection pressure, as provided by the hydrocyclone, is not necessary for AMX granule formation. However, selection pressure did increase the ratio of granules to flocs, namely extent of granulation, in the system.

A process comparable to DEMON SBR is completely autotrophic nitrogen removal over nitrite (CANON), also known as the Paques ANAMMOX® process (Paques a, n.d.), which not only occurs in a continuous flow system but also removes nitrogen through the partial nitritation-anammox process. The difference is that AOB often forms an outer layer around the AMX granule, in the form of ASAG, in CANON reactors (Lackner et al., 2014). To the best of our knowledge, all studies that performed CANON in CFRs and investigated the distribution of AOB and AMX in granules have reported a stratified structure. However, it is our belief that settling velocity-based selection pressure also played an important role in the formation of ASAGs in CFRs. This can be demonstrated by the fact that flocs are more competitive than granular sludge for substrate uptake due to a lower resistance to mass diffusion in the floc structure (Liu et al., 2015). If AMX granules and flocculent AOB biomass are co-inoculated in a hypothetical CFR, some AOB will attach to the surface of the AMX granules just like their ubiquitous attachment to abiotic surfaces (Flemming et al., 2016; Underhill and Prosser, 1987). However, the much higher specific surface area of AOB flocs over ASAGs will allow the former to easily outcompete the latter when selection pressure is not used. When a settling velocity-based selection pressure is applied, many AOB flocs will be washed out of the reactor, allowing the AOB growing on the surfaces of AMX granules to compete for resources, ensuring these granules to develop into mature ASAGs. On the other hand, when no selection pressure is applied, flocculent AOB will remain in the reactor and outcompete the AOB growing on the granule surfaces, preventing the development of the thin film of nitrifiers on AMX granules. Therefore, selection pressure will help develop ASAGs, but is not necessarily required for their formation. This insight also provides a new role of settling velocity-based selection pressure. It should be pointed out that the principles of this thought experiment apply equally well to the development of CAGs.

FAGs were observed by Chen et al., 2017 in a MBR with internal liquid circulation (**Figure 6c**). In this experiment the membrane completely retained the biomass, so no settling- or size-based selection pressure was present. However, the formation of aerobic aggregates was induced by the entanglement of microbial cells by filamentous bacteria as hydraulic circulation induced collisions between them (**Figure 3**). Such aggregation of filamentous microorganisms seems closely related to a similar process (called pelletization) observed for fungal species (Nyman et al., 2013; Zhang and Hu, 2012). This phenomenon is distinct from the granulation process for CAGs which relies on selection pressure and EPS production.

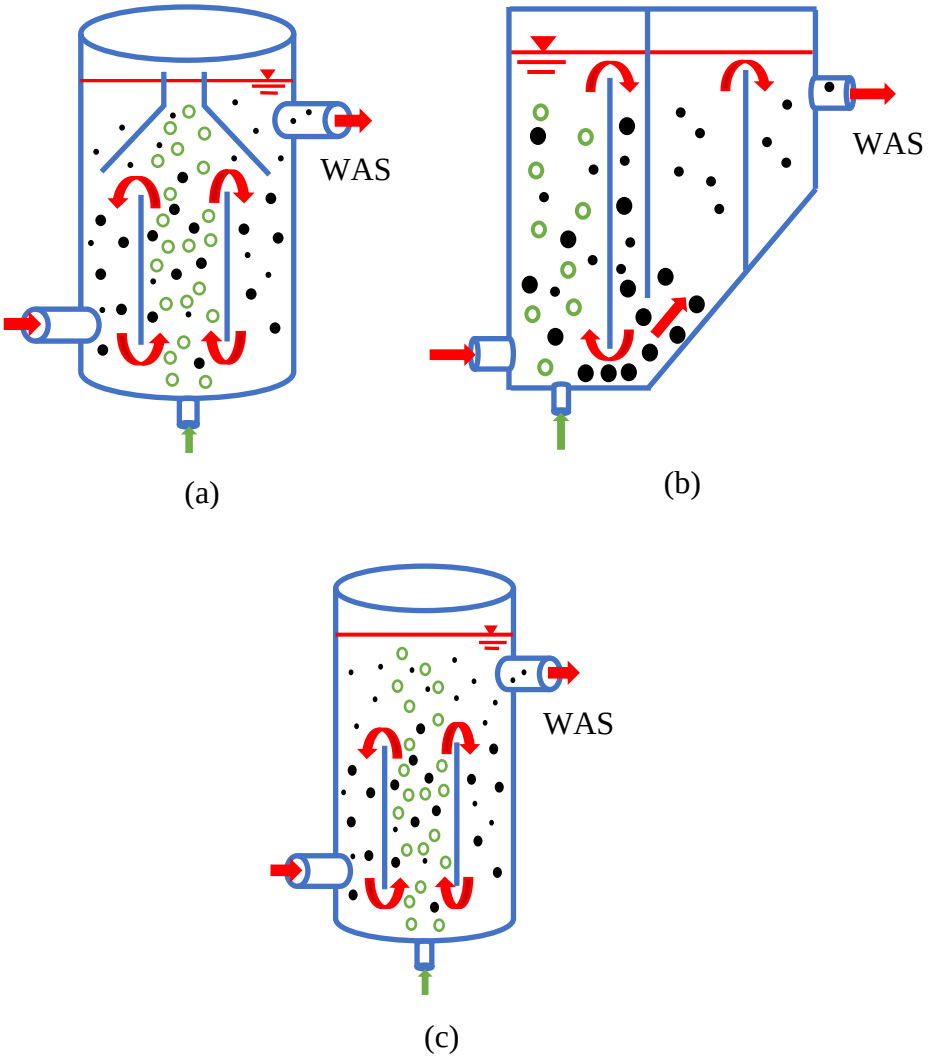

Figure 13. Continuous ALR configurations: (a) an ALR with a three-phase separator on the top (Ramos et al., 2016), (b) an ALR with baffled settling zones (Qian et al., 2017), (c) a hybrid ALR/bubble column (Liu et al., 2015) *(blue – Reactor and membrane; red – water flow; green – air bubbles; small black circle – floc biomass; large black circle - granules)*

2.6.2 Granular sludge recirculation systems

CFRs with external solids/liquid separators (**Figures 6b, 12b, and 14a,b**) have the disadvantage of requiring the return of sludge to the reactor. Although loss of granules due to crushing in sludge return pipes from external settling tanks is a concern (Li et al., 2015; Li et al., 2014), several studies have successfully implemented external settling tanks with their reactors (Chen et al., 2015b; Li et al., 2016d; Li et al., 2016e; Liu et al., 2014).

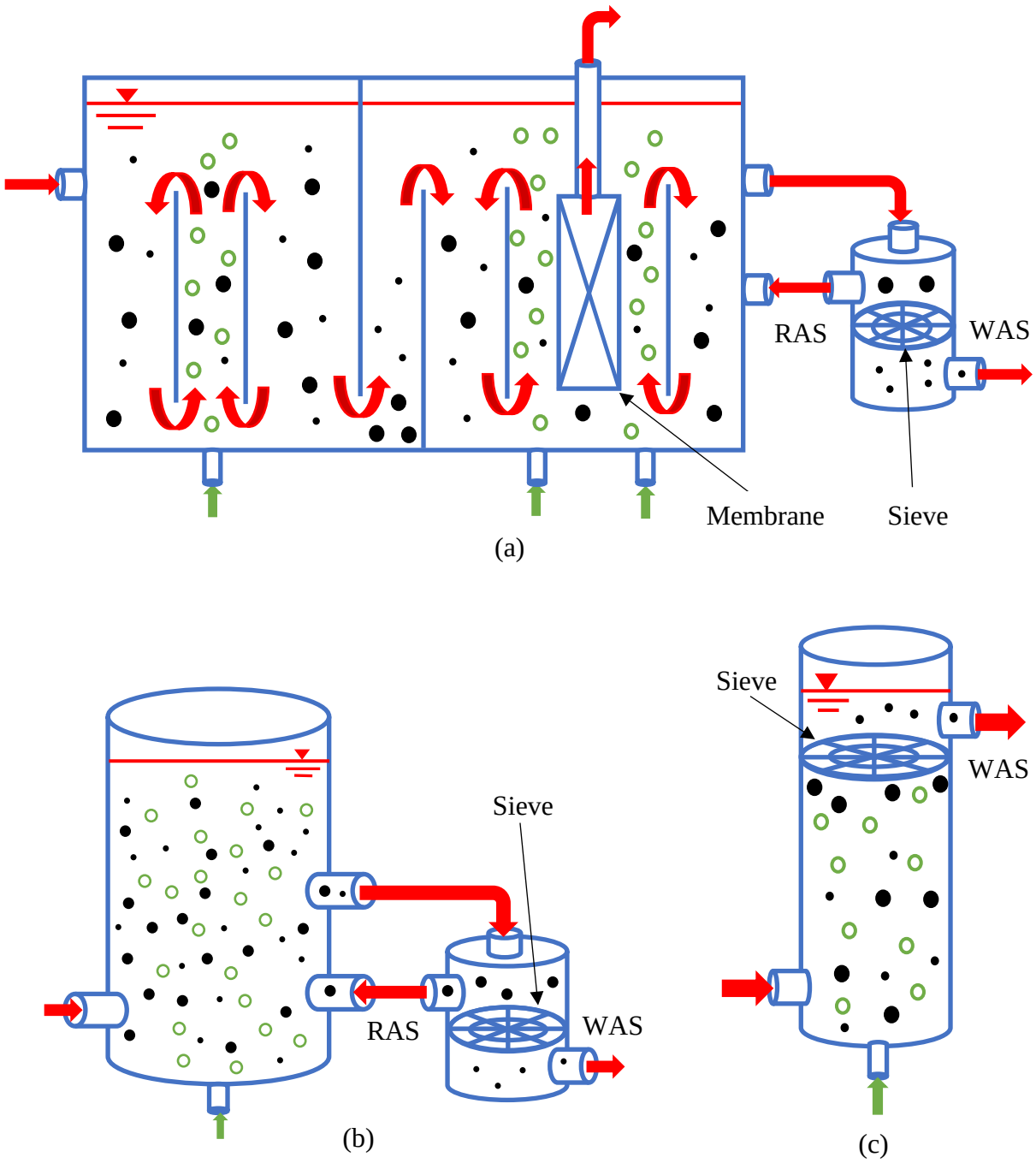

Figure 14. CFRs implementing particle size-based selection pressure: (a) an ALR and a settling tank in series with an MBR and an external settling tank equipped with a sieve screen (Liu et al., 2012), (b) a bubble column and an external selection tank equipped with a sieve screen (Liu et al., 2014), (c) a bubble column with an internal screen (Wang and Peng, 2008). *(blue – Reactor and membrane; red – water flow; green – air bubbles; small black circle – floc biomass; large black circle - granule)*

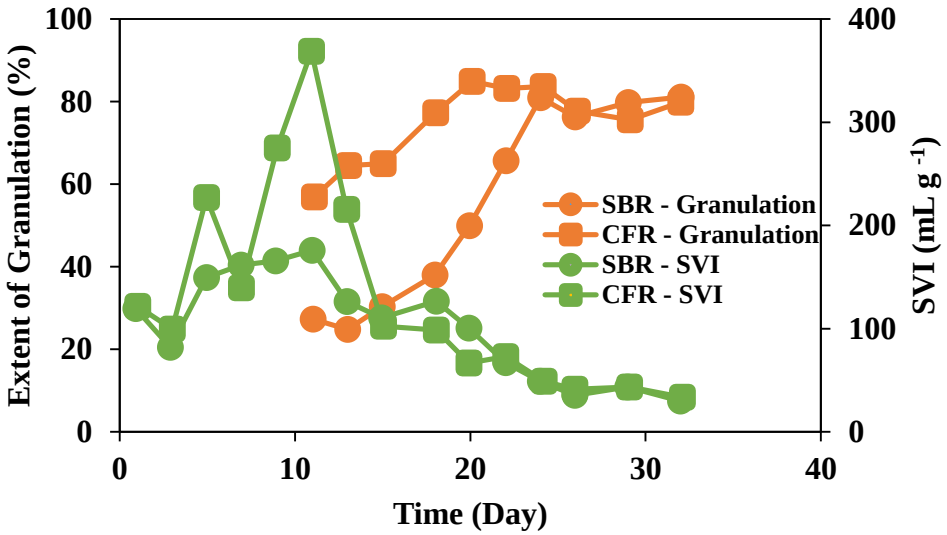

Figure 15. Extent of granulation of total biomass and SVI in an SBR with settling velocity selection and a CFR with granule size selection using a sieve (Liu et al., 2014)

It is interesting to see that Li et al., 2016e and Chen et al., 2015b used peristaltic pumps to return the sludge without crushing the granular sludge. One possible alternative to conventional pumps is the airlift pump. Such a pump functions by bubbling air at the bottom of a submerged tube. The aerated liquid is less dense than the liquid above, causing it to rise up and out of the tube (Oueslati et al., 2017). This principle was utilized in the BIOCOS® process (World Water Works, n.d.), as well as the design by Odegaard, 2016 for transferring biofilm carriers between sidestream and mainstream moving bed biofilm reactors (MBBR). Zou et al., 2018 also used this technology in a pilot-scale study to return heavy biomass from a settling tank. This technology can be easily adapted to granular sludge as well.

2.6.3 Creation of feast/famine conditions

The intentional creation of feast/famine conditions is not common among lab-scale CFRs, even among those that successfully achieved aerobic granulation. Therefore, alternation of high and low substrate concentrations is not as essential on such small scales. Nonetheless, studies by Corsino et al., 2016 and Li et al., 2015 investigated the performance of such a strategy. Both papers used CFRs comprising multiple baffled reaction chambers in series. As substrate-rich influent traversed the long flow path of the reactor, COD and other nutrients were progressively consumed by biomass, resulting in substrate-lean areas far from the inlet. Li et al., 2015 induced a cyclic nature to the feast/famine conditions by using a RFBR, operating in cycles of 2 hours forward-flow (**Figure 8b**) and then two hours reverse-flow (**Figure 8c**). In other words, the location of substrate-rich and substrate-poor zones "cycled" each time the flow direction was reversed. Aerobic granules were formed within 21 days and remained stable for the remainder of the 135-day study, growing

to a final diameter of 0.13 mm. These aggregates are smaller than typical aerobic granules, but having an SVI of 43 mL g^{-1} and compact, round structure supports classifying them as granular sludge. Liu et al., 2012 used a similar method of cycling through forward and reverse flow in a two-reactor system (**Figure 8d-e**), i.e. the effluent from one reactor was the influent to the other. Although the creation of feast/famine was not discussed, it is easy to see that the first reactor (to which influent was fed) could act as a feast phase, while famine existed in the second reactor.

Corsino et al., 2016 achieved feast/famine conditions by maintaining a constant effluent withdraw, but intermittent feeding (**Figure 8a**). In this study, continuous flow with and without intermittent feeding were compared. First, SBR-cultivated aerobic granules were seeded into the reactor operating at a constant feed rate. However, granule density was observed to decrease from 100 to 50 kg dry mass m^{-3} wet granules. The protein-to-polysaccharide ratio (PN/PS), as well as total EPSs, diminished before the system stabilized with small, loose granules. Switching to intermittent flow improved granule density and increased total EPSs from 200 to more than 400 mg EPS g^{-1} VSS, although the percent of granules formed within the total biomass remained approximately the same as before (**Figure 9**). The authors observed that feast/famine, while maintaining stability, failed to promote further formation of granules without the additional influence of settling velocity-based selection pressure. The mixed liquor of the system contained a mixture of granules, flocs, and soluble microbial products (SMPs) from degradation of EPSs during periods of famine. Although not always essential for granulation in lab-scale reactors, evidence suggests that feast/famine conditions may help improve the settleability of sludge in full-scale CFRs (Section 2.8.5).

2.6.4 Hydraulics and shear force

The shear present in a reactor depends in part on the flow patterns therein. ALRs, for example, promote a regular, circular flow that induces significantly higher shear forces than bubble columns (Zhou et al., 2013c). The majority of studies reviewed in this paper utilized upflow reactors fitting one of these two configurations. A more plug-like flow resulting from a serpentine pattern of baffles (Li et al., 2015), sometimes seen in full-scale aeration basins, may supply a weaker shear force. A study by Hasebe et al., 2011 compared the formation of nitrifying granules in column and rectangular reactors. The results suggest that reactor shape is not a major factor in the granulation process.

Table 1. Time-span reported for aerobic granules to form and remain stable under various cultivation strategies. The stable phase is defined as the period of time after granules have been formed and maintained acceptable structure and performance. Unless otherwise indicated in the footnotes, experiments are were ended prior to loss of granule stability. Shading indicates granule type (white – CAGs; light grey – ASAGs; dark grey – FAGs).

Granulation strategy	Reactor type	Formation / acclimation phase (days)	Stable phase (days)	Inoculum/ diameter (mm)	Average Granule Diameter (mm)	SRT (day)	Loading Rate (g COD or N L^{-1} d^{-1})	DO (mg L^{-1})	Temperature (°C)	HRT (hr)	Reference
Adjustable baffles for settling large particles	Modified oxidation ditch	13	107	Anaerobic & aerobic sludge / < 0.05	0.6	—	0.53 – 1.1	—	18 – 30	3	Li et al., 2014
Size-based selection pressure with sieve	Bubble column	7	48	Activated sludge	1.0 – 3.0	—	1.07	3.0 – 6.0	20	9	Liu et al., 2014
Settling-based selection pressure; feast-famine conditions	Reverse flow baffled reactor	21	114	Anaerobic & aerobic sludge / < 0.05	0.135	—	0.54 – 1.6	—	—	5.5 – 16.4	Li et al., 2015
Hydraulically-induced biomass collisions and filamentous entanglement [I]	CMAS	21	70	Sludge from secondary clarifier	0.18 – 1.25	18	1.35	4.2	25 - 27	8	Chen et al., 2015b
Three-phase separator; inoculum from biofilm reactor; high DO to prevent diffusion limitation	ALR	25	55 [II]	Biofilm from biofiltration backwash system	0.6 – 0.9	—	1 – 3	6 – 7.5	21	2	Yang et al., 2014
Three-phase separator; hydrodynamic shear force	ALR	11	36	Activated sludge	0.51	—	1.2 – 1.8	5.8 – 7.6	20	1.8 – 2	Zhou et al., 2014
Internal solids/liquid separator; inoculation of special bacteria to enhance EPS production; Ca-PO_4 precipitate deposition to improve stability	Baffled bubble column	40	32	Activated sludge	0.5 – 2	—	0.4 – 1.05	—	15 – 30	0.55 – 2.37	Xin et al., 2017

Three-phase separator	ALR	20	12	Activated sludge / > 0.045	0.635	—	1.5 – 5	—	20	2 – 3	Zhou et al., 2013a
Three-phase separator	ALR	10	20	Activated sludge	0.7 – 1	—	4.8 – 5	—	20	2.8	Zhou et al., 2013b
Three-phase separator	ALR	12	23 [III]	Activated sludge	0.9	8 – 10	3.5 – 4.8	—	20	2	Zhou et al., 2013c
Internal settling tank; intermittent inoculation from SBR [IV]	MBR	40	80	Aerobic granules	0.625	—	0.6 – 1.2	—	—	8	Sajjad et al., 2016
N/A[V]	ALR	—	23	—	1.5 – 2.6	—	—	4	—	—	Yulianto et al., 2017
Three-phase separator; solids retention by low HRT	ALR	30	45	Activated sludge	1.54	—	0.556 – 2.37	>5	30	5.4 – 22.8	Jin et al., 2008b
Internal solid-liquid separator; appropriate aeration volume	Upflow reactor	100	400	Acclimated activated sludge	0.346	—	0.125 – 0.82	1 - 8	—	14.6	Tsuneda et al., 2003
Three-phase separator; inoculation of mixed aerobic/anaerobic sludge forms stable core	Bubble column	27	38 [VI]	Activated sludge + anaerobic digester sludge	2.5	—	1 – 3.7	0.3 – 0.6	30	10	Chen et al., 2009
ALR with settling tank	ALR + MBR [I] system	—	250 [VII]	Sludge from sediment tank of SBR	—	—	1.0 – 9.0 [VIII]	0.1 – 4.0	30	12 – 24	Hou et al., 2017
Enriching denitrifiers in the presence of high PO_4^{3-} concentration; inorganic precipitation in granule core [V]	Bubble column	—	216	Aerobic granules / 2.3	1.9	—	7.0	—	—	24	Juang et al., 2010
ALR with settling tank; MBR with sieve	ALR + MBR system	30	45	Aerobic granules / 1.0 – 6.0	0.1 – 1.0	—	0.18 – 0.74	2.0 – 3.0	20	13	Liu et al., 2012
External settling tank	Bubble column system	30	90, 40 [IX]	P-removal granules	0.9	10 – 30	0.8 – 1.2 [X]	2.0 [XI]	22	6 [X]	Li et al., 2016b

External settling tank	Bubble column system	30	98	P-removal granules	—	23 – 30	0.64 – 1.07 [x]	2.0 – 3.0 [xi]	22	4.5 – 7.5 [x]	Li et al., 2016a
External settling tank	Bubble column system	24	55	P-removal granules / 0.95	0.95	—	1.2 [x]	2 – 5 [xi]	22	6 [x]	Li et al., 2016c
External settling tank	Bubble column system	—	40, 40 [ix]	P-removal granules / 0.98	0.96	—	0.8 – 1.6 [x]	2 – 5 [xi]	22	6 [x]	Li et al., 2016d
Reactor with novel settling tank; stepwise reduction in settling time	Bubble column system	16	180	P-removal granules / 0.98	0.93	—	1.2 [x]	2.0 – 5.0 [xi]	22	6 [x]	Li et al., 2016e
Switching from continuous to intermittent feeding (effluent removal kept continuous) [I]	Baffled MBR	42 [xii]	30 [xiii]	Aerobic granules / 1.9	1.3 – 1.6 [xiv]	50	3.84	2 / 8 [xvi]	—	7.5	Corsino et al., 2016
Settling zone; gradually reducing HRT to increase EPSs	Aerated CSTR	—	145	Nitritation granules / 0.9	1.2	33 – 56	1.5 – 3.3	0.8 – 1.5	28	0.9 – 2	Qian et al., 2017
Hybrid reactor with improved granule retention; $CaCO_3$ precipitation improved stability	Hybrid ALR / bubble column	—	31	Aerobic granules / 1.5	1.2	—	3	—	25	8	Liu et al., 2015
N/A [I]	MBR	24	46	Glycogen-accumulating granules / 0.8 – 1.5	—	35 – 45	—	—	—	5.3 – 5.8	Wang et al., 2008
Three-phase separator	ALR	—	223	Anammox-partial nitritation granules / 0.9	0.9 – 1.4	75 – 210	0.27 – 0.86	0.7 – 3.6	20	1.4 – 3.6	Poot et al., 2016
Three-phase separator; high DO to prevent diffusion limitation	ALR	—	390	Partial nitritation granules	1.0 – 2.7	107	0.3 – 0.7	0.5 – 4	30	0.9 – 6.3	Ramos et al., 2016

Inclined tube settler + external settling tank	Upflow reactor	—	65	Aerobic granules / 1.18	1.8	—	4.8 – 15 [xv]	—	10 – 20	4	Long et al., 2015b
Inclined tube settler + external settling tank	Upflow reactor	18	—	Activated sludge + aerobic granules	1.2	—	6	—	10 – 20	4	Long et al., 2015a
Cultivation of seed granules under high C/N in SBR [v]	CFR	—	216	Aerobic granules	4.8 – 6.1	—	6 – 31.3 [xvi]	—	25	2.2 – 19	Chen et al., 2016
Three-phase separator; special bacteria inoculation		36	16	Aerobic granules	—	—	0.1	7	28	12	Wan et al., 2013
Three-phase separator	Upflow reactor	—	75	Aerobic granules / 3.5 – 4.5	2.5 – 3.5	—	0.16	—	28	12	Wan et al., 2014c
Three-phase separator; Achieving partial nitritation under low C/N induced EPS production	Upflow reactor	—	180	Aerobic granules / 3 – 4	2 – 3	—	0.05 – 0.1	—	6 – 25	12 – 24	Wan et al., 2014b
Three-phase separator; cryoprotective EPS production for low temperature survival	ALR	—	250	AOB enriched biomass	0.81	80	0.63	0.5 – 2.5	10	2.5	Reino et al., 2016
Three-phase separator + external separator; temporary inorganic carriers provide nucleation sites for biomass attachment	ALR	—	300	nitrifying granules [xvii]	0.7 – 0.9	—	0.75 – 6.1	5 – 7	30	—	Bartroli et al., 2010
N/A [v]	ALR	—	—	Aerobic granules	0.8 – 1.1, 0.4 – 0.5 [xviii]	—	0.4 – 1.0, 0.9 – 4.0 [xviii]	2, 4 – 5.5 [xviii]	30	—	Jemaat et al., 2015
Three–phase separator	ALR	—	150	Aerobic granules / 1.5	1.0 – 1.5	—	0.4 – 1.1	2.0	30	20.4 – 55.2	Jemaat et al., 2014a
Three–phase separator	ALR	—	50	—	0.9 – 1.1	—	1.1	2	30	—	Jemaat et al., 2014b

N/A [v]	ALR	—	450	Nitrifying granules / 0.5	0.5 – 1.5	—	0.27 – 1.4	1 – 5	12.5 – 30.0	—	Isanta et al., 2015
Internal screening	Bubble column	3	33	biofilm	2 – 3	—	4.1 – 22.0 [ixx]	>3	18	1.2, 6.4 [ixx]	Wang and Peng, 2008
Internal settling tank	Upflow reactor	—	70	Aerobic granules	—	—	3.1 – 5.6	—	—	10	Bumbac et al., 2015
N/A [v]	CFR	33	36	Aerobic granules	—	—	0.1, 0.17, 0.5 [xx]	6 – 8	28	12, 7.2, 2.4 [xx]	Wan et al., 2014d
Solid-liquid separator; control of surface loading rate	Upflow reactor	65	75	Aerobic sludge	0.226	—	0.15 – 0.23	>2	22	32 – 48	Kishida et al., 2010
Solid-liquid separator	Upflow reactor	91	59 [iii]	Aerobic sludge	>0.2	—	3.0 – 6.0	—	22	6 – 12	Kishida et al., 2012
N/A [v]	CSTR	—	600	Granular sludge	1.6	—	0.5	6	—	24	Matsumoto et al., 2010
Solid-liquid separator	Uplow reactor	—	14	Nitrifying granules	—	—	2.8 – 19	—	—	0.75 – 4.9	Tsuneda et al., 2006
N/A [v]	CSTR	50	70		—	—	1.0 – 1.9	>4.0	—	0.6 – 1.2	
		—	100		1.0 – 1.2	—	0.83 – 1.2	—	—	28.8	
		—	200		—	—	0.16 – 0.32	—	—	4.5 – 9.0	
N/A [v]	MBR	10	18 [xxi]	Activated sludge	3 – 6	—	—	—	—	—	Zhao et al., 2014
CANON process; widened top section of the reactor slowed liquid upflow velocity, allowing solids to settle	Bubble column	190 [xxii]	43	AMX sludge	1.9 [xxiii]	—	0.007	0.5 – 0.8	35	53 – 98	Varas et al., 2015
N/A [v]	Upflow biofilm reactor	128	242	AMX granules & flocs	2.0 – 5.0	—	52.4 – 104.8	0.6 – 0.8	25	16 – 32	Li et al., 2016f
CANON process	Upflow reactor	—	136	AMX granules / 2.4	—	—	0.10 – 0.95	—	—	6	Carvajal-Arroyo et al., 2014

CANON process	Bubble column	—	120	CANON granules	—	—	2.80	1	35	4	Gonzalez-Martinez et al., 2017
CANON process	Aerated upflow sludge bed reactor	—	—	AOB & AMX sludge	0.8 – 1.0	—	0.19 – 0.58	0.7 – 0.8	30	9.36	Zhang et al., 2010
CANON process	Bubble column	—	260	CANON sludge	—	—	0.6 – 2.8	1	15 – 30	4.0	Gonzalez-Martinez et al., 2016
CANON process	Upflow reactor	—	120 [xxiv]	CANON granules	1 – 2	—	1.49	1.0	35	4	Rodriguez-Sanchez et al., 2017
Total solids retained by membrane with internal liquid circulation [I]	Baffled MBR	37	73	Activated sludge	0.228	110	0.2 – 0.32	—	25 – 31	5	Chen et al., 2017

[I] Lack of or insufficient means for selection pressure
[II] Granules collapsed after this point due to a decrease in DO
[III] Granule stability compromised by filamentous bulking after this point
[IV] Data only from stage II of the experiment, where intermittent seeding from an SBR occurred
[V] It is not clear whether a means for selection pressure is present or not
[VI] Granules formed from mixed aerobic/anaerobic sludge were stable for the remaining 38 days of the experiment; granules fromed from exclusively aerobic granules were stable for only 23 days before disintegrated due to ineffective DO diffusion
[VII] Granules disintegrated due to excessively high pyridine loading
[VIII] Pyridine loading rate
[IX] Two periods of stability, interrupted by a period of instability at elevated COD influent concentration
[X] Based on combined HRT from both aerobic and anaerobic tanks
[XI] Corresponding only to the aerobic tank in the system
[XII] Steady decrease in stability until influent flow was changed from continuous to intermittent in the following phase
[XIII] Extent of granulation became steady at 40% when influent was switched to intermittent feeding; but, granulation did not improve without selection pressure
[XIV] Feast/famine values during phase II (intermittent influent, continuous effluent) of the experiment
[XV] Granules became unstable when OLR increased to 18 g COD L^{-1} d^{-1}
[XVI] The reactor was operated at OLR as high as 39 g L^{-1} d^{-1}, but performance was not stable at this higher loading

[xvii] Biofilm was grown around activated carbon carriers, then the carriers were removed, leaving seeded granules
[xviii] Two reactors used, the first seeded with granules directly. The other operated as an SBR until granules formed, then switched to continuous flow
[ixx] increased HRT, which decreased the OLR, resulted in growth of filamentous bacteria and granule collapse
[xx] At HRT = 2.4 hours, ammonium removal decreased and granules began to washout of the reactor; this is not considered stable performance
[xxi] Reactor influent included antibiotics. Granules became unstable after organic load was decreased.
[xxii] Startup period with unstable nitrogen removal performance due to lack of DO control
[xxiii] Size at DO = 0.2 mg L^{-1}, at which point the system exhibited the best performance
[xxiv] Antibiotics were added to the feed after first 60 days. Although the granules remained, they underwent significant morphological changes. Nitrogen removal efficiency also suffered.

Zhou et al., 2014 investigated the formation mechanism of granules in an ALR by fluorescently labeling the flocculent biomass. They observed that granulation is a dynamic process in which biomass is continuously aggregating and disaggregating from the granules due to hydraulic shear forces. Detached portions of the granules serve as nucleation sites for the formation of new granules. This is consistent with the view of others in this field of study, who generally accept that shear is limited to shaping the granule morphology (Liu et al., 2005). However, this along with several other studies from the same research team also concluded that shear force is the driving force for aerobic granulation (Chen et al., 2017; Chen et al., 2015b; Zhou et al., 2013a; Zhou et al., 2013b; Zhou et al., 2013c; Zhou et al., 2014), rather than settling velocity-based selection pressure. It should be noted, nonetheless, that strong shear force is often present in aerated reactors, and the occurrence of granular sludge has been rarely observed in the long history of conventional treatment systems (Martin et al., 2016). It is possible that these studies credited shear force with more of a role than necessary since the contribution of selection pressure induced by the three-phase separator of the ALR used in those experiments was not mentioned. The studies by Chen et al., 2017 and Chen et al., 2015b described biomass collision, entanglement, and then biological aggregate formation. Although they ascribed shear force as a primary role in granulation, neither of these experiments actually produced CAGs (Section 2.6.1). As in SBRs (Section 2.3.3), shear force in CFRs may influence the microbial structure of aerobic granules. For instance, Gao et al., 2012 concluded that fast-growing aerobes would grow over AMX under low, but not high, shear. This is likely because the aerobic bacteria were stripped off the surface at least as fast as it could grow, preventing the formation of a stratified structure.

2.6.5 Bioaugmentation

Bioaugmentation is an effective means of speeding up aerobic granule formation or improving granule stability in CFRs. Several forms of bioaugmentation have been implemented in the literature.

a) *Seed SBR granules*. An effective way to rapidly start up a CFR granulation process is by seeding granules already cultivated in an SBR (**Table 1**). Seeded granules may be cultivated under special conditions that favor stability in CFRs, as done by Chen et al., 2016. In this study, granules were formed under low NH_3-N conditions (C/N = 153.8) to form protein-rich EPSs (PN/PS > 20) which were maintained under continuous flow for 216 days. The protein in EPSs was believed to improve the hydrophobicity of biomass, which enhances granule stability (Xin et al., 2017; Zhou et al., 2013c). Granules are usually seeded only once at the beginning of the experiment, however, Sajjad et al., 2016 used a novel inoculation technique, i.e. after developing granules in an SBR operated in parallel with a continuous MBR, granules from the SBR were continuously seeded into the MBR. Rather than a single inoculation at the beginning of the experiment (as is done by most researchers), sludge continued to be intermittently transferred between the reactors to maintain granule uniformity (**Figure 11d**). The granules were reported to be stabilized

around 0.625 mm in diameter in each reactor. A problem encountered with seeding pre-formed granules is that they will often partially disintegrate prior to adapting to the conditions of CFRs (Corsino et al., 2016; Li et al., 2016e; Liu et al., 2012). A special type of aerobic granules such as ASAGs, in which AMX is present in the core, is often seeded into CFRs performing ammonia or total nitrogen removal (Poot et al., 2016).

b) *Seed biofilms*. By inoculating biofilms from a biofilter backwash unit, Yang et al., 2014 achieved the growth of nitrifying granules in CFRs within 25 days, followed by 50 days of stable operation. The comparable characteristics of granular sludge and biofilms, e.g. high density, layered structure, and EPS-supported structure, likely allowed more rapid granulation and improved stability. Wang and Peng, 2008 also inoculated biofilms and achieved granulation in three days. This system was unique in that both biofilm-covered carriers and granules co-existed.
c) *Seed special bacteria*. Bacteria with special characteristics may be inoculated into CFRs to improve aerobic granule development. An example is the inoculation of bacterial TN-14, a denitrifier which promotes production of EPSs with high protein content (Xin et al., 2017). This bacteria was inoculated into CFRs using the configuration of **Figure 11a** and achieved successful granulation within 40 days, remaining stable for the additional 32 days afterwards. Likewise, Wan et al., 2013 incorporated *Pseudoxanthomonas Mexicana* into granules cultivated in an SBR to improve stability in a CFR, but no discussion of the mechanism is given. It was also reported that the presence of anaerobes in the inoculum favors the formation of granules that are able to withstand low DO conditions (Chen et al., 2009).
d) *Temporary inorganic carriers.* As previously discussed, biomass grown on spherical carriers are a form of biofilms rather than granules, for purposes of this review. However, Bartroli et al., 2010 used activated carbon as abiotic cores to accelerate aerobic granulation and then used an unspecified technique to remove activated carbon from CFRs. The end product of this process, not having an inorganic carrier, is by definition granular sludge. This technique may be especially helpful for nitrifying granules since nitrifiers are difficult to aggregate without nucleating surfaces (Jin et al., 2008a).

2.6.6 Temperature effect

The formation and stability of aerobic granules in CFRs was found not reliant on the environmental temperature, e.g. the climate, the influence of which relates more to granule performance. Temperature used for aerobic granulation studies in CFRs spanned a broad range (**Table 1**), but the majority were carried out at a constant temperature between 20 to 30 °C. Lee and Chen, 2015 decreased the operating temperature from 28 to 10 °C and noted that COD removal efficiency decreased by at least 18% in three sets of CFR aerobic granules. Likewise, Wan et al., 2014b found that ammonia removal efficiency diminished with a stepwise decrease in temperature from 25 to 15 and then to 6 °C. Reino et al., 2016 successfully cultivated and maintained aerobic granules in a CFR at only 10 °C. It was found that granule stability appeared to be enhanced by psychrotolerant bacteria which produces cryoprotective EPSs to survive in cold temperatures, however, microbial

diversity diminished. A similar decrease in diversity was noted in granules cultivated at 6 °C (Wan et al., 2014b). The effect of temperature on the microbial community was also observed by Gonzalez-Martinez et al., 2016, who noted a shift in the AOB and AMX species, i.e. *Nitrosomonas* to *Prosthecobacter* and *Candidatus Brocadia* to *Candidatus Anammoxoglobus*, respectively, as temperature was gradually reduced from 35 to 15 °C.

2.6.7 Dissolved oxygen effect

DO concentration does not seem to have a determinative role in the formation or stability of granules. Aerobic granulation has been achieved in CFRs operated at DO concentrations ranging from 0.1 to 8 mg L^{-1} (**Table 1**). Although Yang et al., 2014 reported that granules lost stability at DO less than 3 mg L^{-1}, low DO is an important parameter for achieving successful partial nitritation. Low DO, for example, allows for selection of AOB over NOB due to their differences in DO affinity (Van Hulle et al., 2010). Reino et al., 2016 operated a successful aerobic granulation CFR in the range of 0.5 to 2.5 mg DO L^{-1}. In this study, the low DO appears to have been used to maintain a low DO/TAN (total ammonia nitrogen) ratio for partial nitritation, a strategy also employed by Bartroli et al., 2010. Varas et al., 2015 recommends control of DO, as opposed to volumetric flow, to suppress NOB growth in granular sludge CFRs.

2.6.8 Solids and hydraulic retention time

Solids retention time (SRT) and hydraulic retention time (HRT) are important parameters as the former controls the amount of biomass that can be retained in a bioreactor and the latter represents the treatment rate. **Table 1** provides the SRT and HRT used by CFRs in literature. SRT is not usually monitored or controlled during aerobic granulation experiments. Only 11 out of the 57 examined CFR papers reported SRT values. Since some CFRs incorporate membranes, they are able to fully retain biomass, and SRT is controlled by manually wasting the sludge (Ramos et al., 2016; Wang et al., 2008). SRT in other CFRs appears not to be controlled directly, but is related to the HRT (Qian et al., 2017). As can be seen in the case of study by Poot et al., 2016, aerobic granules with diameter ranging from 0.9 to 1.4 mm remained stable under SRT between a wide range of 72 to 210 days, which suggests that SRT is not an essential factor in successful aerobic granulation in CFRs. This is consistent with studies using SBRs (Li et al., 2016b) (Section 2.3.7). However, a long SRT may play a detrimental effect on granule stability. The system in the study by Li et al., 2016b, when operated at an SRT of 30 days and influent COD concentration of 300 mg L^{-1}, developed filamentous bacteria.

When a CFR comprises an internal settling zone, HRT is directly related to the application of settling velocity-based selection pressure. Biomass will only settle if its settling velocity exceeds the upflow velocity of the outgoing water. That upflow velocity is proportional to the HRT at a given settling zone cross-sectional area, per Eq. (2),

$$upflow\ velocity = \frac{Volume}{Cross\ sectional\ area \times\ HRT} \quad (2)$$

For example, optimizing the upflow velocity allowed formation of nitrifying granules in a CFR after 65 days (Kishida et al., 2010), a significantly shorter time than the 300 days required under non-optimal operation in a similar reactor (Tsuneda et al., 2003).

The HRT of the CFR must then be chosen such that it is short enough for the washing out of flocculent biomass (Corsino et al., 2016; Xin et al., 2017). However, too short an HRT has been reported to wash out granules, causing system instability (Wan et al., 2014d). HRT may also influence the granule properties, probably due to the OLR change with HRT. Reducing HRT from 2.0 to 0.9 hours, for instance, increased aerobic granule compactness and size from 0.9 to 1.2 mm (Qian et al., 2017). The same trend was observed by Jin et al., 2008b.

2.6.9 Organic loading rate

OLRs used in aerobic granulation CFRs spanned a broad range across the literature (**Table 1**), mostly in the range of 0.3 to 7 g COD L^{-1} d^{-1}. Zhou et al., 2013c tested the effect of OLRs on aerobic granulation in CFRs. They successfully cultivated aerobic granules from flocculent sludge under OLRs of 3.5 and 4.8 g COD L^{-1} d^{-1}, although excessive growth of filamentous bacteria occurred after 35 days of operation in both reactors. The growth of filaments was blamed on the diffusion limitations due to low substrate availability. This is consistent with the study of Wang and Peng, 2008 in which filamentous growth ruined the settleability of the sludge after a decrease in OLRs. Stable aerobic granules have been maintained at much higher OLRs, e.g. 31.3 g COD L^{-1} d^{-1}, with good COD removal performance (Chen et al., 2016). However, care must be taken not to select an excessively high loading rate as it will promote the growth of granules with mass diffusion limitation, resulting in cores comprising dead cells. This was the case in the CFR operated by Long et al., 2015b at an OLR of 18 g COD L^{-1} d^{-1}. OLRs will impact the biodiversity of granular CFRs, although the nature of the effect has been inconsistently reported. On the one hand, decreasing the OLR has been found to cause a decline in the microbial diversity of the system (Wan et al., 2013; Wan et al., 2014b). However, Li et al., 2016d noted that an increase in OLRs from 0.8 to 1.6 g COD L^{-1} d^{-1} decreased the biodiversity of phosphorous removal granules. High OLRs were also found to induce the production of EPSs (Zhou et al., 2013c), however, Li et al., 2016d noted that increasing the OLRs from 1.2 to 1.6 g COD L^{-1} d^{-1} destabilized their phosphorous removal system by diminishing the polysaccharide content of EPSs from 35 to 20 mg g^{-1} VSS. Thus, OLRs do not directly impact aerobic granule formation; rather it has more bearing on biodiversity and EPS production, which further impact the aerobic granule structural stability.

2.6.10 Time-span reported for aerobic granule formation and stabilization in CFRs

Differences in time required for granule formation are expected to vary due to differences in operating conditions between experiments, as well as in criteria for determining exactly when granulation has occurred. The time it took for aerobic granules to form in CFRs generally ranged from one week to one month (**Table 1**). The nitrifying granules cultivated by Tsuneda et al., 2003 deviated from this trend, requiring 100 days. Three studies have been carried out with CFRs and SBRs running in parallel to compare the time required for granule formation in each (Li et al., 2015; Li et al., 2014; Liu et al., 2014). Li et al., 2014 observed granules within 4 days in a SBR and 13 days in a continuous flow, modified oxidation ditch. The same research team achieved granulation within 21 and 7 days, respectively, in a SBR and a RFBR in a separate study (Li et al., 2015). It should be noted that different settling time and OLRs were applied in the CFR and SBR used in either study, so the results might not be directly comparable. In another study, identical column reactors were operated in SBR and CFR modes, in which the SBR was utilizing settling velocity in Eq. (1) as a selection pressure, and the CFR was equipped with a sieve for particle size-based selection (**Figure 14b**). It was reported that each reactor has cultivated aerobic granules within 7 days (Liu et al., 2014).

Numerous operational strategies have been reported successful in maintaining stable operation of aerobic granulation CFRs for over 100 days (**Table 1**). It is difficult to evaluate the long-term stability of these CFR aerobic granules under each strategy, especially since many experiments were ended abruptly (see **Table 1** and footnotes). CFRs with granules performing ammonia oxidation, however, appeared to run for longer periods of time, e.g. 223 days a in study by Poot et al., 2016. This suggests, as will be addressed later, that such nitrifying granules are especially stable under continuous flow operation.

2.6.11 Precipitation of inorganic compounds

Precipitation of metals is known to improve aerobic granule stability and settleability in SBRs (Gao et al., 2011). The same appears to be true for CFRs. Multiple studies have also shown that Mg, Ca, and Fe precipitates also improve the properties of granules in CFRs (Juang et al., 2010; Lee and Chen, 2015; Liu et al., 2015). More specifically, Juang et al., 2010 observed that an internal denitrification process increased the alkalinity of the granule core, which favored precipitation in the presence of high concentrations of phosphate. In comparison, granules cultivated under a lower phosphate feed (0.1 g K_2HPO_4 L^{-1} and 1.35 g KH_2PO_4 L^{-1}) collapsed after 3 days operation, while those grown at higher phosphate levels (1.65 g K_2HPO_4 L^{-1} and 1.35 g L^{-1} KH_2PO_4 L^{-1}) remained stable for 216 days (Juang et al., 2010). Chemical precipitation by dipping pre-formed granules in supersaturated solution was also used as another strategy (Lee and Chen, 2015). Mg compounds were concentrated above their solubility limit and readily precipitated within the granules (Lee and Chen, 2015).

Liu et al., 2015 raised a concern that inorganic precipitation in continuous flow, aerobic granulation will decrease sludge bioactivity. In their study, as a SBR was allowed to reach steady state prior to switching to CFR mode, it was demonstrated that, although biomass in CFR mode improved settleability, the biological activity kept decreasing. The results also showed that, as compared to the batch operation, continuous mode left granules susceptible to excessive precipitation. This inorganic precipitation replaced the biomass with ash content increasing from 25 to 84% (Liu et al., 2015). Granules are known to have lower specific substrate utilization rate than bioflocs for their smaller specific surface area (Liu et al., 2015). Consequently, the lower concentration of substrate in CFRs allows bioflocs to outcompete granules for faster substrate utilization. Granular sludge was reported to respond by consuming the polysaccharide content of its own EPSs, which exposed protein surfaces to act as nucleation sites for precipitation (Liu et al., 2015). The variation in organic content of aerobic granules in CFRs was also studied by Juang et al., 2010. Based on their reported values of TSS and VSS, the ash content for seeded SBR granules was 21%. This value increased to 55% after 90 days, but declined to 23% by 210 days of operation in the CFR. Obviously, the ash content never reached the extreme values reported above by Liu et al., 2015. Juang et al., 2010 did not discuss what caused the extreme fluctuation of the granule organic content from intermediate to stable stages of granule cultivation. No changes in operating conditions were mentioned, so the variation may be due to a lengthy acclimation period. Liu et al., 2015 only operated their CFR for approximately 40 days, so their poor biomass activity may possibly be the result of not reaching steady state. Another possibility is the difference in the F/M ratio, 0.007 (Liu et al., 2015) and 0.2 (Juang et al., 2010). As Liu et al., 2015 theorized that the granular biomass was consuming the polysaccharide component of EPSs, the higher level of F/M in the experiment by Juang et al., 2010 was likely sufficient to avoid the need for biomass to consume EPSs. In another experiment, Wan et al., 2014a operated their reactors with similar influent concentration of COD, phosphate, and calcium, and observed comparable specific oxygen uptake rates (SOURs) of granules formed in a SBR and a CFR operated in parallel (**Figure 16**). This observation suggests that excessive inorganic precipitation, such that biological activity is significantly lowered, is not necessarily an intrinsic problem of aerobic granulation in CFRs.

Xin et al., 2017 proposed that inorganic precipitation facilitates the granulation process in CFRs. They added 40 mg Ca^{2+} L^{-1} to their influent, crediting successful granulation of the sludge, in part, to calcium phosphate nucleation for the attachment of bacterial cells. On the other hand, Zhou et al., 2013b examined the mechanisms of granulation directly from bioflocs in two CFRs with different calcium concentrations. Aerobic granules formed in both reactors within 10 days, although the granules with high calcium content grew to a larger size. Thus, it is logical to conclude that calcium precipitation is not required for granulation.

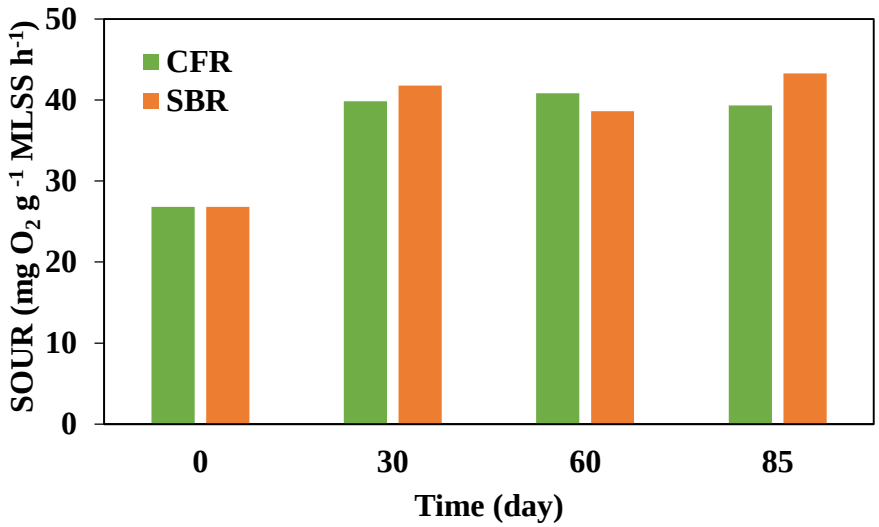

Figure 16. SOURs in SBRs and CFRs over an 85-day cultivation period (Wan et al., 2014a)

2.7 Characteristics of aerobic granules formed in CFRs

In general, aerobic granular sludge was found to possess similar properties whether they are developed in CFRs and SBRs. It seems that substrate properties and operating conditions, rather than the mode of fluid flow, are the primary parameters that determine granule characteristics.

2.7.1 Granule size

Average aerobic granule diameter in CFRs varies from 0.14 to 6.10 mm as summarized in **Table 1**, although in more than 60% of the studies it did not exceed an average of 2 mm. Studies comparing size of granules formed in CFRs and SBRs reported comparable sizes, although batch mode generally favored the formation of larger granules (**Table 2**) (Bumbac et al., 2015; Li et al., 2015; Li et al., 2014). Sajjad et al., 2016 operated an SBR and a continuous flow membrane reactor equipped with a settling tank, with the same influent conditions. The smaller granule size in CFRs was explained as a result of the low substrate concentration and the resulting poor penetration into the granule. This also resulted in granules with a relatively looser structure (Bumbac et al., 2015; Li et al., 2016e; Liu et al., 2012). The other major factor influencing granule size is shear force which works to strip off the outer layers of biomass. It was claimed that continuous aeration of CFRs, as opposed to the intermittent aeration of SBRs, induced a greater number of aggregate collisions to further limit the size of granules (Sajjad et al., 2016). After 100 days of operation, granules in the SBR reached 0.8 mm, while aggregates in the membrane reactor with settling velocity-based selection pressure only achieved 0.2 mm under the same loading rate. The smaller size granules formed in the MBR was attributed, at least in part, to shear from collisions. In the final stage of their experiment, granules were periodically transferred from the SBR to the CFR,

and size in both reactors stabilized around 0.6 mm. The exception to this trend was reported in the study by Chen et al., 2016, where granules had diameters of 4.5 to 4.7 mm in an SBR but 4.8 to 6.1 mm in a CFR. It is not clear why granules in the CFR achieved such a larger size in the study.

Table 2. Comparison of size and settling properties between SBR and CFR granules

Reactor	SVI (mL g^{-1})	Settling Velocity (m h^{-1})	Diameter (mm)	Settling time (min)	Granule formation time (days)	Reference
Continuous modified oxidation Ditch	46	23.3	0.28	60	13	Li et al., 2014
SBR	35	27.9	0.31	20	4	
Reverse flow baffled reactor	43	—	0.13	30	21	Li et al., 2015
SBR	32	—	0.22	15	7	
Continuous bubble column with sieve*	35	30.68	1.0 – 3.0	0	7	Liu et al., 2014
SBR	30	35.03	1.0 – 2.0	5	7	

*implemented size-based, rather than settling velocity-based, selection pressure

As can be seen in **Table 1**, several CFRs were seeded with granules cultivated in SBRs. It has been commonly observed that granules will disintegrate when initially seeded into CFRs due to their adaption to the new environment, poor diffusion properties, and the associated substrate deficiency (Corsino et al., 2016; Liu et al., 2012). The disintegrated biomass must then adjust to continuous flow conditions, possibly regaining some of its former size (Li et al., 2016c; Li et al., 2016e).

2.7.2 Granule density

Example densities for aerobic granules developed in CFRs are 1052 to 1059 kg m^{-3} (Li et al., 2016c) and 1010 – 1070 kg m^{-3} (Jin et al., 2008b), which is slightly greater than that of the water. Li et al., 2016c observed that the density of phosphorous-removal granules cultivated from a SBR dropped significantly in large granules (diameter > 0.6 mm) during acclimation to the CFR, but final values were approximately the same as the seeded granules. Generally, changes in density correlate with changes in granule stability in that denser granules usually come with greater structural strength (Corsino et al., 2016).

2.7.3 Granule strength

Granule strength was found comparable for aerobic granules cultivated in SBRs and CFRs. Multiple studies reported that granules had higher strength, as determined by ultrasound methods, after being cultivated under continuous flow conditions than when they were seeded from SBRs (Lee and Chen, 2015; Wan et al., 2013; Wan et al., 2014b; Wan et al., 2014c). Wan et al., 2014a seeded granules previously stored under saline conditions into a SBR and a CFR, respectively, for comparison. With ultrasonic treatment, seed granules, CFR granules, and SBR granules disintegrated in 15, 25, and 20 minutes, respectively, implying CFR granules possess greatest physical strength. Li et al., 2016c observed comparable strengths of phosphorous-removal granules under batch and continuous modes within different phases of an experiment.

2.7.4 Extent of granulation

The extent of granulation is taken to mean the fraction of total biomass that exists in granular form. This property is shown to be dependent on the effectiveness of the settling- or size-based selection pressure, i.e. a more effective means of removing small or poorly settling biomass will improve the relative amount of granular biomass. Granules seeded into a CFR by Corsino et al., 2016 slowly diminished in size over a 42-day period, resulting in an extent of granulation of approximately 40%. Without provision of a settling velocity-based selection pressure, this value was not improved when the remaining granules were stabilized by switching to an intermittent feeding mode to create feast/famine conditions (**Figure 9**). Zhou et al., 2013c reported values of 58.6% to 71.9% for extent of granulation in continuous flow ALRs. However, a much higher level of granulation, e.g. 90 %, was obtained in CFRs by Liu et al., 2012. Although they described the first reactor in their system as an SBR, it was actually hydraulically connected to a settling tank and thus functioned as a continuous ALR (**Figure 14a**). Extent of granulation in this ALR reached 90%, although it decreased to 40 to 70% in the downstream MBR. A particle size-based selection pressure was applied to the MBR with partial discharge to the sieve only once per day. This intermittently applied selection pressure, along with a continuous influx of flocculent sludge from the ALR, is likely what led to a poor and variable extent of granulation. Size-based selection pressure cannot itself be blamed since Liu et al., 2014 observed approximately equal extent of granulation (e.g. 80%) between a SBR with settling velocity selection pressure and a CFR with granule size selection.

Flocs will always be present in granular sludge systems since they are less resistant to mass diffusion and, therefore, more competitive for substrate utilization (Liu et al., 2015). Since CFRs are not as efficient in applying settling velocity-based selection pressure as SBRs, the mixture of granules and flocs will inherently be more pronounced. In this way, granular CFRs are similar to integrated fixed-film activated sludge (IFAS) systems (Ekama, 2015). Such systems combine granular and flocculent sludge, lowering the sludge age and increasing the treatment capacity. The coexistence of flocs and granules also allows for the division of treatment objectives. This principle

is similar to that used in some autotrophic nitrogen removal systems where most AOB exists in a flocculent state and AMX accumulates within granules (Shi et al., 2016). Complete granulation of biomass, in fact, would harm performance, since such systems may be unable to fully remove particulate matters due to the lack of enmeshment and bioflocculation capacities and thus require post-treatment (de Bruin et al., 2004; Van Winckel et al., 2016). In theory, there exists an optimal extent of granulation value for best performance of a given CFR, however, this value is yet to be determined.

2.7.5 SOUR

The SOUR of aerobic granules in CFRs has not been well documented, but there seems to be a trade-off between high SOUR and granule stability. Liu et al., 2015 noted that the SOUR of granules decreased from 61 to 23 (mg O_2 g^{-1} MLSS h^{-1}) after switching from batch to continuous flow. This decline was attributed to the excessive precipitation of $CaCO_3$. Such extreme precipitation, however, is not inherent to aerobic granules under continuous flow (Section 2.6.11). For instance, Wan et al., 2014a compared SOURs of granules stabilized in CFRs and SBRs inoculated with granules previously formed in SBRs and stored under saline conditions. SOUR was monitored for 85 days and plotted in **Figure 16**, showing significant similarity between granules from the two modes of reactor operation.

2.7.6 Settling velocity

The settling velocity of granules in a SBR (27.9 m h^{-1}) was found slightly greater than that (23.3 m h^{-1}) of granules in a continuous flow, modified oxidation ditch (**Table 2**) (Li et al., 2014). Li et al., 2016c swapped granules from batch to continuous flow conditions and noted an initial drop in settling velocities. The velocity, however, recovered close to its original value when a steady state was reached. In contrast, when CFRs are operated using a sized-based selection strategy, rather than settling velocity-based, granules develop poorer settling properties (Liu et al., 2014). This must be an inherent limitation to size-based selection since large biomass having low settling velocity cannot be washed out of the reactor (Liu et al., 2012).

2.7.7 SVI

Literature SVI_{30} values for CAGs formed or developed in CFRs range from 23 mL g^{-1} (Li et al., 2016e) to approximately 60 mL g^{-1} (Xin et al., 2017). This is consistent with the study by Martin et al., 2016, who suggested an upper limit SVI of 60 mL g^{-1} for granular sludge. FAGs grown by Chen et al., 2015b, comprising poorly settling filaments, had a higher SVI of about 100 mL g^{-1}. Granules cultivated in the study by Liu et al., 2015 showed an SVI of 2 mL g^{-1}, but this was due to excessive precipitation and loss of biological activity in the granules. Studies that side-by-side compared performance of granules in CFRs and SBRs showed that SVI was comparable between the two (**Table 2**), being slightly larger for that of CFRs.

One proposed characteristic of granular sludge, by which the successful achievement of granulation may be confirmed, is that SVI_5 should approximately equal SVI_{30} (Schwarzenbeck et al., 2004b). The CFR studies examined in this review suggest that this is not always a reliable criterion by which successful granulation can be judged. Sajjad et al., 2016, for example, observed that SVI_5 and SVI_{30} were approximately equal both before and after successful granulation had been achieved in the CFR. Moreover, Yang et al., 2014 cultivated aerobic granules within 25 days, as confirmed by a regular, dense structure (**Figure 10f)**, although the difference between SVI_5 and SVI_{30} did not approach equality until after day 40.

2.7.8 EPSs

Li et al., 2015 compared granules from a SBR and a continuous RFBR in **Figure 8b,c**. The seed sludge had 304.0 mg EPSs g^{-1}, which increased to 473.4 mg g^{-1} in the SBR and 587.2 mg g^{-1} in the RFBR. Corsino et al., 2016 operated a reactor in the continuous flow mode with effluent being constantly withdrawn. However, the feeding scheme comprised two stages, the first with continuous flow and the second intermittent. With continuous influent flow, EPSs of seeded granules decreased from 500 to 200 mg g^{-1} VSS. However, intermittent feeding, which created feast-famine conditions, allowed for an increase in EPSs to greater than 400 mg g^{-1} VSS and in PN/PS ratio from approximately 2.5 to 4. The contribution of EPSs to aggregation of biomass was considered essential to the proposed granulation mechanism (Chen et al., 2009). Yang et al., 2014 achieved a uniform distribution of EPSs within granules cultivated in a continuous flow ALR. Zhou et al., 2013a also operated a continuous flow ALR to determine the EPS distribution within granules formed under continuous flow. This paper noted that both β-polysaccharides and proteins were distributed uniformly throughout the granules, as well.

PN/PS is a significant variable concerning granule stability. Although the importance of PN/PS is recognized, studies have been inconsistent as to the nature of the effect (Xin et al., 2017). Protein in particular is known to improve the hydrophobicity of biomass (Xin et al., 2017; Zhou et al., 2013c), granules having higher PN/PS ratio being more hydrophobic (Chen et al., 2009). Indeed, large values of PN/PS, e.g. 11 (Li et al., 2015), have been credited to forming stable aerobic granule sludge. On the other hand, Li et al., 2016d observed the importance of PS, which contributes to the adhesion of microbes to each other. In their experiment, granules were stable at a PN/PS of approximately 0.5, and a decrease in PS led to a loss in stability. These values mark the extremes of a wide range of EPSs reported during successful CFR experiments. It appears that the value of PN/PS is not a major factor in determining aerobic granule stability. Further research should be dedicated to evaluating the true effect.

2.7.9 CFR granule morphology

Settling velocity-based selection pressure has a significant impact on the morphology of sludge as it aggregates in CFRs. When appropriate selection mechanisms are employed, granular sludge grows in CFRs from activated sludge (**Figure 10a**) into loose aggregates (**Figure 10b**), which with time develop into round, compact granules (**Figure 10c**) (Xin et al., 2017). The same sequence and results were observed for fluffy biofilm inoculum (**Figure 10d-f**) (Yang et al., 2014). Such round granules (Juang et al., 2010; Yang et al., 2014; Zhou et al., 2013c) with compact structure (Liu et al., 2014; Wan et al., 2014c; Xin et al., 2017; Yang et al., 2014; Zhou et al., 2013a; Zhou et al., 2014) are common in CFRs and similar to those formed in SBRs (Chen et al., 2015a; Rosman et al., 2014). Chen et al., 2015b inoculated sludge (**Figure 10j**) into a CFR connected to a clarifier with a 2-hour settling time. This settling time was much longer than that reported for efficient selection in literature and the aggregates that formed were excessively loose, appearing somewhat translucent (**Figure 10k**). These aggregates showed an appearance and properties (e.g. SVI of 50 to 90 mL g^{-1}) similar to large flocs rather than granular sludge, demonstrating the necessity of using stronger settling velocity-based selection pressure.

Some researchers who used pre-formed granular sludge as inoculum reported a different final morphology. The seeded granules (**Figure 10g**) in the experiment of Li et al., 2016c likewise partially disintegrated (**Figure 10h**) and developed irregular, loose morphologies (**Figure 10i**). Both papers noted that the change in structure was due to diffusion limitations of DO or substrate in large granule under the continuous flow mode.

There is limited observation or discussion of the stratification of aerobic granule structure formed in CFRs. Surface layers of filamentous bacteria were reported (Jin et al., 2008b), and granules cores are sometimes distinguished from the outer layers, e.g. in terms of density (Qian et al., 2017; Zhou et al., 2013a). The formation of stratified layers is at least partially due to the differences in the growth rate of different types of bacteria. Shear is also relevant as excessively strong forces will prevent the faster-growing organisms from dominating at the granule surface (Gao et al., 2012). A well-known advantage of stratification is the development of functional layers with different oxidation state environments. Going outward from the granule center, anaerobic, anoxic, and aerobic layers can co-exist in the same granule to support the simultaneous activity of microbes requiring different, even conflicting, metabolic conditions (Chen et al., 2009).

Interestingly, a compact, dense core has been linked to granule stability in CFRs (Wan et al., 2014b; Zhou et al., 2013a). Although the development of an anaerobic core may destabilize aerobic granules (Yang et al., 2014), there are some cases where it may strengthen the granule stability. For example, denitrifiers have been shown to precipitate inorganic materials, improving stability. Chen et al., 2009 compared the operation of granules developed from aerobic, anaerobic, and mixed sludge in low DO conditions. The aerobic granules showed the least stability and collapsed when diffusion limitation killed biomass in the core. Granules formed from inoculum with both aerobic and anaerobic sludge, on the other hand, had anaerobic cores which improved granule

stability. This finding is opposite to the conclusions made by Lee et al., 2010 who believed that anaerobes should be suppressed. The stabilization observed by Chen et al., 2009 was likely due to the higher PN/PS ratio and hydrophobicity in those granules. It is also clear that anaerobic cores will not collapse in the absence of oxygen, as aerobic cores will. Besides biomass, inorganic materials, either carriers or precipitates, may be present in the granule cores. These inorganic carriers have been successfully used to promote the formation of granules, but the long-term stability in CFRs has not yet been determined. The role of inorganic precipitates in promoting stability is discussed in Section 2.6.11.

In the realm of aerobic wastewater treatment, stratification of biomass layers is especially relevant to nitrogen removal. For instance, Jin et al., 2008b reported a layered structure in aerobic granules which allowed for AMX to grow in CFRs. The stratification of AOB and NOB as another example, allows partial nitritation by means of DO and substrate gradients. This is the strategy successfully implemented by Poot et al., 2016 in a continuous flow ALR for suppression of NOB growth. By promoting the growth of AOB on the exterior of granules, sufficient DO is consumed to inhibit growth of NOB and, consequently, suppress nitrate production. However, such a layered structure is not inherent to continuous processes as Yang et al., 2014 developed CFR granular sludge in which AOB and NOB were uniformly distributed. Moreover, Tsuneda et al., 2003 observed nitrifying granules wherein both AOB and NOB grew on the granule surface, lacking a clear stratification of the two. Probably, such a layer formation can be attributed to the special cultivation strategies used in these studies.

Stratification can be especially essential in ASAGs since AMX requires anaerobic conditions for growth. In this case, AOB provides the two-fold function of creating an oxygen gradient in the granule and preventing AMX washout. The latter function is necessary due to the extremely slow growth rate of AMX. Interestingly, co-existence of AOB and AMX throughout ASAGs, without a stratified structure, was observed by Li et al., 2016f. This is likely due to the porous structure of the granules allowing diffusion of DO into the granule interior. It is not entirely clear, nor discussed in that paper, how AMX survived in a bulk DO of 0.8 mg O_2 L^{-1} without stratification.

2.7.10 Microbial community of aerobic granules in CFRs

The microbial community of aerobic granules depends on the reactor operational parameters and the nature of influent wastewater. Changes in HRT (Li et al., 2016a), substrate concentration (Li et al., 2016d; Wan et al., 2014b), and temperature (Reino et al., 2016; Wan et al., 2014b) all play a role in the speciation and diversity of granular sludge. This is consistent with the microbial community dependency on influent composition and operational parameters as have been comprehended in SBRs (Gao et al., 2011; Liu et al., 2005). While the mode of flow in a reactor will not largely affect the microbial makeup of aerobic granular sludge, it has been shown to alter the relative abundances of particular organisms. Li et al., 2015, after operating a continuous RFBR and SBR in parallel at similar OLRs, observed that the microbial species present in the granules of both reactors were generally the same. Differing intensities of bands from their denaturing

gradient gel electrophoresis analysis, however, indicated that certain species had high relative abundances in one reactor or the other. These differences were attributed to the different conditions inherent to continuous and batch flows. The same observations were noted in the comparison of a continuous flow, modified oxidation ditch reactor and a SBR, although the reactors were operated at different OLRs (Li et al., 2014). When Wan et al., 2014a reactivated stored granules in a CFR and a SBR, they gradually reduced the OLR in both reactors from 2500 to 200 mg COD L^{-1}. The microbial diversity decreased in both reactors over the first 30 days, but decreased more in the CFR probably due to the different washout characteristics of continuous flow. However, diversity also recovered more rapidly in the CFR in later operation. The species of biomass grows in an aerobic granule is largely dependent on the type of substrate provided in the wastewater. For examples, nitrifiers grow well in the presence of ammonia and phosphate reducers accumulate in the presence of phosphorous, as described in the following sections.

Literature suggests that aerobic granulation mechanism in CFRs is not dependent on a particular community, although the microbial makeup will affect stability. Aerobic granules containing nitrifying (Jin et al., 2008b), denitrifying (Xin et al., 2017), and phosphorus accumulating organisms (Li et al., 2016e) all achieved successful and stable aerobic granulation in CFRs. This implies that the source of the sludge is not essential to the ultimate formation of aerobic granules. On the other hand, granules comprised of nitrifiers are known to be particularly stable (Liu et al., 2004). Other examples of particular species that improve granule stability include flavobacteria, which induces EPSs production (Li et al., 2014; Zhou et al., 2014), and *Pseudoxanthomonas Mexicana* (Wan et al., 2013; Wan et al., 2014d), which was discussed in Section 2.6.5.

Although bacteria are the dominant organism in aerobic granular sludge, it should not be forgotten that small populations of fungi and archaea are also present (Liu et al., 2017a). These include ammonia oxidizing archaea that function well in low DO environments, making them suitable alternatives to AOB in nitritation-anammox processes (Liu et al., 2016).

Nitrification is carried out in a two-step process in which AOB first convert NH_4^+ to NO_2^-, followed by oxidation to NO_3^- by NOB. When grown in CFRs, AOB were found primarily to belong to *Nitrosomonas* (Qian et al., 2017; Ramos et al., 2016; Reino et al., 2016; Tsuneda et al., 2003; Wan et al., 2013; Wan et al., 2014b). However, this may change with adjustments of operating conditions, as dominance was found switched to *Prosthecobacter* when temperature and influent ammonium were gradually decreased from 35 °C and 470 mg N L^{-1} to 15 °C and 100 mg N L^{-1}, respectively (Gonzalez-Martinez et al., 2016). *Nitrospira* (Li et al., 2015; Qian et al., 2017; Hasebe et al., 2017) and *Nitrobacter* (Reino et al., 2016) were the most commonly detected NOB in CFRs, although often at low levels. Under proper conditions, AOB and NOB may form stratified layers around the granules core, as discussed in Section 2.7.9.

The recent discovery of comammox bacteria, which belong to the *Nitrospira* genus and completely oxidize ammonia to nitrate, has expanded our understanding of the microbial mechanisms of ammonia oxidation (van Kessel et al., 2015). Comammox compete at low substrate concentrations

and have been theorized to grow well inside biofilms, where diffusion limitation keeps ammonia levels low (Daims et al., 2015). This would be especially true for granular CFRs since a low substrate concentration is also maintained in the bulk water. Indeed, the presence of comammox was presented as a likely explanation for the uneven distribution of AOB and NOB in nitrifying granules cultivated in a CFR (Hasebe et al., 2017).

ASAGs are common in autotrophic nitrogen removal processes, such as CANON. Although granules comprising AMX cores are typically seeded into the CFR (Jin et al., 2008b; Varas et al., 2015; Zhang et al., 2010), nitrifying granules have been reported to develop AMX cores during continuous flow operations (Qian et al., 2017). Qian et al., 2017 credited this AMX growth to partial washout of AOB, combined with high nitrogen loading rate and EPS content. The exact speciation of AMX present in CFRs varied and included *Brocadia Anammoxidans* (Zhang et al., 2010) and *Candidatus Kuenenia* Qian et al., 2017. As has been shown to be the case with nitrifiers, the species of AMX also depends on operating parameters. Gonzalez-Martinez et al., 2016 noted a switch from *Candidatus Brocadia* to *Candidatus Anammoxoglobus* as temperature and influent NH_4^+ were lowered from 35 °C and 470 mg N L^{-1} to 15 °C and 100 mg N L^{-1}, respectively.

The microbial community of phosphate-accumulating organisms (PAOs) also depends on the operating conditions of the CFR. For example, Li et al., 2016d investigated the change in phosphorus removal granules as the influent COD was adjusted. While the feed remained at 200 or 300 mg COD L^{-1}, *Rhodocyclaceae* was the primary PAO. A step increase to 400 mg COD L^{-1} allowed the filamentous *Thiothrix spp.* to thrive, compromising granule stability and phosphorus removal efficiency. When COD was stepped back down to 200 mg L^{-1}, *Candidatus Accumlibater*, which competed more efficiently with filamentous bacteria, grew and restored proper phosphorus removal.

2.8 Application of CFR aerobic granulation for wastewater treatment

Aerobic granular sludge developed in CFRs have been shown to efficiently remove COD and phosphorus. High performance of ammonia oxidation is also possible, although the conditions in aerobic CFRs are generally not favorable for total nitrogen removal. The notable exception is ASAGs comprising AMX in their cores, which has been implemented in full-scale wastewater treatment. Aerobic CFRs may also be linked to anoxic reactors to allow for nitrogen removal. Overall, CFRs and SBRs have comparable pollutant removal capabilities (Bumbac et al., 2015).

2.8.1 COD removal

Many CFR aerobic granulation studies achieved COD removal efficiencies greater than or equal to 90% (Li et al., 2016e; Li et al., 2015; Li et al., 2014; Wan et al., 2013; Zhou et al., 2013c) although some could only achieve greater than 80% (Chen et al., 2017). Chen et al., 2016

monitored organics removal over OLRs ranging from 6 to 39 g L^{-1} d^{-1}. It was found that COD removal fluctuated around 84% until the OLR was increased from 6 – 12 to 18 g L^{-1} d^{-1}. With OLRs further increasing, COD removal efficiencies exceeded 90% until OLR reaching 34.3 g L^{-1} d^{-1} at which COD removal efficiency dropped to 37%. Wan et al., 2014a, reactivating aerobic granules stored under saline conditions, was able to maintain greater than 94% COD removal in both SBRs and CFRs for 85 days with a stepwise decline in influent COD from 2500 to 1000 and then to 200 mg L^{-1}. Lee and Chen, 2015 demonstrated that coating granules with precipitates help maintain stable performance, while a decrease in temperature will harm COD removal efficiency.

2.8.2 Nitrogen removal

Aerobic granulation CFRs have achieved NH_4^+-N removal through ammonia oxidation at efficiencies greater than 90% (Hou et al., 2017; Li et al., 2014; Wan et al., 2014b), even approaching 100% removal in some cases (Jin et al., 2008b; Li et al., 2015). The ammonia oxidation process is, in fact, essential to nitrifying granule formation. This was shown by Kishida et al., 2012 who observed the formation of such granules in a standard CFR performing ammonia oxidation, but not in an identical reactor fed with an ammonia oxidation inhibitor. However, ammonium and total nitrogen removal depends on the operating conditions, such as HRT (Qian et al., 2017), DO (Varas et al., 2015), temperature, and carbon source (Wan et al., 2014b). Slow-growing nitrifying bacteria is known to improve the strength of aerobic granules grown at low C/N ratios in SBRs (Liu et al., 2004). The same principle was found true in CFRs. In fact, AOB and NOB are particularly suited for continuous flow conditions since they are able to grow in low nutrient environments (Yang et al., 2014). A study by Kishida et al., 2010 suggests that feast/famine conditions are not as essential to granulation of nitrifiers, since SVI and granule appearance were very similar in parallel SBR and CFR systems.

It usually takes a long time, however, to cultivate nitrifying granules from nitrifying bioflocs in CFRs. Ali et al., 2016 was only able to obtain 15% nitrifying sludge with particle size greater than 0.2 after 199 days cultivation. Interestingly, Tsuneda et al., 2003 was able to cultivate granules from nitrifying bioflocs after 100 days. They tested the effect of aeration volume and determined an appropriate range, e.g. 0.071 to 0.20 L min^{-1} L^{-1} sludge bed, must be implemented in order to achieve granulation. The rate of granule formation may be accelerated by optimizing the influent upflow velocity, as discussed in Section 2.6.8. Using nitrifying biomass from biofilms (Yang et al., 2014) or seeding activated sludge followed by acclimating to nitrifying conditions (Jin et al., 2008b) are also promising strategies. Many authors simply inoculate their reactors with pre-formed granules (Poot et al., 2016; Qian et al., 2017; Wan et al., 2013; Wan et al., 2014b; Wan et al., 2014c).

Continuous flow is a convenient operation mode when desiring to achieve partial nitritation which was the objective of multiple papers. Poot et al., 2016 successfully suppressed nitrate production by intentionally maintaining an ammonium residual and stratified granular structure in CFR aerobic granules. Although the advantages of continuous flow were not discussed in the work, it

is clear that it was easy to maintain a constant residual concentration of ammonium in CFRs. Whereas, in a SBR, ammonium levels were bound to fluctuate with the cyclic feast/famine conditions. A common strategy for suppressing nitrate accumulation is DO/NH_4^+ ratio control (Bartroli et al., 2010; Isanta et al., 2015; Jemaat et al., 2015; Qian et al., 2017).

The small particle size of granules developed in CFRs impedes denitrification because it allows for penetration of DO deep into the granule, preventing the formation of an anoxic core in which denitrifiers can grow (Corsino et al., 2016; Liu et al., 2012). Denitrifier growth, however, has been reported and is important for biological precipitation of metals (by increasing the alkalinity of the environment) to improve CFR granule stability (Juang et al., 2010). In addition, Qian et al., 2017 reported growth of AMX in their aerobic granular reactors. They believe enhanced EPS production inhibited diffusion of oxygen to the granule core, providing the anaerobic environment necessary for AMX to grow. A dense core also allowed the development of an anoxic zone in the experiment by Wan et al., 2014b. Jin et al., 2008b also developed AMX in their continuous aerobic reactors. The mechanism was not discussed but is likely due to the larger size of the granules (47% granules had a diameter >1.5 mm after 75 days) allowing for an anoxic center zone to become established.

The presence of AMX in the core of some aerobic granules allows for the CANON process to proceed because partial nitritation and nitrogen removal may be performed in a single granular particle. After an outer layer of AOB performs partial nitritation, the AMX converts the produced nitrite and diffused ammonia into nitrogen gas (Gao et al., 2011; Zhang et al., 2008). Li et al., 2016f achieved successful nitritation-anammox in a granular upflow reactor operated at 25 °C and 70 mg N L^{-1}, showing the process is achievable for mainstream wastewaters at warm temperatures. When utilized in CFRs, the effect of operating or environmental conditions for nitrogen removal were usually the research focus rather than the granule stability because these studies were more interested in the performance of the conversion processes than the granules themselves (Gonzalez-Martinez et al., 2016; Varas et al., 2015).

2.8.3 Phosphorus removal

Enhanced phosphorus removal requires an anaerobic tank (known as a selector) prior to the aerobic zone (**Figure 12b)**. This selector gives PAO's an advantage over other heterotrophic organisms that cannot grow without an electron acceptor. In addition, such selectors improve the settleablility of the sludge as filamentous bacteria are suppressed (Metcalf and Eddy, 2014), which may contribute to the granulation process.

A significant amount of work has been conducted with regard to phosphorus removal by aerobic granules in CFRs (Li et al., 2016a; Li et al., 2016b; Li et al., 2016c; Li et al., 2016d; Li et al., 2016e). For example, some studies examined the stability of phosphorus-removal granules after being seeded from an SBR into a CFR. In this case, granules from a SBR that performed COD removal at 98% efficiency and phosphate removal at 99% efficiency were used (Li et al., 2016c). Although the respective efficiencies temporarily decreased to 79% and 64% upon inoculation, the

granules approached its original performance within 24 days. This behavior corresponded with a relapse and recovery in average granule size. The seeded granules shifted from a smooth, round appearance to a loose, irregular structure. After an acclimation period, granules were stabilized for the rest of a 55-day continuous operation (Li et al., 2016c). The phosphorus removal CFR in the study by Li et al., 2016d operated well at OLRs less than 4 mg COD L^{-1}, at which point granule EPSs were diminished and growth of filamentous bacteria was promoted. In contrast, a study using a granular SBR for phosphorus removal was able to operate under OLR of 500 mg COD L^{-1} (Yu et al., 2014). Two issues common to all CFRs, including phosphorus-removal systems (Li et al., 2016c; Li et al., 2016e), are retaining biomass and controlling settling time. Li et al., 2016e implemented a unique, external settling tank (**Figure 12b**) to stepwise decrease settling time from 9 to 3 minutes. Rapid startup and accumulation of PAO's was achieved within 16 days and operation remained stable for 6 months. The final three-minute settling time was considered comparable to that of an SBR. However, since granules settling in CFRs must overcome the additional resistance of fluid flow, settling is more difficult to achieve. PAO-dominated granules are heavy, and since only the heaviest granules will settle under continuous flow, PAO's are more easily enriched in granular sludge in CFRs than in SBRs designed with similar settling times.

Other researchers have also explored the phosphorus removal capabilities of aerobic granules in CFRs. For instance, Liu et al., 2012 observed a phosphorus removal of approximately 60% for influent containing 10 to 25 mg P L^{-1}. Liu et al., 2014 compared the performance of granules in a CFR with size-based selection pressure and a SBR. The specific phosphorus removal rate was measured as 1.479 kg total phosphorus kg^{-1} MLSS d^{-1}, slightly higher than the 1.371 kg total phosphorus kg^{-1} MLSS d^{-1} achieved in the SBR.

2.8.4 Special wastewater treatment

The type of wastewater is believed, for the most part, not to be determinative towards successful aerobic granulation in CFRs. Just like in SBRs (Gao et al., 2011; Liu et al., 2005), aerobic granules cultivated in CFRs have been shown to treat a variety of special wastewaters (Tsuneda et al., 2006), including synthetic (Jin et al., 2008b; Tsuneda et al., 2003), domestic (Yang et al., 2014; Zhou et al., 2013a), industrial (Bumbac et al., 2015), and mixed domestic/industrial wastewater (Li et al., 2014; Zhou et al., 2013c). Aerobic granules have even been shown to effectively perform nitrogen removal from the wastewater produced by a semiconductor factory (Hasebe et al., 2017). In fact, CFRs with granular sludge are especially advantageous when treating toxic compounds since they will be maintained at lower concentrations than SBRs (Ramos et al., 2016). CFR aerobic granules, for example, have been shown capable of efficiently treating wastewater containing pyridine (Hou et al., 2017) and aromatic compounds (Ramos et al., 2016). In the case of aromatic compounds, aerobic granular sludge has been shown to stably handle variable concentrations (Jemaat et al., 2014b) and even spikes (Jemaat et al., 2014a). Saline wastewater was also found suitable for continuous flow because the presence of salts induced EPS production and thus compact granule structure (Wan et al., 2014c).

The removal of antibiotics and personal care products is a rising concern in wastewater treatment. Both degradation and adsorption are important mechanisms for this process in aerobic granular CFRs (Rodriguez-Sanchez et al., 2017). For instance, prednisolone, naproxen, and ibuprofen have been reduced by greater than 60% in a continuous flow, granular MBR (Zhao et al., 2014), while Rodriguez-Sanchez et al., 2017 removed more than 50% of each of azithromycin, norfloxacin and trimethoprim in a CANON reactor. Results differ regarding observed granule stability, possibly due to differences in wastewater composition or the identity of the antibiotics used. The granules in an MBR fed with approximately 1100 mg COD L^{-1} formed in less than 10 days, but destabilized into loose aggregates after a month of operation (Zhao et al., 2014). Granules in a CANON reactor remained intact, although they decreased in size and developed a more compact surface (Rodriguez-Sanchez et al., 2017). The internal structure also changed dramatically as antibiotic-resistant fungi developed.

The study of Wagner et al., 2015 may suggest that aerobic granulation CFRs are more adept than SBRs at treating wastewater containing particulate matter. In that study, a poor extent of granulation was achieved in an upflow SBR fed with an insoluble component, as filamentous organisms grew to significant numbers. By increasing the duration of an anaerobic phase, during which particulates were solubilized, filamentous growth on the granules was suppressed; however, short settling time allowed washout of biomass, leading to a low SRT and poor effluent quality, i.e. high concentration of effluent solids. System performance was greatly improved by also switching to a "simultaneous fill-and-draw mode". This allowed a constant volume and reduced settling velocity selection due to the upflow of the influent. During this phase of the experiment, both suppression of filaments and a high SRT were achieved.

2.8.5 Full-scale application

ASAGs have already been incorporated into full-scale application for continuously treating sidestream wastewater rich in ammonia. The ANAMMOX® process of Paques (CANON) is a commercially available, continuous flow process utilizing stratified partial nitritation-anammox granules in an upflow reactor with a liquid-solid separator. This system has been applied to treat high ammonium containing wastewaters from dewatering liquor from anaerobically digested biosolids, food, yeast, and tannery plants in China and the Netherlands (Paques a, n.d.). The success of this technology was demonstrated by 90% removal of ammonium from a 18,900 m^3 d^{-1} flow of wastewater comprising 600 mg L^{-1} NH_4^+ (Paques a, n.d.).

A recent study interviewed personnel at 39 North American wastewater treatment plants and identified four facilities that had conditions favoring possible aerobic granulation (Martin et al., 2016). Specifically, these four plants contained sludge having an annual average SVI of 60 mL g^{-1}, which was considered the cut-off between activated sludge and aerobic granules in terms of settleability. Although only one of these four plants reported granule formation, the "granulation potential" in three of the four plants was attributed to creation of feast/famine conditions. These results not only indicated that feast/famine is a key factor in full-scale granulation, but also identify

strategies for applying such conditions. One option is the exposure of return activated sludge (RAS) to a high substrate concentration prior to returning it to the aeration basin (i.e. utilizing a selector zone). A second layout is a multi-pass system with step-feeding. In this case, the influent is fed to every other pass (feast) but not the intermediate passes (famine). Another study focused on the occurrence of large flocs at the Trinity River Authority which exhibited a granule-like settleability (Bruce et al., 2014). Possible reasons included a large OLR with a high soluble COD fraction and accumulation of slow growing nitrifiers and PAOs, both of which have already been shown in this review to contribute to the formation of large granules. A third explanation was the rectangular configuration of the settling tank.

Feast/famine, therefore, is a useful technique that may be used to promote good settleability of the sludge. If a selection pressure, based on settling velocity or size, can also be achieved in full-scale CFRs, the requirements for granular sludge should be met. The key is to determine how to apply such a selection pressure to full-scale continuous systems. One option that has been tested is the use of hydrocyclones (**Figure 17a,b**) within which vortexing separates the biomass based on density and size. This type of selection is termed "vortex selection pressure" herein. Specifically, mixed liquor is tangentially fed toward the top of the cyclone, after which the cone-shape of the cyclone induces a circular motion (Cobb et al., 1973). Heavier material, such as granular sludge, will be forced against the cyclone wall by centrifugal forces and traverse downward to the bottom outlet. Motion of lighter particles toward the cyclone wall is resisted by the water, leading to washout through the top outlet. It is clear that the inclusion of hydrocyclones in future treatment installations will decreases the required size for clarifiers in the process.

So far, three full-scale facilities have examined the possibility of using hydrocyclones to apply a vortex selection pressure to form aerobic granules in continuous, mainstream treatment for nitrogen removal. Two of these plants, namely Strass Wastewater Treatment Plant in Strass, Austria (Wett et al., 2015) and Ejby Mølle WWTP in Odense, Denmark (Willoughby et al., 2016), were bioaugmented by periodically seeding AMX granules from a sidestream DEMON SBR into the mainstream treatment system. Both the DEMON SBR and mainstream reactors incorporated hydrocyclones for retention of AMX granules. In the case of the mainstream, the dense granular sludge was returned to the beginning of the process facilitate the formation of ASAGs. Ejby Mølle WWTP, in particular, successfully maintained 35% granular sludge, on a mass basis, in their mainstream MLSS after two years of operation (Willoughby et al., 2016). The Strass Plant maintained growing granules in the MLSS. However, although the average diameter increased during the 9-month test period, the aggregates were still small compared to most granules formed in laboratory reactors. By the conclusion of the study, only 4% of the granules achieved diameters in the range of 0.3 to 0.4 mm (Wett et al., 2015). It is noteworthy that the plant in Strass, Austria subsequently removed the hydrocyclones and installed sieves for retaining ASAGs in both the sidestream and mainstream reactors. It is clear that these sieves will select for larger granules, as previously discussed. The particular sieves used at Strass are rotating drums manufactured by Zierler ABZ. **Figure 17c** shows an example rotating drum apparatus with a 77 μm screen.

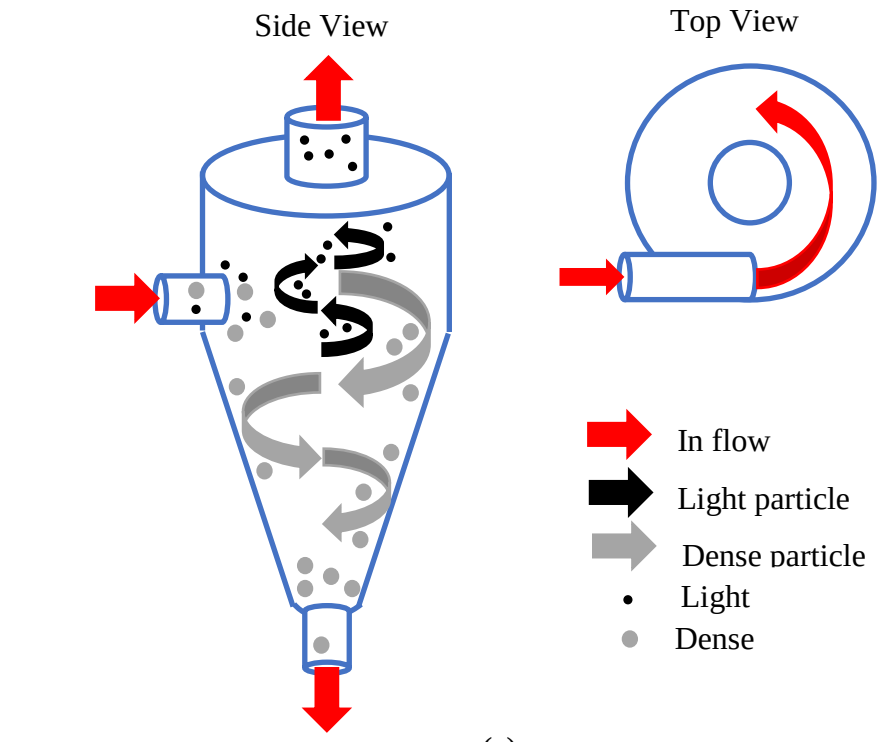

(a)

(b)

(c)

Figure 17. Separation technology for full-scale operations: (a) a schematic of hydrocyclone separating biomass particles based on density and size, (b) a photo of hydrocyclones installed at HRSD, (c) a photo of a rotating sieve drum used in Strass, Austria treatment plants

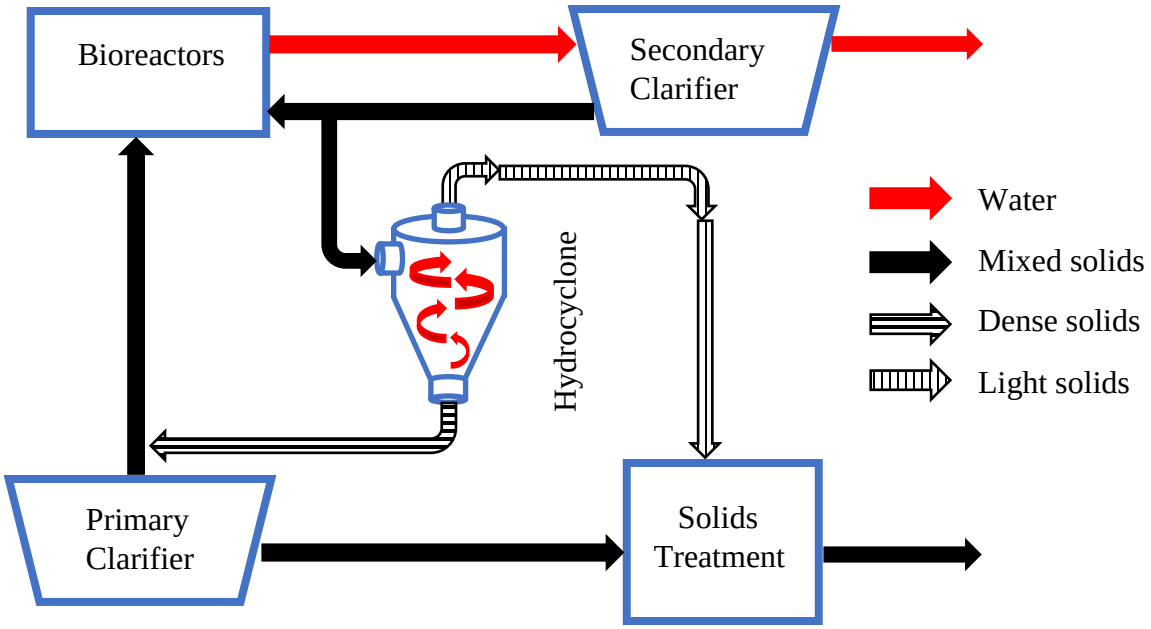

Figure 18. Continuous flow processes at the James River WWTP implementing a hydrocyclone for separation of biomass with good settling properties (Ford et al., 2016).

The third full-scale facility with hydrocyclone installation for aerobic granulation is located at the James River WWTP (**Figure 18**) operated by Hampton Road Sanitation District (HRSD) (Ford et al., 2016). This is a four-stage Bardenpho facility with IFAS, a particular configuration specialized for nitrogen removal. To our knowledge, this is the only full-scale facility that did not seed side-stream AMX granules into the mainstream. Although the retained fast settling biomass did not show clear granular morphology, HRSD's study shows the feasibility of using hydrocyclones to selectively enrich dense biomass. The accumulation of inorganic materials and stability of biological phosphorous removal were reported to be the key to achieving dense particles. Since vortex selection pressure was applied, it is difficult to mechanistically explain why the morphology of granular sludge was not observed. The absence of feast/famine, which has been shown to be essential for settleability improvement, may be part of the reason. It also stands to reason that the time required for granulation will be longer in full-scale plants than observed in a laboratory setting. The hydrocyclones were operated for approximately one year which may not have been long enough for granule formation (Ford et al., 2016). Another concern is the loss of % VSS (reaching 40%) in the hydrocyclone underflow outlet stream returned to the bioreactors, likely due to the accumulation of inorganic material. Two more plants in the United States, namely Alexandria Renew Enterprises Water Resource Recovery Facility (Alexandria, VA, US) (Willoughby et al., 2016) and Blue Plains WWTP (Washington D.C) (Van Winckel et al., 2016), are expected to implement full-scale treatment in the near future. Although the data has yet to be published, management at the Alexandria Renew Enterprises facility, which has implemented hydrocyclones, have reported observing particles larger than 0.25 mm comprising about 20% of the sludge during early testing.

In summary, the combined results of these full-scale studies suggest that hydrocyclones are an effective means for improving the settling properties of sludge in mainstream (Ford et al., 2016; Willoughby et al., 2016). Due to complex mechanisms and the long time required for formation from flocculent sludge, seeding SBR granules appears to be the most efficient strategy for mainstream applications. Selectors providing a feast phase prior to the mainstream basins is also known to improve settleability (Martin et al., 2016; Metcalf and Eddy, 2014). However, further investigations are necessary to better understand the processes at play in these systems.

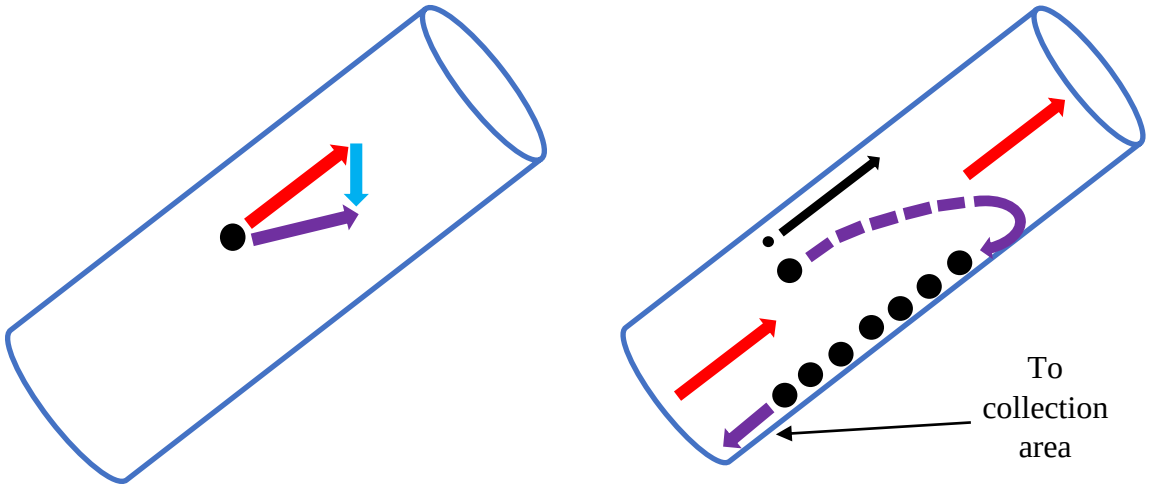

(a) (b)

Figure 19. Inclined tube settlers: (a) the forces acting upon a single granule, (b) the trajectory of a granule and a floc in an appropriately designed inclined tube settler *(dark blue – inclined tube settler; red – water flow; light blue – gravitational force; purple – granule trajectory; black line – trajectory of the floc; large black circle – granule; small black circle – floc)*

The use of inclined plate and tube settlers to supplement clarification is known to be effective in drinking water treatment (Edzwald, 2011), and is used to increase the surface area over which solids may settle (Tarpagkou and Pantokratoras, 2014). This technology has not been commonly used in wastewater treatment, although it has been tested in pilot studies (Faraji et al., 2013; Saleh and Hamoda, 1999). One example of full-scale application in the wastewater industry is the use of inclined plate settlers (also called lamella plate settlers) in the primary settling tanks of the SBR-based Ringsend plant in Dublin, Ireland (Celtic Anglian Water). Inclined plates have also been installed in the CIRCOX® process (Paques b, n.d.) to selectively favor the growth of biofilms on carriers. Given the success with biofilm formation, these unique settlers appear to be a promising alternative for applying a selection pressure in granular CFRs. **Figure 19a** shows the forces acting upon a granule as it is carried through an inclined tube. The net force acting on this granule is toward the wall of the tube (Edzwald, 2011). Granules, as they accumulate on the wall, will slide down toward a collection area (**Figure 19b**). If the inclined tube and flow characteristics are appropriately designed, flocs (which do not settle as well as the granular sludge) will be washed

out from the top of the tube before they meet the tube wall. This technology, since it is already being used in drinking water treatment, should be easy to adapt to full-scale WWTPs. Inclined plate settlers may either improve the settling performance of a current settling tank or else allow a smaller installation to achieve the same performance. This technology, or alternatives such as hydrocyclones, should be chosen if compactness is desired in a new treatment plant. Although they permit for compact systems, membranes provide total sludge retention (Section 2.6.1) and are, therefore, not advisable for mainstream application when aerobic granulation is the goal due to the lack of selection pressure.

2.9 Effect of granule size on autotrophic microbial activity and abundance

When the activities of AOB, NOB, and AMX in different granule sizes have been compared in the literature, the factor of interest is usually the resistance to the diffusion of DO into the granule structure. An increase in granule size leads to a corresponding decrease in DO penetration (Volcke et al., 2012; Luo et al., 2017) and, therefore, a decrease in aerobic volume fraction (Winkler et al., 2011; Volcke et al., 2010). An increased anoxic zone allows for the increased growth of AMX which may compete with NOB for NO_2^- (Volcke et al., 2012; Winkler et al., 2011). Similarly, the availability of DO is the determinant factor for the ratio of AOB and AMX growth (Vlaeminck et al., 2010).

The observed trend in the literature is that AOB activity decreases as granule size increases (Vlaeminck et al., 2010; Wang et al., 2014). Growth of NOB follows the pattern of AOB, favoring small granules (Winkler et al., 2011; Zhu et al., 2018; Volcke et al., 2012; Wang et al., 2014; Liu et al., 2017b) and having a lower NO_2^- oxidation rate as aggregate size increases (Vlaeminck et al., 2010; Morales et al., 2016). Generally, the abundance of AOB (Vlaeminck, et al. 2010; Luo et al., 2017) and NOB (Vlaeminck et al., 2010; Winkler et al., 2011) followed the same trend as that of the microbial activity, i.e., decreasing with increasing granule size. This knowledge suggests that granule size should be taken into account when considering different strategies for NOB suppression (Zhu et al., 2018).

However, it is not the individual trends that need to be considered for nitrite accumulation, but rather the AOB:NOB ratio. Few researchers have analyzed this important relationship for granular sludge, although the data available in some publications allows for the computation of AOB:NOB ratios (**Table 3**). Opposing trends can be seen with regard to the effect of granule size on this ratio. Analysis of the results from the study by Zhu et al., 2018 in **Table 3** indicates that the ratio of AOB:NOB abundance increased with increasing granule diameter. NOB became nearly non-existent in aggregates greater than 50 µm. These results are explained by the researchers as resulting from the competition for limited DO based on relative oxygen affinities (Zhu et al., 2018). Winkler et al., 2011 observed the same trend. In fact, Winkler et al., 2011 and Morales et al., 2016 suggested selectively discarding the smaller aggregates that favor NOB activity. Vlaeminck et al., 2010, however, observed the opposite trend in AOB:NOB activity ratios with the highest ratio in

the smallest granule size. This cannot be explained by DO limitation, so there must be more factors at play. For example, high influent TAN (250 to 350 mg N L^{-1}) in the study of Vlaeminck et al., 2010 suggests the possibility of FA inhbition. Further research must be done to investigate the mechanisms responsible for the AOB:NOB activity and abundance patterns observed in granular sludge, particularly the potential impact of FA.

Table 3. Activity and abundance ratios of AOB to NOB for several granule sizes

Granule Size (mm)	AOB:NOB (Activity)	AOB:NOB (Abundance)	Reference
0.1 – 0.25	28.1	–	Vlaeminck et al., 2010
0.25 – 0.5	2.8	–	
0.5 – 1	3.9	–	
1 – 1.6	4.4	–	
1.6 – 2	3.8	–	
>2	4.4	–	
0.007	–	1.6	Zhu et al., 2018 [II]
0.015	–	1.7	
0.030	–	2.2	
0.050	–	117.2	
0.090	–	820	
0.78 [III]	1.9	35	Winkler et al., 2011
0.93 [III]	23	233.3	

[I] Ammonium oxidation in this case includes contributions by AOB and ammonia oxidizing archaea

[II] Data used for the determination of AOB:NOB ratios from this source were read from a plot (Figure 8) in the source paper. Further granule sizes are provided, but reading of nearly zero NOB concentrations makes determination of AOB:NOB ratios difficult.

[III] Average diameter of the size range. Samples taken from the top of the reactor, where small granules were prevalent, and bottom of the reactor, where large granules were dominant. No further separation of particle size was implemented.

2.10 Free ammonia inhibition as a means of NOB suppression

The exact mechanism of FA inhibition is unknown, although the effect is believed to more strongly target the anabolism rather than the catabolism of NOB (Vadivelu et al., 2007). Another theory is that ammonia deactivates the complex of the nitrite and enzyme such that oxidation does not occur (Gee et al., 1990). Several factors complicate the application of FA inhibition to mainstream nitrogen removal. First, the influent TAN, i.e. the sum of NH_4^+ and NH_3, of domestic wastewater is significantly lower than that in sidestream processes. This makes it difficult to maintain a significant FA concentration in WWTPs. Second, there are differences in the literature as to how

the effect of FA on NOB is quantified. One approach is to report a minimum value at which FA exhibits inhibition of nitrite oxidation, although methods for determining this value also vary. Anthonisen et al., 1976 increased FA in a continuous flow reactor and considered the minimum inhibitory value as that at which nitrite began to accumulate. This study suggested a range of 0.1 – 1 mg NH_3 L^{-1} which has been accepted by many in the field. Other studies determined NOB activities at different FA levels in batch experiments (Ushiki et al., 2017; Villaverde et al., 2000). One area of concern with these batch tests is how the onset of FA inhibition is defined. Ushiki et al., 2017 seems to consider the minimum FA value to occur when the first noticeable drop in NOB activity occurs. It is unclear how Villaverde et al., 2000 determined the cutoff between inhibition and non-inhibition. Another issue with these methods is that the inhibitory value determined by the experiment is limited by the number of data points utilized. For example, Ushiki et al., 2017 did not further investigate if inhibition actually began at a FA between the measured values. As an alternative, it is common to quantify FA inhibition by providing an inhibition constant, $K_{I,FA}$. However, different inhibition models have been used to predict NOB's response to FA. As can be seen in **Table 4**, the most commonly accepted models are either uncompetitive or mixed inhibition. Both forms of inhibition result in a decrease in the apparent μ_{max}. However, uncompetitive inhibition would lead to a decrease in substrate affinity, K_S, while mixed inhibition increases K_S (Gil and Choi, 2001).

Table 4. FA inhibition parameters and models

$K_{I,FAapp}$ (mg NH_3-N L^{-1})	Inhibition Threshold (mg NH_3-N L^{-1})	Inhibition Type	Reference
7.0, 25.5 [I] 13.2, 34.6 [I]	0.85 4.3	Mixed	Ushiki et al., 2017
— —	50 0.04 – 0.08	— —	Blackburne et al., 2007
—	0.08 – 0.8	—	Anthonisen et al., 1976
0.2	—	$\frac{K_{I,FA}}{K_{I,FA} + S_{FA}}$	Hiatt and Grady, 2008
0.62, 0.67 [I]	—	Uncompetitive	Park and Bae, 2009
5.7	1.6	Haldane	Li et al., 2011b
0.2	—	—	Wu et al., 2016
1.6 – 20 [II]	—	$\frac{K_{I,FA}}{K_{I,FA} + S_{FA}}$	Wett and Rauch, 2003
3.9, 11.1 [I]	—	Mixed	Pambrun et al., 2006
173	—	Uncompetitive	Gee et al., 1990
—	—	Mixed	Gil and Choi, 2001

[I] Inhibition constants related to the affinity and maximum activity, respectively

[II] Change in $K_{I,FAapp}$ is credited to adaption of the NOB to FA

2.11 Free ammonia inhibition of NOB in biofilms and granular sludge

FA inhibition studies have been focused on flocculent sludge, and it is not yet clear how a granular structure may influence the inhibitory levels of FA. Granular sludge is larger and more compact than flocculent sludge, leading to external and internal resistances to the diffusion of substrates necessary for nitrogen removal. Ammonium will clearly encounter a diffusion resistance as it penetrates into the granule structure. This diffusion resistance was observed by Piculell et al., 2016 who exposed biofilms with thickness of 50 and 400 μm to reject water. Nitrite accumulation by inhibition of NOB was noted to be more successful in the thinner biofilms in their study. Although many parameters were variable in this study, the results suggest that diffusion did play a role in FA inhibition of NOB in granular sludge and biofilms. However, this study did not seek to establish useful parameters in quantifying the effect of FA. Even when the ammonia inhibition constant has been determined for granular sludge, such as in the study by Cui et al., 2017, the influence of diffusion has not been investigated.

The effect of diffusion limitation can be reflected by a change in the apparent half-saturation coefficient, $K_{S,app}$. In fact, the study of Manser et al., 2005 indicates that K_{O2} for AOB and NOB can change dramatically as oxygen diffuses through the granular structure. The diffusion limitation that substrates encounter in granules and biofilms depends on several factors. Most obvious are the size and density of the flocs, granules, or biofilms (Manser et al., 2005; Wu et al., 2017a). Other factors include the growth of nitrifiers in 3-dimensional microcolony structures (Picioreanu et al., 2016) and nitrifier enrichment (Wu et al., 2017b). The factors that limit diffusion of oxygen will also likely influence the measurement of ammonia inhibition coefficients because NH_4^+ is, like oxygen, consumed by the growth of AOB. Consumption of NH_4^+, and thus TAN, will also lower available FA by Eq. (11). Diffusional resistance to the transport of FA in microbial aggregates will in fact result in the NOB at different depths experiencing different local concentrations of FA. The true, or intrinsic, $K_{I,FA}$ has been used to quantify the FA inhibition in a modified Monod equation in Eq. (18) in which the local FA concentration (S_{FA}) in proximity to the bacterial cell has to be used. However, this local FA concentration is difficult to estimate inside the structures of granules or biofilms unless the very complicated differential equation from Fick's law in Eq. (15) is used. For that reason, an apparent $K_{I,FAapp}$ in Eq. (12) has been commonly used to quantify the FA inhibition on granules or biofilms by using the bulk FA concentration which is easily measured. Therefore, this $K_{I,FAapp}$ is a lump sum parameter that takes into consideration both the FA inhibition and diffusion limitation effects.

Besides diffusional resistance to NH_4^+, pH will also play a role since ammonium oxidation releases H^+ [Eq. (3)] even though nitrite oxidization does not [Eq. (4)]. This is important to note because pH directly influences the acid/base equilibrium of the TAN system. In fact, the pH gradient may have more of an impact than diffusion on the available FA in the granule interior (Poot et al., 2016). The pH in nitrifying biofilms has been found not only to depend on the ammonia concentration, but also on the supplied alkalinity and its diffusion into the granule or biofilm. A small drop in pH across the granule, e.g. 0.4 to 0.6, is only possible at high HCO_3^-/DO ratios, e.g.

HCO_3^-/DO > 5 (Zhang and Bishop, 1996). The low alkalinity of domestic wastewater suggests that a significant pH drop will occur in biofilms and granules incorporated into mainstream WWTPs (Shanahan and Semmens, 2015).

$$NH_4^+ + \frac{3}{2}O_2 \rightarrow NO_2^- + H_2O + 2H^+ \quad (3)$$

$$NO_2^- + \frac{1}{2}O_2 \rightarrow NO_3^- \quad (4)$$

Inhibition in SBRs may alternate from FA to free nitrous acid (FNA) under the proper conditions (Li et al., 2011a), since FNA inhibition increases with decreasing pH. While the cyclic nature of an SBR is absent in CFRs, Hou et al., 2014 simulated a similar effect by adjusting the supplied alkalinity in a continuous flow, moving bed biofilm reactor (MBBR). Changes in pH allowed for switching from FA to FNA inhibition. A similar phenomenon was predicted by the model of Park et al., 2010 when the molar bicarbonate/TAN ratio was set to 0.15. The stratification of AOB and NOB in granular sludge allows for a similar effect in the granule structure itself (Ren et al., 2016), even when the influent is kept stable. A potential concern was raised by Yang et al., 2004 who observed that a FA concentration of 23.5 mg L^{-1} prevented granulation of biomass in an SBR. This was attributed to the suppression of cell hydrophobicity and polysaccharide production under the excessively high FA.

2.12 Stratification of AOB and NOB in aerobic granular sludge

The stratification of nitrifying bacteria, i.e. comprising a coherent layer of AOB over a layer of NOB (**Figure 20a-c**), has been reported in some publications (Vlaeminck et al., 2010; Poot et al., 2016). However, this unique biomass distribution is not universally observed (**Figure 20d-i**), indicating that the proper conditions must first be established (Yang et al., 2014; Gieseke et al., 2003). In fact, "the question remains what are the reasons behind the stratification in the early stages of granule" according to Picioreanu et al., (2016). The mechanisms that have been proposed to date usually involve a form of DO limitation. Kindaichi et al., 2006 and Perez et al., 2009 have argued that differences in oxygen affinity can lead to the spatial separation of AOB and NOB. The literature does in fact generally agree that AOB has a lower K_{O2} than NOB (Ma et al., 2016; Ge et al., 2015). However, Picioreanu et al., 2016 has pointed out that AOB and NOB do not exist in granules as individual cells but rather form aggregated colonies. Colonies of AOB tend to provide more significant diffusional resistance to DO, resulting in an effective affinity for oxygen that is less than that of NOB colonies. In this situation, DO affinity cannot explain the formation of a layer of AOB over a NOB interior. In fact, Picioreanu et al., 2016 claims that stratification is actually a prerequisite to the inhibition of NOB based on DO affinity. The colonies of AOB, in other words, must already be near the granule surface in order to have a competitive advantage over NOB. Previous modelling studies have predicted that AOB and NOB actually mingle together

on the granule or biofilm surfaces without clear separation from each other even when DO is low (Mozumder et al., 2014; Vannecke and Volcke, 2015; Volcke et al., 2010).

The missing link to this mechanism, according to Poot, et al., 2016, is providing a low DO:TAN ratio. According to this theory, the high TAN concentration accelerates AOB growth, consuming the majority of the oxygen and limiting its availability to NOB (Perez et al., 2009; Poot et al., 2016). Ammonia oxidation [Eq. (3)], after all, consumes three times as much oxygen compared to nitrite oxidation [Eq. (4)] (Perez et al., 2009; Ma et al., 2016). By applying a low DO:TAN ratio, DO may be significantly limited within the granules even at high bulk DO concentrations. Bartroli et al., 2010, for example, achieved complete suppression of NOB by maintaining a sufficiently high TAN to set the DO/TAN ratio at 0.18 even at DO above 5 mg L^{-1}. Similarly, Vlaeminck et al., 2010 achieved granule structural stratification in an upflow CFR operating at a DO of 2 to 3 mg L^{-1}.

It is possible that the speciation of NOB may play a role in the mechanism of stratification. *Nitrobacter* and *Nitrospira* are the dominant NOB found in wastewater treatment systems and their relative abundances depend on operational conditions (Huang et al., 2010). For example, *Nitrospira* is believed to have a higher affinity for oxygen than *Nitrobacter* due to the former's lower K_{O2} (Vazquez-Padin et al., 2009). **Figure 20e-g** show that *Nitrobacter*, when present in significant numbers, is commonly observed at the granule surface, where DO is highest in the biofilms. The ability of *Nitrospira* to grow in low DO environments has led Almstrand et al., 2013 to suggest *Nitrospira* will naturally grow in the internal regions of biofilm where diffusion limits DO concentration (**Figure 20c**). This is similar to the arguments based on oxygen affinity previously discussed. However, the data from two reactors of Almstrand et al., 2013 bring his conclusions into question. In **Figures 20c** and **21a** *Nitrospira* does indeed form a distinct layer underneath the AOB at the surface for biofilms in a pilot nitrifying trickling filter (NTF). In the full-scale NTF (**Figure 21b**), however, from the same study, *Nitrospira* is actually most prevalent at the biofilm surface. Significant growth of *Nitrospira* on NTF biofilm surface was also observed by Lydmark et al., 2006 (**Figure 20d**). Such results verify that, although NOB speciation may be relevant to stratification mechanisms, DO is not the only important factor for the mechanism of stratification.

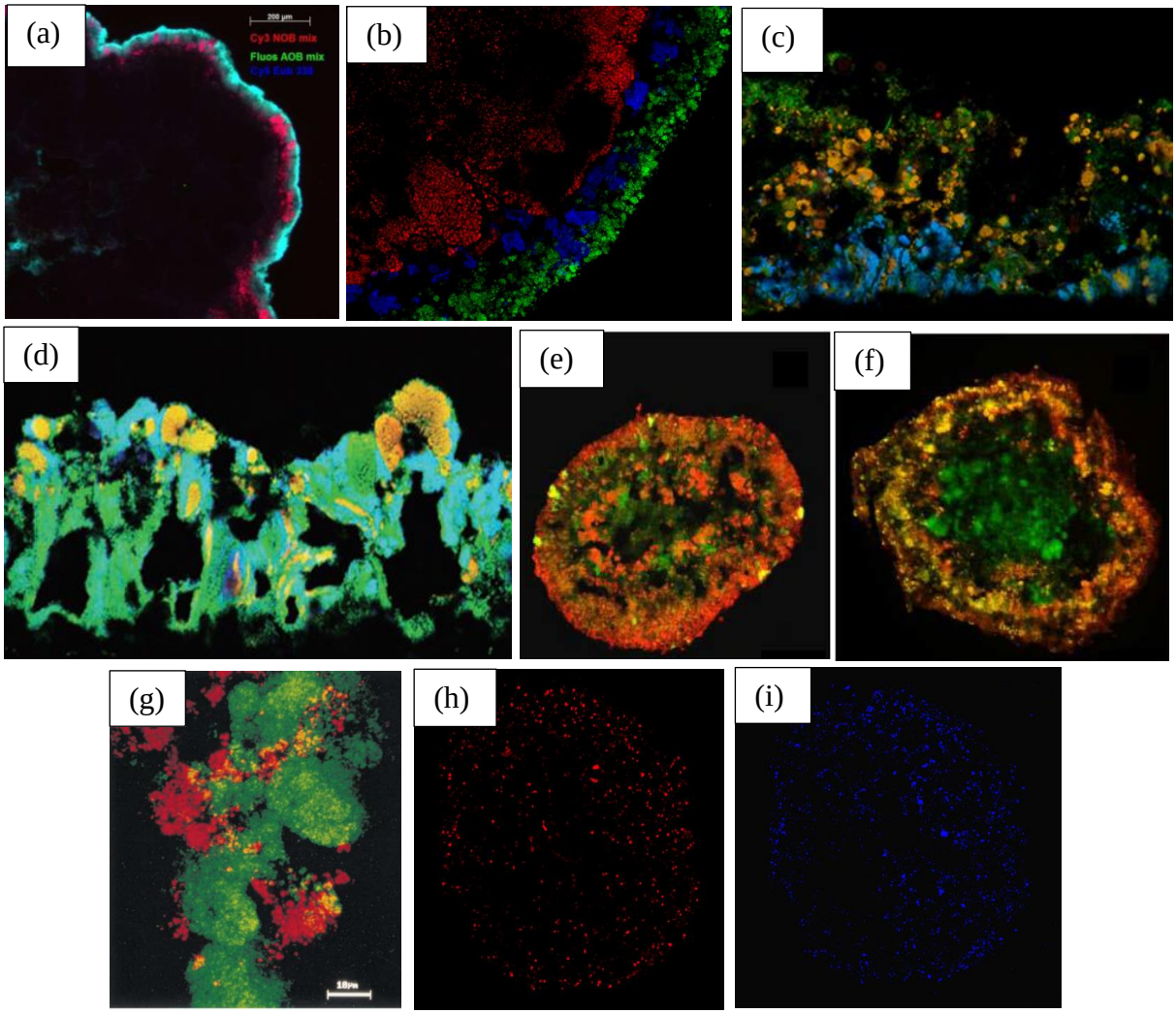

Figure 20. Fluorescent in-situ hybridization (FISH) images showing granules and biofilm with stratified (a-c) and non-stratified (d-i) distributions of AOB and NOB: *(a) blue – AOB, red – NOB (Poot et al., 2016); (b) green – AOB, blue – NOB (Vlaeminck et al., 2010); (c) yellow – AOB, blue – NOB (Almstrand et al., 2013); (d) blue – AOB, yellow – NOB (Lydmark et al., 2006); (e) yellow – NOB; (f) yellow – AOB (Tsuneda et al., 2003); (g) green – AOB, red – AOB (Schramm et al., 1996); (h) red – AOB; (i) blue – NOB (Yang et al., 2014).* (*Permission for reproduction of copyrighted material in this figure has been obtained*)

Discussion on the potential role of FA inhibition as a mechanism for stratification is missing in the literature. Many studies do not address the possibility of FA as an explanation at all. When TAN is maintained at a high concentration to apply a low DO:TAN ratio, the FA is also potentially high enough to inhibit NOB. Yet, FA inhibition was never considered in these papers. This is the case for Poot et al., 2016 who achieved pseudo-steady state FA concentrations ranging from 0.02 to 0.54 mg N L^{-1} in the several phases of their experiment. In fact, the FA for much of the experiment was in the range provided by Anthonisen et al., 1976 for the minimum inhibitory level. Although Vlaeminck et al., 2010 did not report effluent concentrations, the high influent TAN and pH

suggest high levels of FA may have been achieved. The study by Perez et al., 2009 did consider the impact of FA and concluded that inhibition was not an effective means for the compartmentalization of AOB and NOB in biofilms. Careful analysis of this paper, however, indicates that by "compartmentalization", the authors mean the complete separation of AOB and NOB in separate biofilm reactors. This is not directly applicable to biofilms in a single reactor schemed in this study. Further, stratification does not require the complete inhibition of NOB but only that NOB be limited to the granule interior.

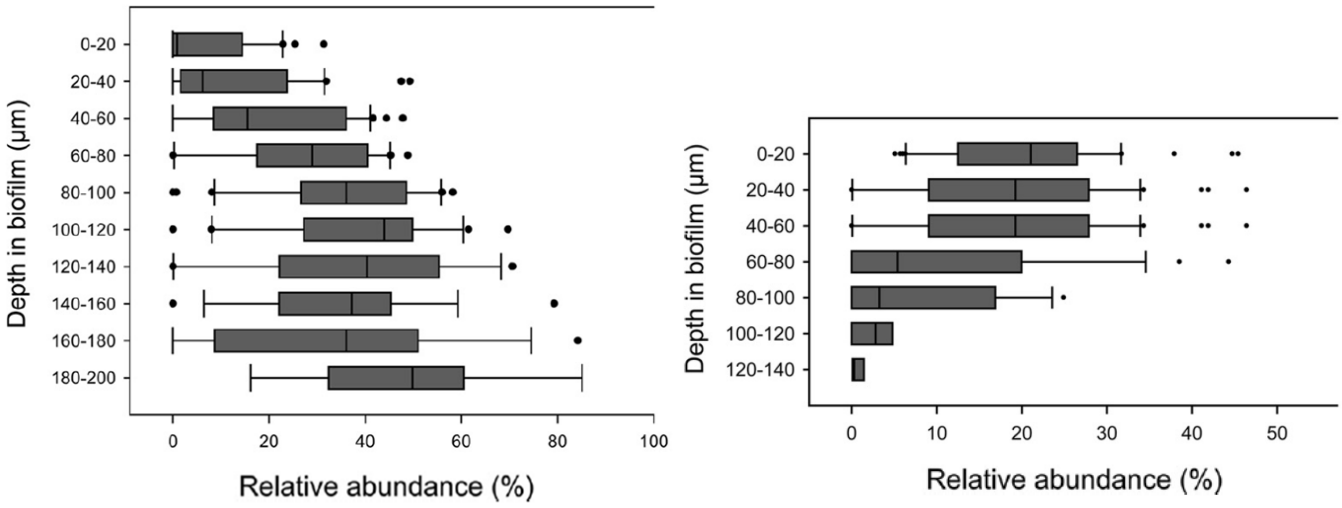

(a) (b)

Figure 21. Relative abundance of Nitrospira in biofilms by FISH quantification for (a) a pilot NTF and (b) a full-scale NTF (Almstrand et al., 2013) (*Permission for reproduction of copyrighted material in this figure has been obtained*)

Chapter 3 – Experimental Methods

3.1 Partial nitritation reactor

3.1.1 Reactor setup and inoculation

The partial nitritation reactor in **Figure 22a** comprised an upflow, 1.5 L ALR. The reactor diameter was 6 cm with a 3 cm diameter riser tube. A three-phase separator was provided at the top of the reactor near the effluent port to retain granular sludge by providing a settling velocity-based selection pressure (**Figure 22b**). Influent was fed from a chilled reservoir by means of a peristaltic pump. The ALR was seeded with refrigerated sludge originating from a DEMON reactor operated by HRSD, Virginia Beach, VA.

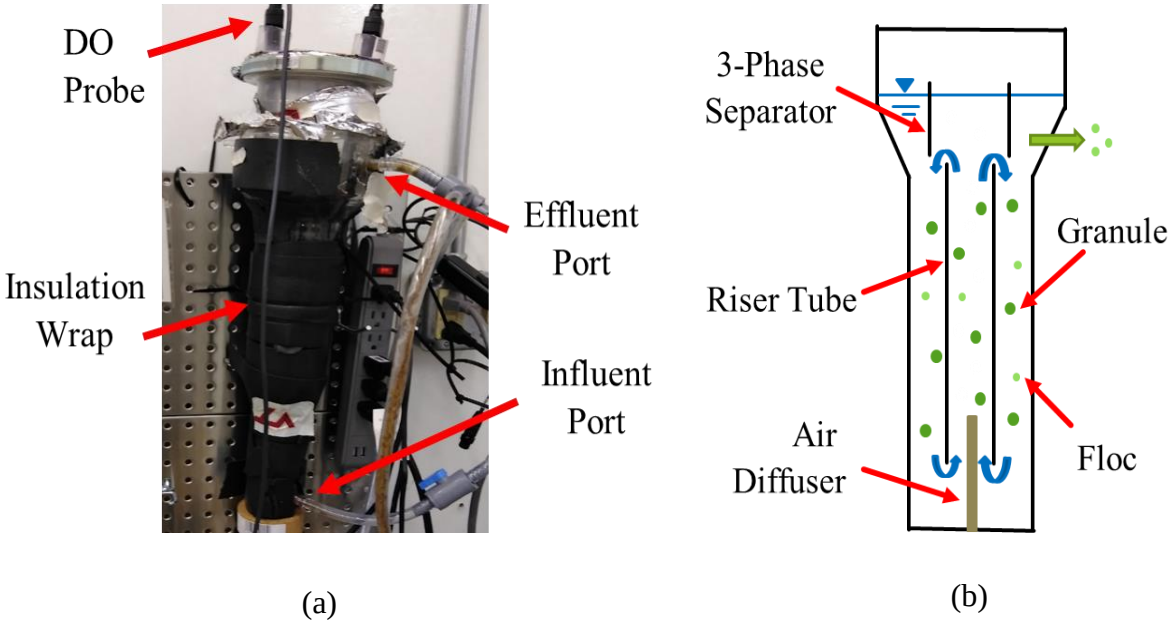

Figure 22. Airlift CFR used in this study: (a) photographic and (b) schematic illustration

3.1.2 Operating conditions

The ALR was operated under a continuous flow mode with a HRT of 5.2 h. The medium used for each batch experiment comprised approximately (per 1 L) 50 – 60 mg NH_4^+-N, 1100 mg $NaHCO_3$, 350 mg Na_2HPO_4, 75 NaH_2PO_4, and trace elements as described in the study by Poot, et al., 2016. Flow rates from an air pump and N_2 gas cylinder were manually adjusted to maintain an average DO < 1 mg L^{-1}. The reactor temperature was not directly controlled but averaged 20.6 °C in a temperature-controlled room.

3.1.3 Effluent monitoring

Effluent NH_4^+, NO_2^-, and NO_3^- were measured using a spectrophotometer and Hach salicylate/cyanurate, NitriVer 3, and TNTplus 835 kits, respectively, according to Hach methods 8155 (Reardon et al., 1966), 8507 (US EPA, 1979), and 10206 (US EPA, 2017). DO was measured every 30 minutes by a submersed, luminescent DO probe (Hach, Intellical™ LDO101, Loveland, CO, USA). Average bulk concentrations for the final 4 months of reactor operation are provided in **Table 5**. The average NH_4^+ and NO_2^- are approximately equal showing successful partial nitritation. The extent of the conversion of NH_4^+ to NO_2^- depended on the DO concentration, which varied around the average, 0.76 mg L^{-1}. **Figure 23** shows this dependency, and further, verifies that the NH_4^+ / NO_2^- ratio is approximately 1 at a DO of 0.76 mg L^{-1}, i.e. the average effluent concentrations accurately reflect the conditions of the reactor at this DO and was used for modelling work in Section 3.3.

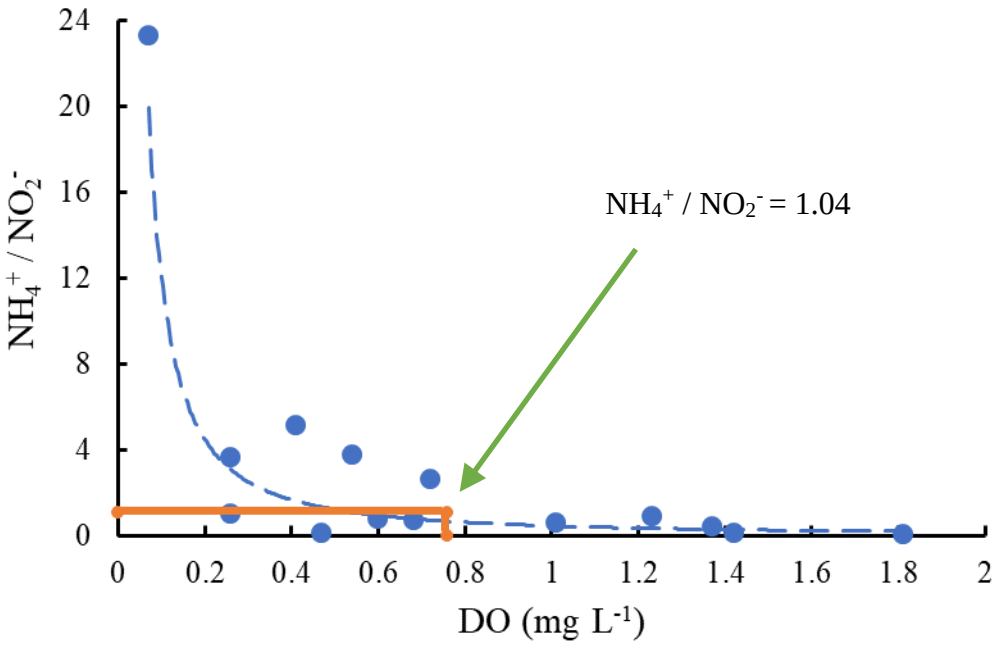

Figure 23. NH_4^+ / NO_2^- ratio plotted for various DO concentrations in the partial nitritation-anammox reactor. The ratio using average NH_4^+ and NO_2^-, e.g. 1.04, is identified by a red arrow

3.1.4 Granule stability analysis

Granule stability after almost eight months of operation was evaluated by the following tests.

(1) A microscope was utilized to image the granule structural integrity for a series of granule size ranges (see Section 3.2.1).

(2) The turbidity of a sample of effluent was determined using a turbidity meter (Hach, 2100N, Loveland, CO, USA).
(3) Particle size distribution was analyzed using a laser scattering particle size distribution analyzer (Horiba, LA-950, Kyoto, Japan).

Table 5. Four-month average bulk concentrations and temperature measured in a partial nitritation-anammox CFR

Variable	Value	Standard Error	Unit
NH_4^+	21.7	3.7	g N m^{-3}
NO_2^-	20.8	3.4	g N m^{-3}
NO_3^-	3.4	0.7	g N m^{-3}
DO	0.76	0.02	g m^{-3}
T	20.6	0.01	°C

3.2 Granule size effect on activity and inhibition

3.2.1 Experimental setup

A suspension medium was prepared, comprising approximately (per 1 L): 500 mg $NaHCO_3$, 35 mg NaH_2PO_4, and trace elements as described in Poot, et al., 2016. Concentrated stock solutions of 5 g $NaNO_2$ L^{-1} and 20 g NH_4Cl L^{-1} were also prepared. Temperature during the experiment was maintained at approximately room temperature. Granular sludge from the partial nitritation reactor was first passed through a series of sieves to separate the biomass into distinct size ranges as follows (in µm): 106 – 149, 149 – 250, 250 – 297, 297 – 350, 350 – 420, and 420 – 500. The sludge in each size range was subsequently re-suspended in suspension medium.

3.2.2 Relative AOB:NOB activity measurement

For each size of range of the biomass, the suspended sludge was washed, allowed to react for at least 1 hour on a shaker plate to completely consume any residual substrate, and washed again. Kinetic experiments took place in 70 mL BOD bottles on a stir plate operating at 80 to 100 rpm to keep the granules suspended. In order to ensure that DO was not transferred from the environment, e.g. by means of leaking, grease was applied around the mouth of the BOD bottle. A sample of each size sludge was added to one of these bottles and the pH of the medium was ensured to be in the range of 7.8 to 8.0, by adding NaOH or HCl if necessary. This range is optimal for both *Nitrospira* and *Nitrobacter* (Blackburne et al., 2007), guaranteeing the maximum activity of NOB. This range is consistent with other reported values of optimal pH in the literature (Grunditz and Dalhammar, 2001). Initial DO was ensured to be in the range of 7 to 8 mg L^{-1} to achieve oxygen non-limiting conditions. Activity was quantified by means of the oxygen uptake rate (OUR) [Eq.

(5)] in a modified procedure similar to that in the study by Moussa et al., 2003. The change in DO with time was measured every minute for 15 minutes to establish the endogenous oxygen uptake rate, namely OUR_1. Straight trend lines (**Figure 24**) with constant slopes indicated OUR was maintained at OUR_{max}, i.e., non-limiting conditions, or in other words, full penetration of DO throughout the granules was preserved.

$$OUR = \frac{d(DO)}{dt} \tag{5}$$

After establishing the endogenous OUR_1, $NaNO_2$ was spiked into the BOD bottle to achieve an initial concentration of approximately 100 mg NO_2^--N L^{-1}. Using 100 mg NO_2^--N L^{-1} (0.004 mg HNO_2-N L^{-1} at pH = 7.8 and T = 20 °C) maintains nitrite non-limiting conditions while keeping the HNO_2 well below the threshold inhibitory value of 0.011 mg HNO_2-N L^{-1} (Ge et al., 2015). The DO was again monitored and used to calculate the OUR, namely OUR_2. NH_4Cl was then dosed to the bottle to ensure approximately 100 mg N L^{-1} initial concentration was achieved and DO was again monitored to provide an OUR_3. The following equations provide the estimation of endogenous respiration rate, as well as AOB and NOB oxygen utilization rates, based on this experimental design.

$$OUR_{endo} = OUR_1 \tag{6}$$

$$OUR_{NOB} = OUR_2 - OUR_1 \tag{7}$$

$$OUR_{AOB} = OUR_3 - OUR_{NOB} - OUR_1 \tag{8}$$

OURs for both AOB and NOB were converted to their relevant nitrogen utilization rates assuming the stoichiometric oxidation of NH_4^+ (3.43 g O_2 g^{-1} NH_4^+) and NO_2^- (1.14 g O_2 g^{-1} NO_2^-) according to Eqs. (3) and (4) on a mass basis (Ma et al., 2016). This allows easy quantification of the AOB:NOB activity ratio based on nitrogen conversion rates.

3.2.3 Confirmation of the presence of AMX

NO_2^- and NH_4^+ were supplied in excess to a similar setup as described in Section 3.2.2 which was inoculated with 350 – 400 µm granules. Once DO had been depleted by nitrifiers in the BOD bottle, a sample was quickly taken for analysis using a Hach total nitrogen (TN) kit based on the persulfate method (APHA, 2012). Three samples were taken, i.e. once per day, to establish the loss of TN in the system. Since there is no carbon source provided in this study, the amount of TN loss can be attributed to level of AMX activity.

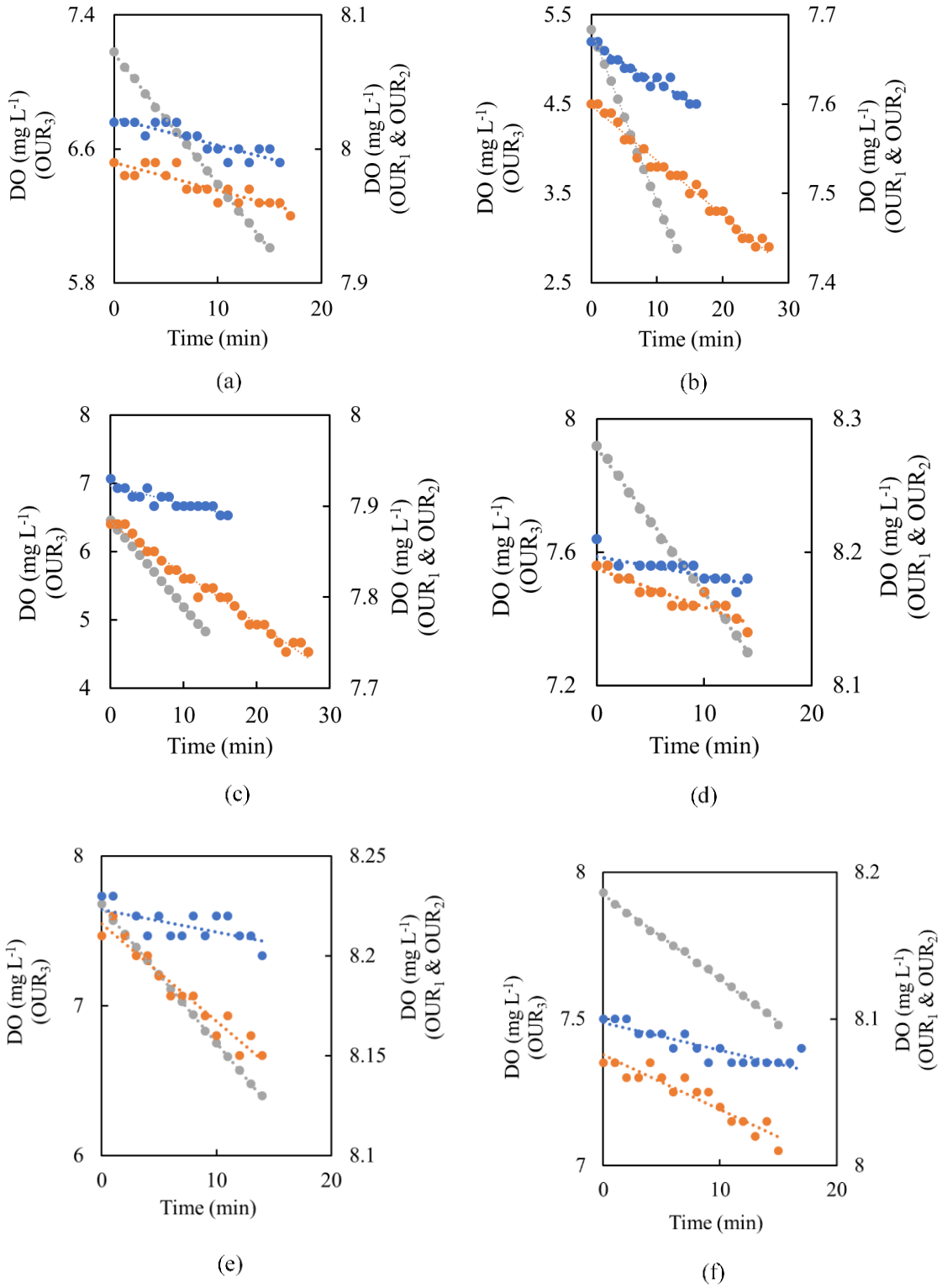

Figure 24. OUR measurements to determine the AOB:NOB activity ratio for each granule size range: (a) 106 – 149 µm, (b) 149 – 250 µm, (c) 250 – 297, (d) 297 – 350, (e) 350 – 420 µm, and (f) 430 – 500 µm. *blue – OUR_1 (endogenous respiration); orange – OUR_2 (endogenous respiration + NOB activity); grey – OUR_3 (endogenous respiration + AOB and NOB activities)*

3.2.4 Diffusion effect on the FA inhibition coefficient for NOB ($K_{I,FAapp}$)

A sample from each granule size range was taken and placed in bottles containing 250 mL of suspension solution at approximately 100 mg N L^{-1} of nitrite. The bottle was placed on a shaker to ensure good mixing. Samples of 2.5 mL or less were extracted before and after a 30 to 40-minute reaction period to establish the uninhibited NOB activity. Ammonium (approximately 25 mg N L^{-1}) was immediately added and a 2.5 mL sample was taken after another reaction period. Aeration was supplied to keep DO non-limiting. This step was repeated for 50 mg L^{-1} of ammonium, and samples were each analyzed for bulk TAN and NO_3^- concentrations to define initial and final values for each period. The difference in NO_3^- observed over the reaction period allowed for the computation of the nitrate production rate, namely R_{NO3}. The bulk FA for each period was calculated using the average of the initial and final TAN values and Eqs. (9) to (11) from the study by Metcalf & Eddy (2014).

$$R_{NO3} = \frac{NO_{3,final}^{-} - NO_{3,initial}^{-}}{reaction\ period} \tag{9}$$

$$FA_{avg,bulk} = \frac{FA_{final,bulk} + FA_{initial,bulk}}{2} \tag{10}$$

$$FA = \frac{TAN(10^{pH})}{\exp\left(\frac{6334}{273+T}\right) + 10^{pH}} \tag{11}$$

Further, the FA inhibition constant $K_{I,FAapp,}$ was determined by assuming an uncompetitive inhibition model, which is commonly applied per **Table 4**. Eq. (12) was adapted from Park and Bae, 2009 to model this type of inhbition, using the nitrite oxidation rate determined at each of the average FA concentrations. Plotting R_{NO3} as a function of FA concentration, followed by linear regression, provides the apparent inhibition constant, $K_{I,FAapp,}$ for each granule size range. In Eq. (12), $R_{NO3,init}$ is the initial, uninhibited nitrite oxidation rate. **Figure 25** shows the results for individual granule size. The generally good linearity of the plots justifies the use of an uncompetitive inhibition model for FA.

$$\frac{1}{R_{NO3}} = \frac{FA_{avg,bulk}}{K_{I,FAapp}}\left(\frac{1}{R_{NO3,init}}\right) + \frac{1}{R_{NO3,init}} \tag{12}$$

Further, since changes in NH_4^+ and NO_3^- were measured during this experiment, approximations of the AOB:NOB activity ratios could be calculated. These were plotted against the values from Section 3.2.2, where nitrogen conversion rates were indirectly calculated from OUR, to determine the correlation between the two data sets.

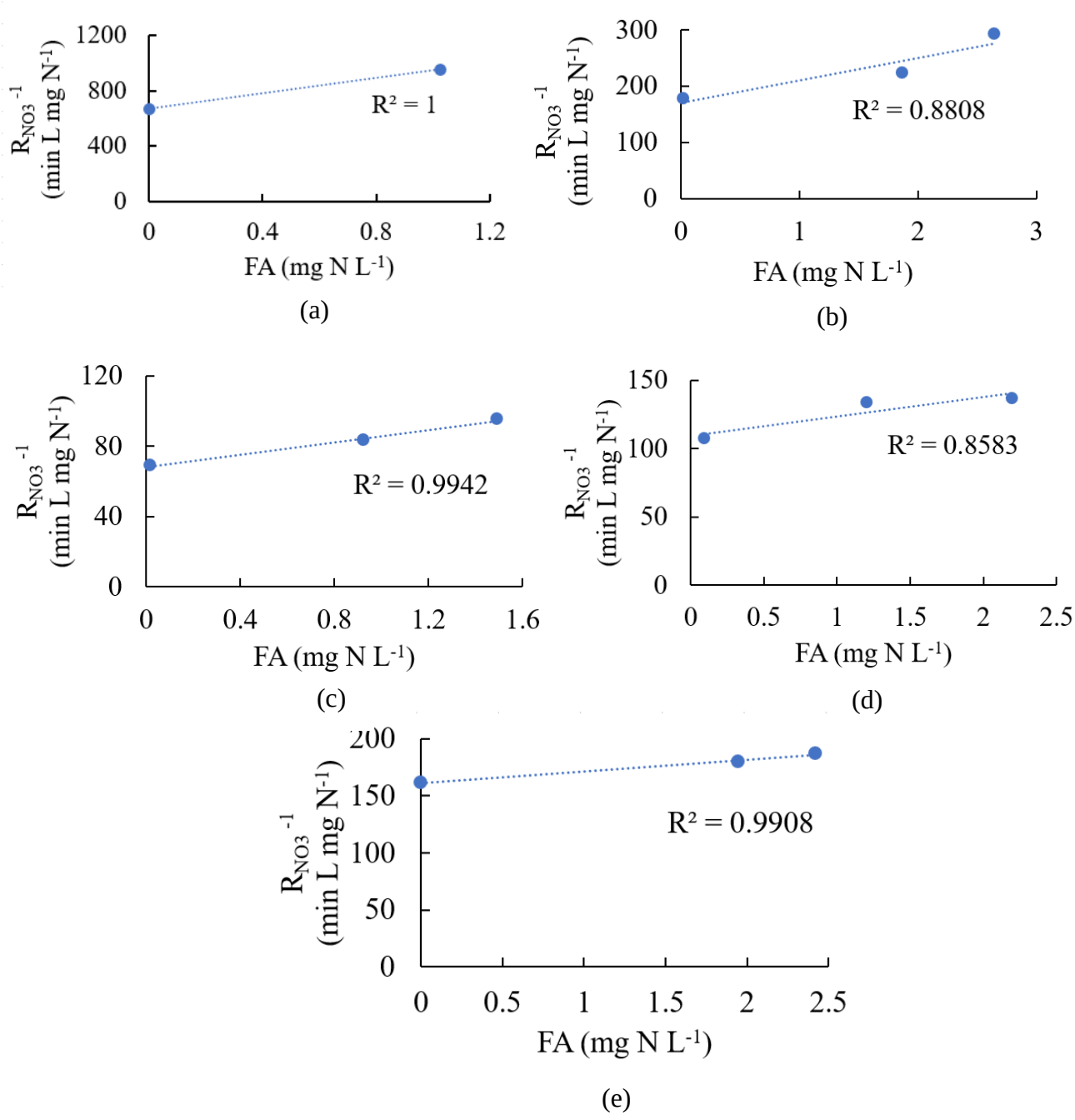

Figure 25. R_{NO3}^{-1} as a function of FA for several granule sizes: (a) 106 – 149 µm, (b) 149 – 250 µm, (c) 250 – 297, (d) 297 – 350, (e) 350 – 420 µm, and (f) 430 – 500 µm

3.3 Model Development

An explanation for the observed AOB:NOB ratios was obtained by implementing a biofilm model programmed in MathWorks® MatLab (R2018a). Simulations were run to predict the distribution profiles of AOB, NOB, AMX, nitrogen, and DO in granular sludge with various particle size. Average radii were used as representative of each size range from Section 3.2.1. In this way two scenarios were considered, specifically the operation with and without FA inhibition of NOB. A regressed $K_{I,FA}$ was used in Eq. (18) to show the impact of FA. The case without FA inhibition was achieved by setting $K_{I,FA}$ to 10,000 mg N L^{-1}, which reduces Eq. (18) to the standard Monod form. Average bulk water concentrations for DO and nitrogen species from **Table 5** were fixed in the model and assumed as steady-state values in continuous flow reactors. Since no COD was provided to the reactor, heterotrophic bacteria do not need to be considered.

3.3.1 Microbial kinetics and substrate utilization

The equations and parameters for microbial kinetics and substrate utilization are summarized in **Tables 6** to **8**, respectively. Temperature sensitive parameters were converted to values at the average operating temperature of the reactor, i.e. 20.6 ℃, by using Eq. (13), where μ_T is the maximum growth rate at temperature T in Kelvin, μ_{293} is the maximum growth rate at 293 Kelvin, and θ is the temperature coefficient. Eq. (13) was taken from the work of Hao et al., 2002, along with the values of θ for AOB, NOB, and AMX. A similar equation is used for the decay coefficient, b. No COD was supplied in the influent to the reactor, therefore, although biomass decay will provide a limited amount of COD, no appreciable growth of heterotropic organisms is expected. Hetertrophic activity is ignored in this model for simplicity.

$$\mu_T = \mu_{293} e^{[-\theta(293-T)]} \tag{13}$$

Monod kinetics was assumed for bacterial growth, although the expressions for NOB and AMX were modified to account for inhibition in Eqs. (18) and (20), respectively. In the case of AMX, this meant including a term for DO. Previous modeling of FA inhibition on NOB has incorporated a variety of different inhibition mechanisms, uncompetitive being commonly used (**Table 4**). Uncompetitive inhibition by FA, therefore, was assumed for NOB growth in this model, which is reasonable supported by the linear plots in **Figure 25**. The $K_{I,FA}$ for NOB was the only variable without an input value and was regressed with Eq. (18) to fit the predicted AOB:NOB activity ratio to data from the experiment in Section 3.2.2. Given that the inhibitory threshold for FA inhibition of AOB is 7 to 150 mg NH_3 L^{-1} (Anthonisen et al., 1976), the model is simplified by ignoring an inhibition term in Eq. (16) which is assumed negligible. The consumption of substrate species i due to microbial growth was modelled by the following equation,

$$R_i = \frac{\mu_{max,j} X_j}{Y_j} \quad (14)$$

where R_i is the utilization rate of substrate i, X_j is the relevant biomass concentration of microbial species j, and Y_j is the growth yield of microbial species j over substrate i. Values for $\mu_{max,j}$ and Y_j were obtained from the literature (**Table 8**). The stoichiometry matrix for the utilization of each substrate species is given in **Table 7**. The output of the kinetic equations in **Table 6** yields an AOB:NOB ratio in terms of biomass concentrations. For comparison of the model predictions to the experimental values, concentrations of AOB and NOB are converted to the equivalent nitrogen utilization rates, namely activities, by Eq. (14).

The K_{O2} is of particular importance in the competition of AOB and NOB at low DO concentrations. The organism with the lower K_{O2} is said to have a higher oxygen affinity and would be expected to dominate under such low DO conditions. A range of values for K_{O2} have been reported in the literature, ranging from 0.2 mg O_2 L^{-1} (Manser et al., 2005) to 1.0 mg O_2 L^{-1} (Ciudad et al., 2006) for AOB and 0.1 mg O_2 L^{-1} (Manser et al., 2005) to 1.4 mg O_2 L^{-1} (Ciudad et al., 2006) for NOB. Values of 0.2 mg O_2 L^{-1} and 0.4 mg O_2 L^{-1} (**Table 8**) were used in this model to simulate the situation where AOB has a competitive advantage over NOB at low DO concentration, since this has been suggested by some researchers as the means for NOB suppression (Kindaichi et al., 2006; Perez et al., 2009).

3.3.2 Effect of diffusion on substrate species concentrations within the granule structure

The diffusivity of each chemical species was assumed to be 80% their values in water according to the study by Sen and Randall (2008). The diffusivity in water for each species is listed in **Table 8**. The diffusion in granules from each size range was accounted for in the model by dividing the granules into 21 layers. The equation for diffusion in a sphere, Eq. (15), was solved for each of these layers. In this equation. D_i is the diffusivity of substrate i, C_i is the concentration of substrate i, r is the distance from the granule center, and R_i is the utilization rate of substrate i.

$$D_i \left(\frac{d^2 C_i}{dr^2} + \frac{2}{r} \frac{dC_i}{dr} \right) - R_i = 0 \quad (15)$$

Table 6. Biological processes for model development

Process	Process Rate	Equation	Reference
Growth of X_{AOB}	$\mu_{max,AOB} X_{AOB} \frac{S_{NH_4^+}}{K_{NH_4^+,AOB} + S_{NH_4^+}} \frac{S_{O_2}}{K_{O_2,AOB} + S_{O_2}}$	(16)	Jubany et al., 2008
Decay of X_{AOB}	$b_{AOB} X_{AOB}$	(17)	Jubany et al., 2008
Growth of X_{NOB}	$\mu_{max,NOB} X_{NOB} \frac{S_{NO_2^-}}{K_{NO_2^-,NOB} + S_{NO_2^-}(1 + S_{FA}/K_{I,FA})} \frac{S_{O_2}}{K_{O_2,NOB} + S_{O_2}}$	(18)	Park and Bae, 2009
Decay of X_{NOB}	$b_{NOB} X_{NOB}$	(19)	Jubany et al., 2008
Growth of X_{AMX}	$\mu_{max,AMX} X_{AMX} \frac{S_{NH_4^+}}{K_{NH_4^+,AMX} + S_{NH_4^+}} \frac{S_{NO_2^-}}{K_{NO_2^-,AMX} + S_{NO_2^-}} \frac{K_{O_2,AMX}}{K_{O_2,AMX} + S_{O_2}}$	(20)	Volcke et al., 2010
Decay of X_{AMX}	$b_{AMX} X_{AMX}$	(21)	Ni et al., 2009

Table 7. Stoichiometry matrix for utilization of O_2, NH_4^+, NO_2^-, and NO_3^-

Process	O_2	NH_4^+	NO_2^-	NO_3^-	X_{AOB}	X_{NOB}	X_{AMX}
Growth of X_{AOB}	$-\left(\frac{3.43 - Y_{AOB}}{Y_{AOB}}\right)$	$-\frac{1}{Y_{AOB}}$	$\frac{1}{Y_{AOB}}$		1		
Growth of X_{NOB}	$-\left(\frac{1.14 - Y_{NOB}}{Y_{NOB}}\right)$		$-\frac{1}{Y_{NOB}}$	$\frac{1}{Y_{NOB}}$		1	
Growth of X_{AMX}		$-\frac{1}{Y_{AMX}}$	$-\frac{1}{Y_{AMX}}$				1

FA was modeled using Eq. (11). The temperature drop within the granule can be considered negligible, so that the bulk temperature may be used in all calculations. The CO_2/HCO_3^- buffer system was assumed to be the controlling factor for changes in pH along the granule radius. In this manner, pH could be simply calculated at each point in the granule by using Eq. (22).

$$pH = pH_{bulk} - \log(K \frac{S_{CO2}}{S_{HCO3}}) \quad (22)$$

where K is the equilibrium constant for the CO_2/HCO_3^- system and equal to $10^{-6.3}$ (Jensen, 2003). Consumption of HCO_3^- occurs as H^+ produced by AOB is neutralized. This drop in bicarbonate inside the granule was modelled to stoichiometrically match the production of H^+ by Eq. (3). Due to this significant alkalinity demand of AOB, $NaHCO_3$ was supplied to the ALR in a ratio of approximately 14 mg HCO_3^- L^{-1} per 1 mg NH_4^+-N L^{-1} to prevent HCO_3^- from becoming limiting.

Table 8. Variable list for model development

Variable	Variable Meaning	Value	Unit	Reference
X_j	Concentrations of bacteria j	N/A	g COD m^{-3}	N/A
S_i	Concentrations of substrate i	N/A	g m^{-3}	N/A
$K_{I,FA}$	Inhibition coefficient for NH_3	N/A	g N m^{-3}	N/A
$\mu_{max,AOB}$	Max specific growth rates of AOB	0.50*	d^{-1}	Cui et al. 2017
$\mu_{max,NOB}$	Max specific growth rates of NOB	0.78*	d^{-1}	Jubany et al., 2008
$\mu_{max,AMX}$	Max specific growth rates of AMX	0.020*	d^{-1}	Azari et al., 2017
b_{AOB}	Decay rate of AOB	0.070*	d^{-1}	Liu and Wang, 2014
b_{NOB}	Decay rate of NOB	0.047*	d^{-1}	Liu and Wang, 2014
b_{AMX}	Decay rate of AMX	0.0016*	d^{-1}	Ni et al., 2009
Y_{AOB}	Growth yields of AOB	0.18	g COD g N^{-1}	Jubany et al., 2008
Y_{NOB}	Growth yields of NOB	0.08	g COD g N^{-1}	Jubany et al., 2008
Y_{AMX}	Growth yields of AMX	0.17	g COD g N^{-1}	Strous et al., 1998
$K_{O_2,AOB}$	AOB half-saturation coefficients for O_2	0.2	g m^{-3}	Manser et al., 2005
$K_{NH_4^+,AOB}$	AOB half-saturation coefficients for NH_4^+	1.1	g N m^{-3}	Volcke et al., 2010
$K_{O_2,NOB}$	NOB half-saturation coefficients for O_2	0.4	g m^{-3}	Sun et al., 2017
$K_{NO_2^-,NOB}$	NOB half-saturation coefficients for NO_2^-	0.5	g N m^{-3}	Volcke et al., 2010
$K_{O_2,AMX}$	AMX half-saturation coefficients for O_2	0.01	g m^{-3}	Volcke et al., 2010
$K_{NO_2^-,AMX}$	AMX half-saturation coefficients for NO_2^-	0.005	g N m^{-3}	Volcke et al., 2010
$K_{NH_4^+,AMX}$	AMX half-saturation coefficients for NH_4^+	0.03	g N m^{-3}	Volcke et al., 2010
$D_{HCO_3^-}$	Diffusion coefficient of HCO_3^-	0.00010	m^2 d^{-1}	Flora et al., 1999
D_{CO_2}	Diffusion coefficient of CO_2	0.00017	m^2 d^{-1}	Flora et al., 1999
$D_{NH_4^+}$	Diffusion coefficient of N	0.00019	m^2 d^{-1}	Picioreanu et al., 1997
$D_{NO_2^-}$	Diffusion coefficient of N	0.00017	m^2 d^{-1}	Picioreanu et al., 1997
$D_{NO_3^-}$	Diffusion coefficient of N	0.00017	m^2 d^{-1}	Picioreanu et al., 1997
D_{O_2}	Diffusion coefficient of O_2	0.00020	m^2 d^{-1}	Picioreanu et al., 1997

*Parameters were converted from the original data in the paper to values at 20.6 °C by Eq. (13)

Chapter 4 – Results

4.1 Long-term granule stability in a continuous flow, partial nitritation reactor

Partial nitritation was successfully implemented in an airlift CFR with average monthly effluent concentrations as shown in **Table 5**. A low DO/TAN ratio, e.g. 0.04, was maintained and verified as an effective operational strategy for suppressing NOB activity. The combined average effluent concentrations (**Table 5**) yielded an average TN of 45.9 mg N L^{-1}, less than the total input TAN (50 to 60 mg N L^{-1}). The difference in nitrogen content supports the presence of AMX activity since the absence of COD prevented the growth of denitrifiers. Although less conclusive, the presence of AMX was further suggested by an observed decrease in TN during a batch experiment with the 350 to 420 µm granules (**Figure 26**). The trend of AMX increasing with increasing granule size is predicted by the model simulation (**Figure 33a-f**) and is expected given the differences in the diffusional resistance to DO. These results are significant because it indicates that both ASAGs with radius ≥ 136.75 µm and CAGs with radius ≤ 99.75 µm coexisted in the same reactor (**Figure 33a-f**).

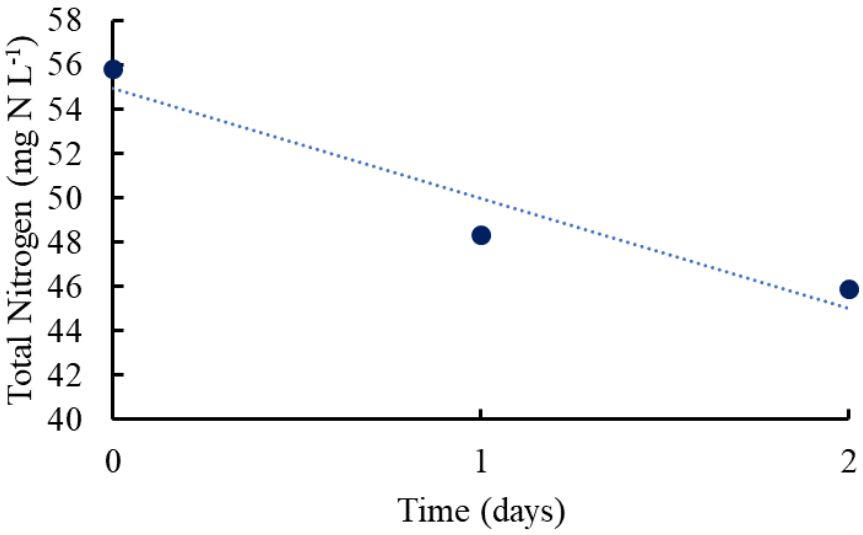

Figure 26. Decreases in TN during a batch experiment for 350 to 420 µm granules without carbon source addition

The partial nitritation reactor was operated for eight months by the conclusion of this study. In order to gain a snapshot of granule stability, the particle size distribution, water turbidity, and granule morphology were analyzed. Images of granules from each size range, as shown in **Figure 27**, display that the granules had well-defined, round shapes with smooth surfaces. The particle size distribution, having a mean of 247 µm, is shown in **Figure 28**. The turbidity of the effluent

was determined to be 2.3 NTU, compared to the 1.6 NTU of the influent, verifying good retention of biomass and integrity of the granular sludge.

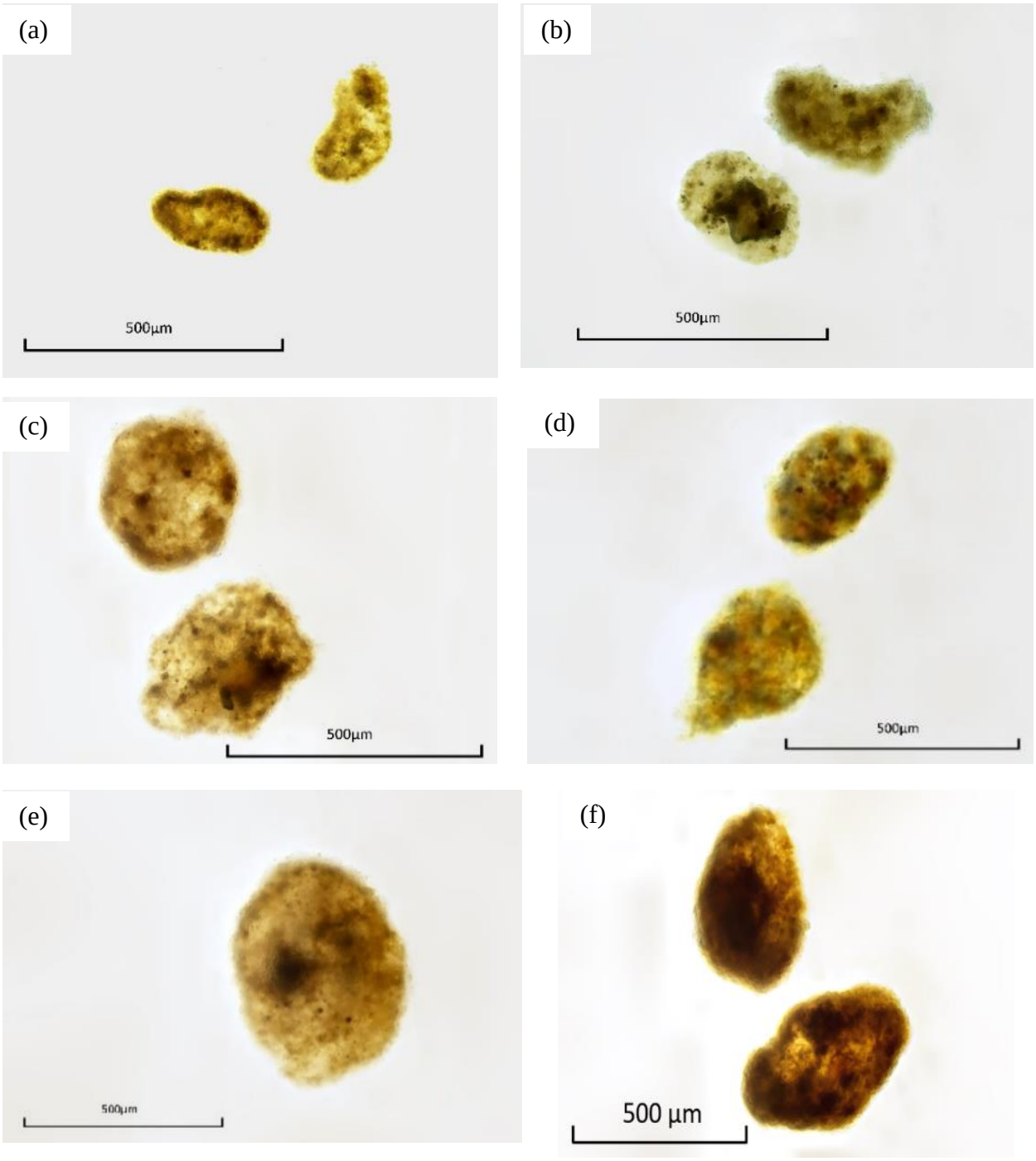

Figure 27. Images of the granule structure for each size range tested. (a) 106 – 150 µm, (b) 150 – 250 µm, (c) 250 – 297 µm, (d) 297 – 350 µm, (e) 350 – 420 µm, and (f) 420 – 500 µm

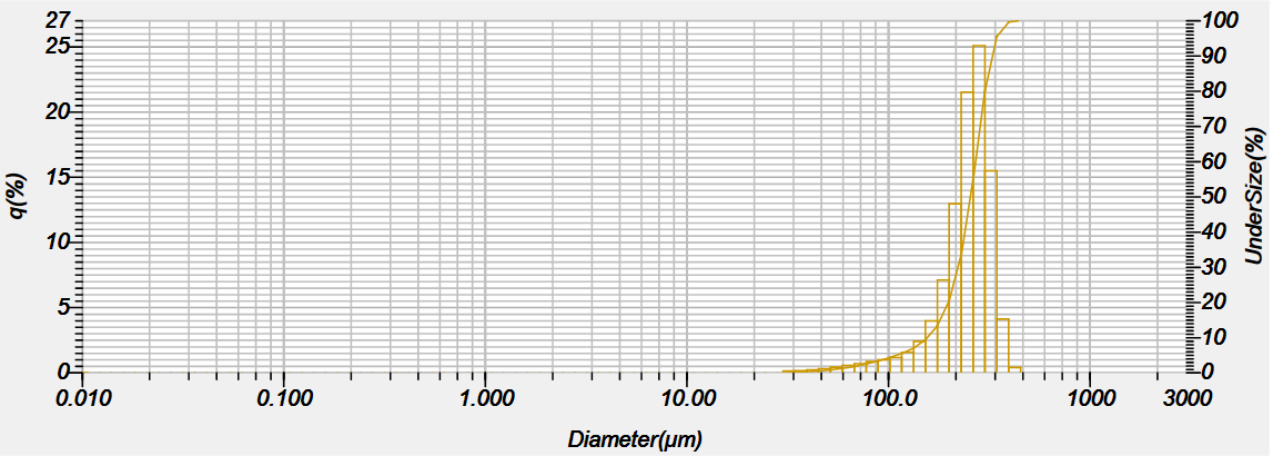

Figure 28. Particle size distribution for the partial nitritation CFR at the end of 8-month operation (*q* - percent of total particles by volume; *undersize* - percent of total particles having smaller size)

4.2 Effect of granule size on the FA inhibition of NOB in aerobic granules

4.2.1 Change in AOB:NOB ratio with granule size

Relative activities of AOB and NOB for each granule size from the batch experiment described in Section 3.2.2 involving OUR measurements (see **Figure 24**) are plotted in **Figure 29** showing a declining AOB:NOB ratio as granules become progressively larger. These data were used for model calibration with equations in **Table 6**, resulting in a regressed $K_{I,FA}$ of 0.35 mg N L^{-1} and the curve shown in **Figure 29**. The good correlation of the AOB:NOB ratio obtained between the OUR experiment and the model prediction in **Figure 29** indicates that the model is able to accurately describe the system.

A second experiment where changes in NO_3^- and NH_4^+ were directly measured (Section 3.2.4) further verified the trend. The values for the AOB:NOB ratios of each granule size resulting from the first experiment, in which activities were determined from OUR, are plotted in **Figure 30** alongside the values obtained in the second experiment, in which nitrogen conversion rates were directly measured. The same trend is observed between data measured from these two separate experiments. Statistical analysis yielded a p value of 0.3 (two-sided test with $\alpha = 0.05$) indicating no statistical difference between the two data sets and further implying that the AOB:NOB ratios obtained in this study are reliable.

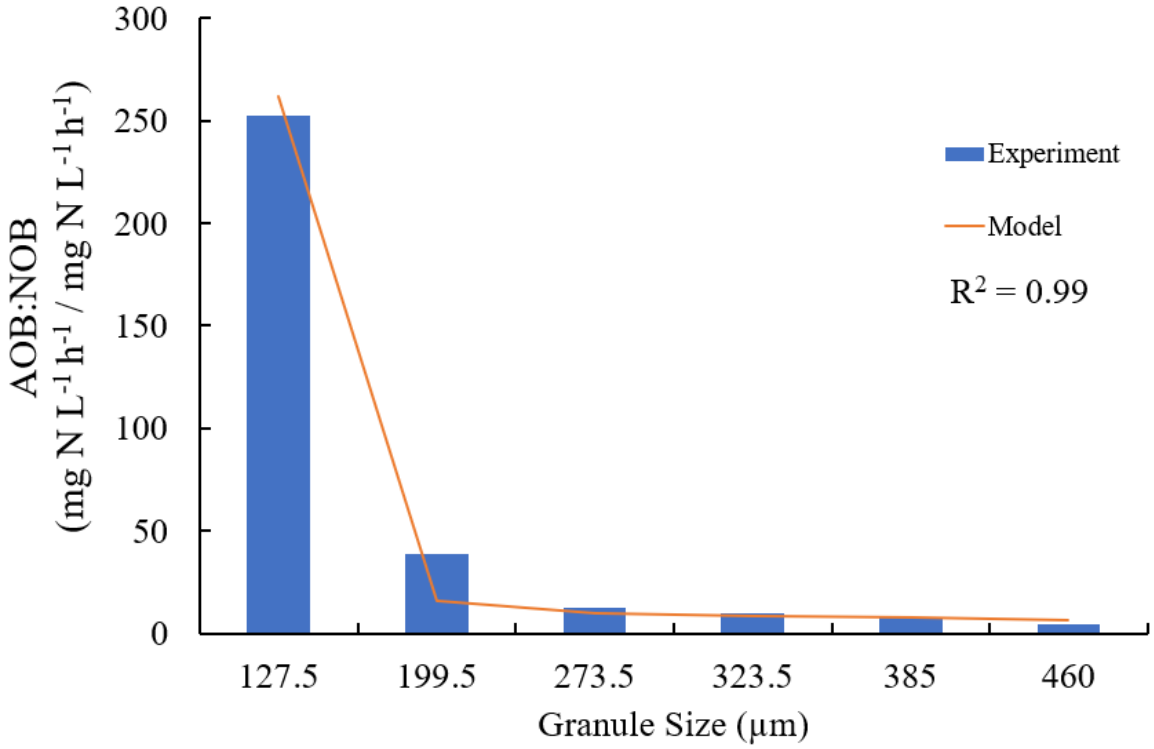

Figure 29. Model simulated and experimentally measured AOB:NOB activity ratios for tested granule sizes

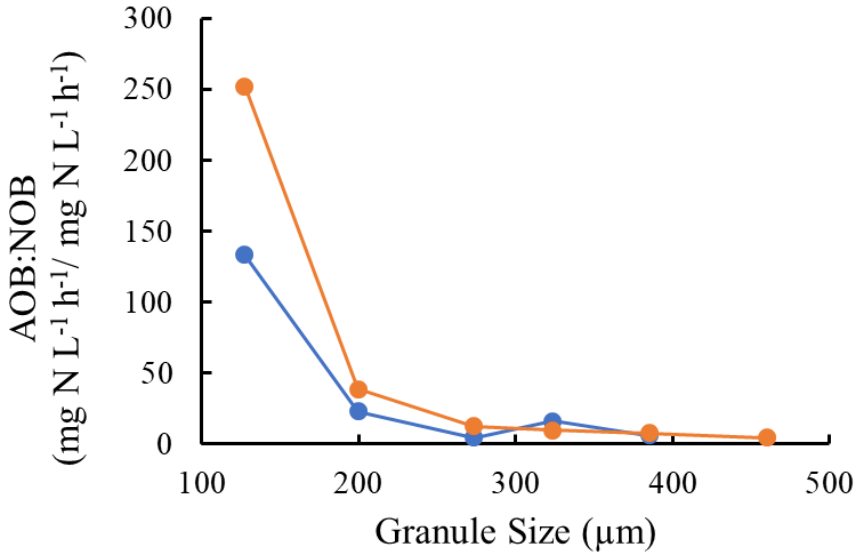

Figure 30. Correlation of AOB/NOB activity ratio measured from OUR- (*orange*) and Nitrogen-based (*blue*) experiments

Model simulation in **Figure 31** shows the AOB:NOB abundance ratio with and without FA inhibition in granules with increasing sizes. As can be seen, totally opposite trends will be resulted under the two scenarios. The increase of AOB:NOB ratio with increasing granule size in **Figure 31** actually has been broadly observed previously (Zhu et al., 2018; Winkler et al., 2011). DO limtation, in the absence of inhbitory concentrations of FA, will be the driving force for competition between AOB and NOB. In small granules, DO will fully penetrate, and NOB will be able to dominate, especially at the surface (Section 4.3). As granules become larger, however, DO will become limiting inside the granule. AOB, with its higher oxygen affinity, will be able to outcompete NOB at low DO concentrations. The addition of FA inhbition obviously has a substantial impact on the AOB:NOB ratio, reversing the trend with granule size under the conditions of this study (**Figure 31**). Clearly FA inhbition of NOB, which occurs primarily at the granule surface (Section 4.2.2), rather than DO limitation, is responsible for the decreasing AOB:NOB ratio observed in **Figure 29**. Further, as expected, the AOB:NOB ratio for abundance follows the same trend as for activity in **Figure 29**.

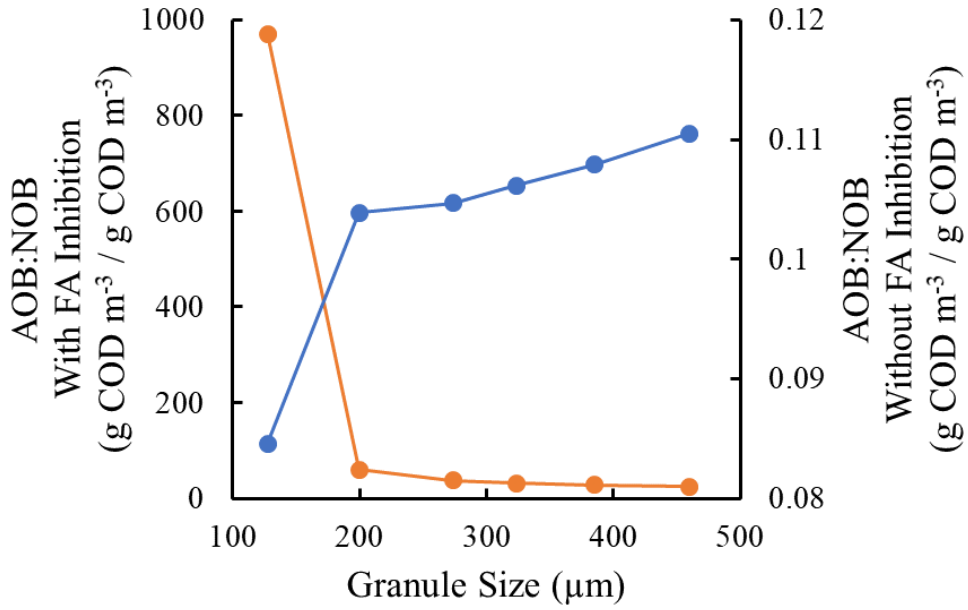

Figure 31. AOB:NOB abundance ratios for the scenarios when (a) FA inhibition is considered (*orange*) and (b) when FA inhibition is absent (*blue*)

4.2.2 Impact of FA and DO distribution on NOB inhibition within aerobic granules as a result of mass diffusion limitation

The average effluent concentrations from the reactor (**Table 5**) demonstrate effective suppression of NOB by FA inhibition. Indeed, the percent nitrite accumulation, given by Eq. (23), was 86%.

$$\%\, NO_2\ accumulation = \frac{NO_2^-}{NO_2^- + NO_3^-} \quad (23)$$

Since the primary distinction between granules of different sizes is the resistance to the transport of substrate and DO, diffusion should have a key role in determining the relative activities of AOB and NOB. **Figures 32** and **34** show the impact of diffusion of the relevant chemical species along the granule radius. It can be seen that the concentration of NH_4^+ decreases along the granule radius for each size modelled. This decline is especially steep near the granule surface. This is consistent with the AOB profiles in **Figure 33**, where AOB is most prevalent in the first 80 µm of the granule. The NO_2^- profile for each granule size in **Figure 32** is nearly identical, indicating limited NOB activity. This is confirmed by only slight changes in NO_3^- across the granule radius for granules with a radius ≥ 99.75 µm. Almost no NOB activity is observed in the smallest granule size, i.e. 63.75 µm. **Figure 33** confirms low abundance of NOB in all granules. Although the impact of diffusion can be seen to influence the profiles of NO_2^- and NH_4^+ in **Figure 32**, their values are always maintained at sufficiently high values, i.e. >20 mg N L^{-1}, to prevent limitation for NOB or AOB utilization, respectively. It is known that AMX can compete with NOB for NO_2^- (Winkler et al., 2011), however this is not expected to be a source of NOB suppression in this experiment. After all, the abundance of NO_2^- in the vicinity of NOB (**Figure 32**) is well above the K_{NO2} of NOB, i.e. 0.5 mg L^{-1}, and is not expected to be limiting.

The concentration of FA is determined by three factors in Eq. (11), namely TAN concentration, temperature, and pH. The decrease in NH_4^+ (**Figure 32**) will tend to also decrease the FA across the granule. However, according to the study by Poot et al., 2016, pH will have a more significant impact on the decrease in FA than will the drop in NH_4^+. It is expected that pH will decrease in the region of AOB activity since ammonia oxidation releases H^+ ions according to Eq. (3). The model predicts such a decline in the pH profile inside the granule structure. **Figure 34** illustrates good correlation between the drops in FA and pH along the granule radius, confirming the strong link between these two parameters, supporting the hypothesized influence of FA inhibition on AOB:NOB ratio measured in **Figures 29** and **30**. Comparison of the data shown in **Figures 33** and **34** provide insight into the FA concentration required for complete inhibition of NOB. The total drop in FA for each granule size was from approximately 0.57 to 0.51 mg N L^{-1}. Although NOB was able to grow at 0.51 mg NH_3-N L^{-1}, NOB was still significantly suppressed. This is consistent with the results of Anthonisen et al. (1976) who found that the minimum inhibitory value of FA was in the range of 0.1 to 1 mg FA L^{-1}.

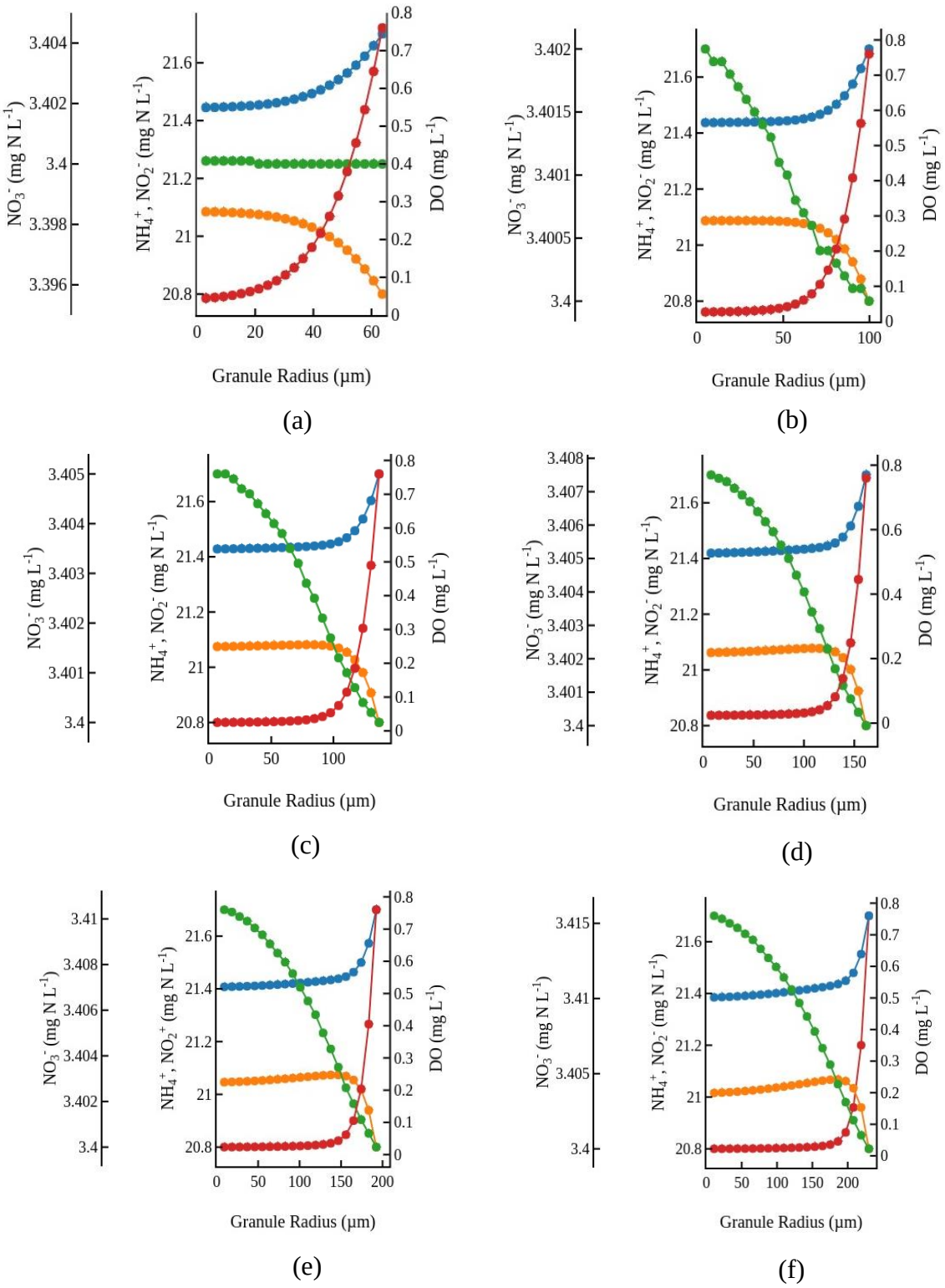

Figure 32. Model simulated substrate profiles along the radius for each granule size range tested: (a) 63.75 μm, (b) 99.75 μm, (c) 136.75 μm, (d) 161.75 μm, (e) 192.5 μm, and (f) 230 μm *(blue – NH_4^+, orange – NO_2^-, green – NO_3^-, red – DO)*

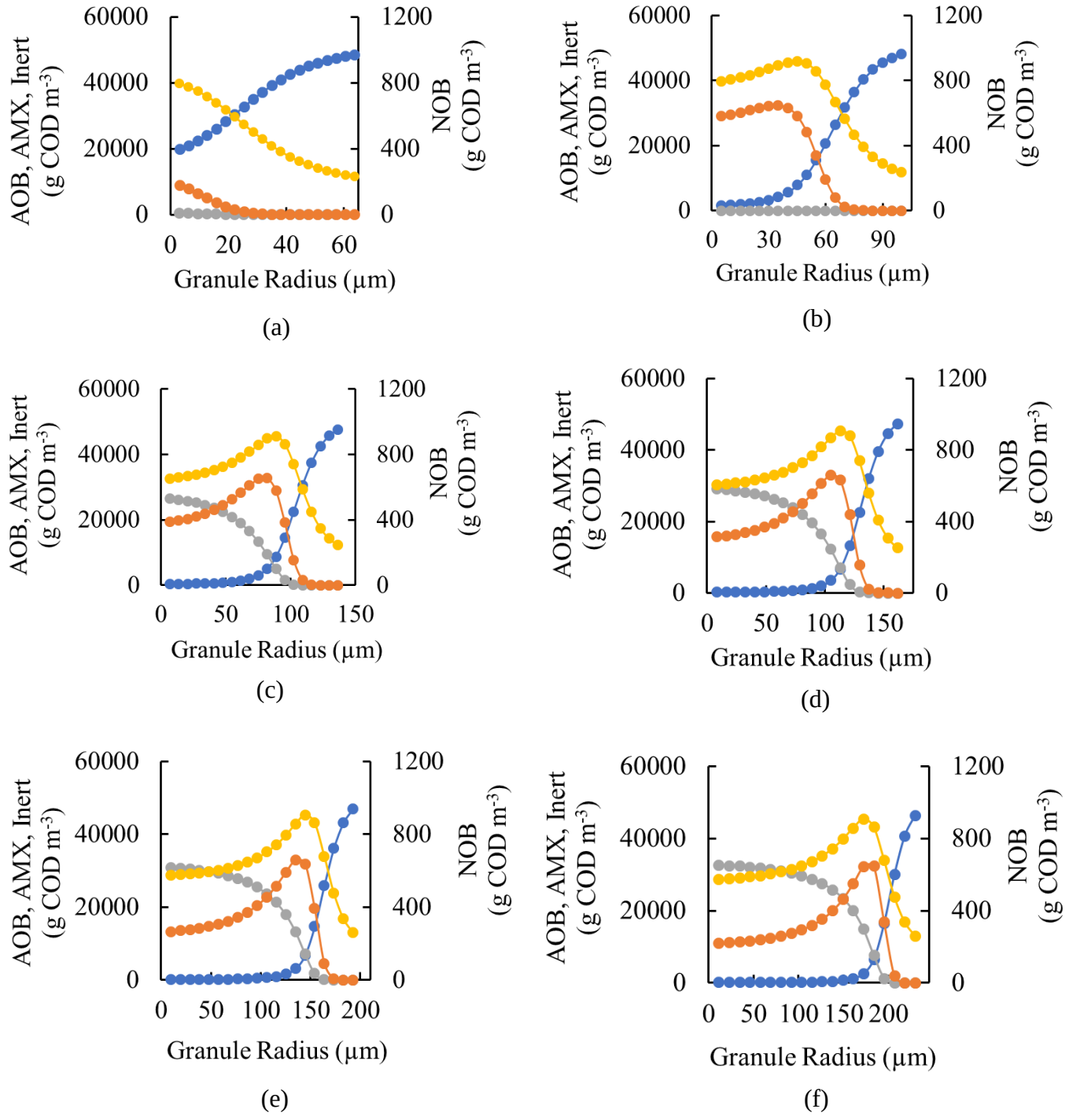

Figure 33. Model simulated biomass profiles along the radius of the tested granules with difference sizes: (a) 63.75 µm, (b) 99.75 µm, (c) 136.75 µm, (d) 161.75 µm, (e) 192.5 µm, and (f) 230 µm *(blue – AOB, orange – NOB, grey – AMX, yellow – Inert)*

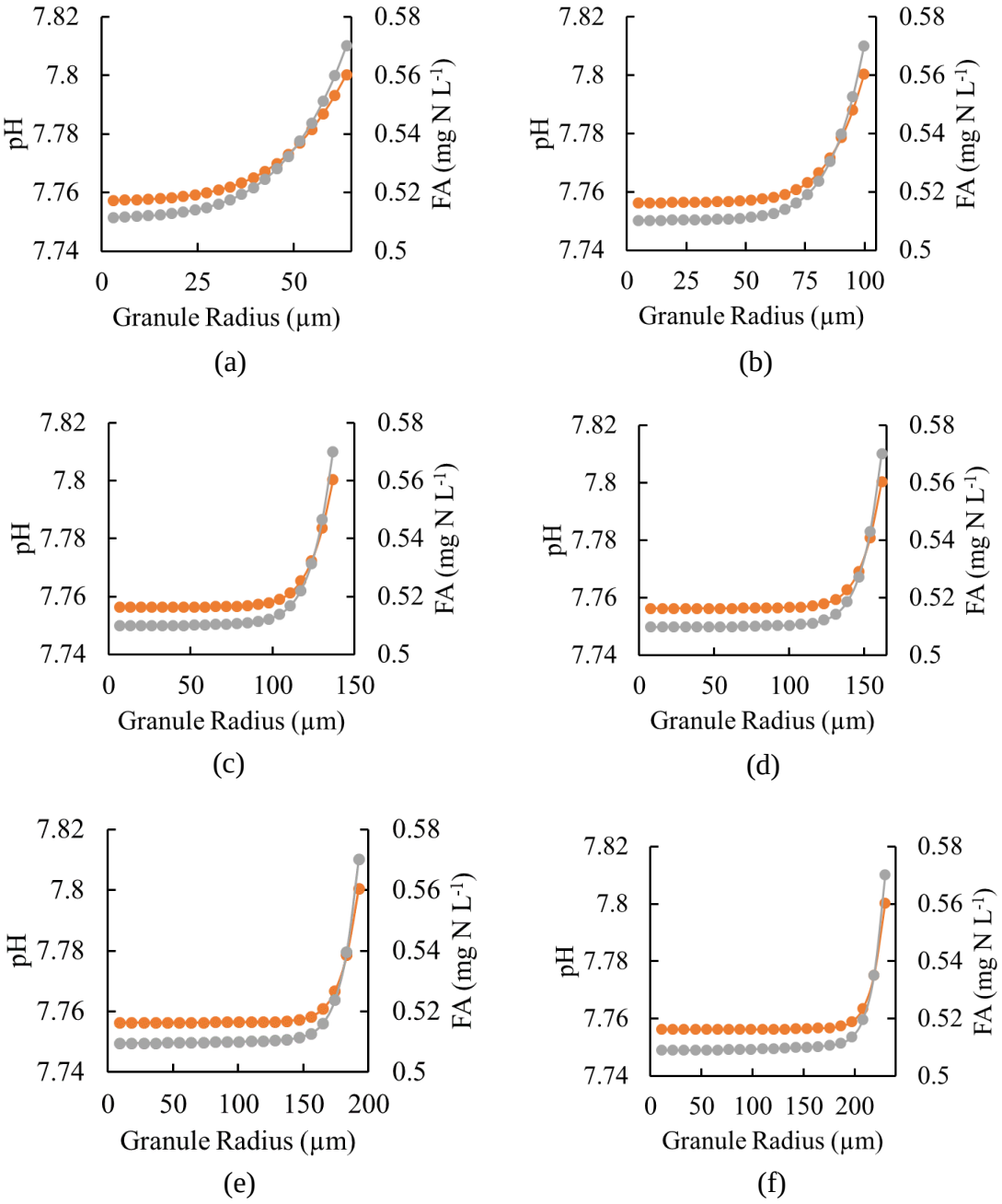

Figure 34. Model simulated FA and pH profiles along the radius of the tested granules with difference sizes: (a) 63.75 µm, (b) 99.75 µm, (c) 136.75 µm, (d) 161.75 µm, (e) 192.5 µm, and (f) 230 µm *(orange – pH, grey – FA)*

AOB has the lower DO affinity (K_{O2} = 0.2 mg L^{-1}) and is favored over NOB (K_{O2} = 0.4 mg L^{-1}) at lower DO concentrations, especially within the granule interior, where DO is at its lowest, i.e. below 0.1 mg L^{-1}. In fact, concentration profiles from the model simulation indicate nearly complete depletion of DO in granules having a diameter greater than 150 µm because it is only 5% of its bulk concentration after penetrating to approximately 50 µm under the granule surface

(**Figure 32**). The impact of DO limitation on NOB is evident since a peak in NOB's abundance is also observed at the same depth (**Figure 33**), i.e. the low concentration of DO approximately 50 μm deep within the granule suppresses the ability of NOB to grow, leading to a sharply decreasing trend of NOB abundance further inside the granule. DO limitation, however, should not be the only factor influencing the relative activities of AOB and NOB since there would have been more AOB inside the granules given its higher DO affinity. Since this is actually not the case in **Figure 33**, the diffusional decrease in FA (**Figure 34**) must have a significant impact on the AOB:NOB ratio in different size granules. Interestingly, the model was found only capable of predicting behavior consistent with the experimental data when FA inhibition of NOB was taken into consideration (**Figures 29** and **31**), i.e. the model only matched the experimental data when a low $K_{I,FA}$, typical of strong FA inhibition, was regressed.

It is further observed in **Figure 33** that the model predicts no AMX will grow in granules with diameter < 136.75 μm. This is due to the penetration of DO in these small granules. Once DO penetration is limited, AMX is able to grow in the granule interior. In fact, the abundance of AMX increases as the granule size increases (**Figure 33**).

4.2.3 Effect of granule size on the FA inhibition coefficient for NOB ($K_{I,FAapp}$)

Reported values for the $K_{I,FAapp}$ vary over a wide range, as shown in **Table 4.** One explanation for the discrepancy is that the measured value of $K_{I,FAapp}$ is influenced by diffusion limitation of the microbial aggregates, which is not accounted for in the Monod equation. In addition, different equations for the effect of FA exist, each representing a different inhibition mechanism. In this case, the measured value does not accurately reflect the true $K_{I,FA}$, but is rather a lump sum of inhibition effects into an apparent K_{FA}, namely $K_{I,FAapp}$. The $K_{I,FA}$ regressed in the model in **Table 6** was 0.35 mg N L^{-1}, which is on the lower end of the range in **Table 4**. Since this value represents a true $K_{I,FA}$ with no impact of diffusion on the growth rate of NOB [Eq. (18)], the low value should be expected. **Figure 35** shows the $K_{I,FAapp}$ for the granule sizes evaluated in this study. These experimentally determined $K_{I,FAapp}$ values from Eq. (12) which include the diffusion effect, ranging from 0.2 to 173 mg N L^{-1}, were much larger than 0.32 mg N L^{-1}. Thus can be seen, $K_{I,FAapp}$ clearly increased with granule size, reflecting an increased impact of diffusion resistance. This further supports the conclusion that diffusion limits the effectiveness of FA inhibition of NOB in large granules.

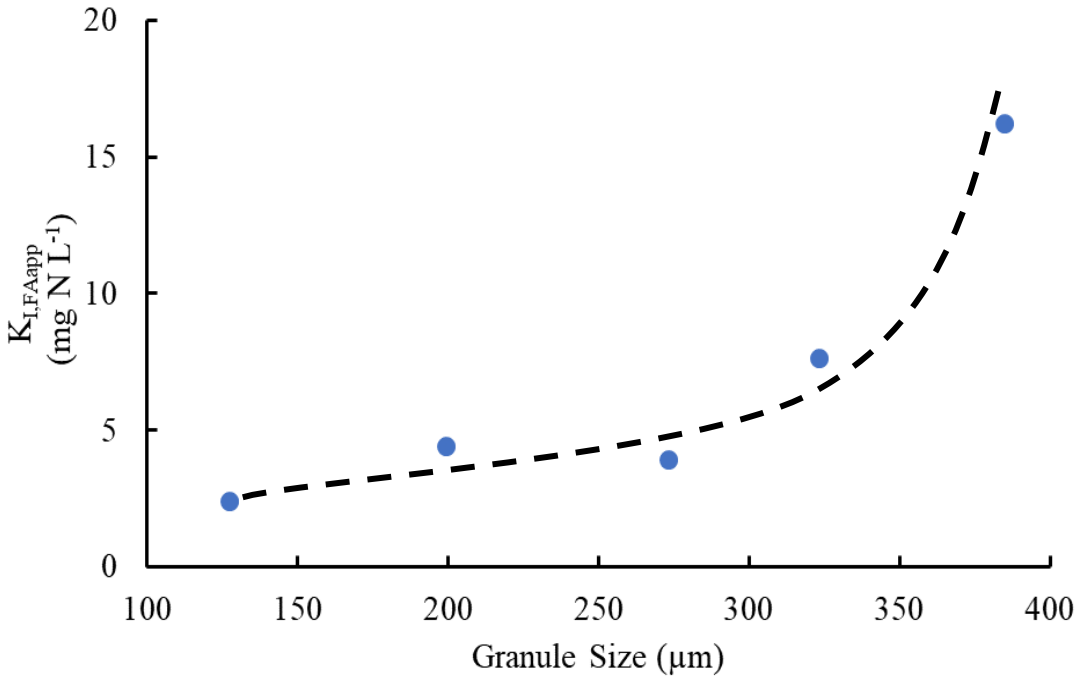

Figure 35. Experimentally measured $K_{I,FAapp}$ for granules with several sizes

4.3 Relationship between granule stratification and FA inhibition

Figure 33 illustrates a stratified structure in each granule size modelled in this study. Specifically, AOB dominates at the granule surface and NOB exists only in the granule interior. When AMX is present, i.e. in granules ≥ 136.75 µm, AMX will grow even further within the granule, where DO has been depleted. The $K_{I,FA}$ in Eq. (18) was again set to 10,000 mg N L^{-1} to simulate a situation in which FA inhibition was absent from the system. **Figure 36** compares the cases for when FA inhibition is and is not considered, highlighting the distribution of AOB and NOB in the top layers of the granule for the smallest, i.e. 63.75 µm (**Figure 36a,c**), and the largest, i.e. 230 µm (**Figure 36b,d**), granule sizes studied in this work. In the case of no FA inhibition, DO limitation is the only factor contributing to NOB suppression. It can be seen that NOB dominates over AOB at the surface of the granule if FA inhibition is ignored. This is expected given the value of K_{O2} for AOB, i.e. 0.2 mg L^{-1}, was half that of NOB, i.e. 0.4 mg L^{-1} (**Table 8**). AOB is more competitive at low DO and should dominate inside the granule where DO has been depleted to its lowest values. NOB dominates at the granule surface also due to the high NO_2^- concentration in the bulk water. Such a situation would not be sustainable since NOB growth would drive down the NO_2^- concentration over time, leading to a failure of partial nitritation. In other words, NO_2^- accumulation in this system cannot be explained solely by DO limitation. Not only does this situation conflict with the successful partial nitration observed in this study (**Table 5**), but **Figure 31** also shows that the case without FA inhibition predicts an increasing AOB:NOB ratio with granule size. The experimental data in **Figure 29** is opposite to such a trend, i.e. AOB:NOB decreases as the granule size increases.

The results in **Figures 29** and **31** suggest that the biomass distribution for the case of FA inhibition (**Figure 36c,d**) is the correct structure. In other words, stratification of AOB over NOB in this system is a result of FA inhibition since FA prevents NOB from growing at the granule surface. However, the decrease in FA concentration due to diffusional resistance (**Figure 34**) allows NOB to grow in the granule interior (**Figure 33**).

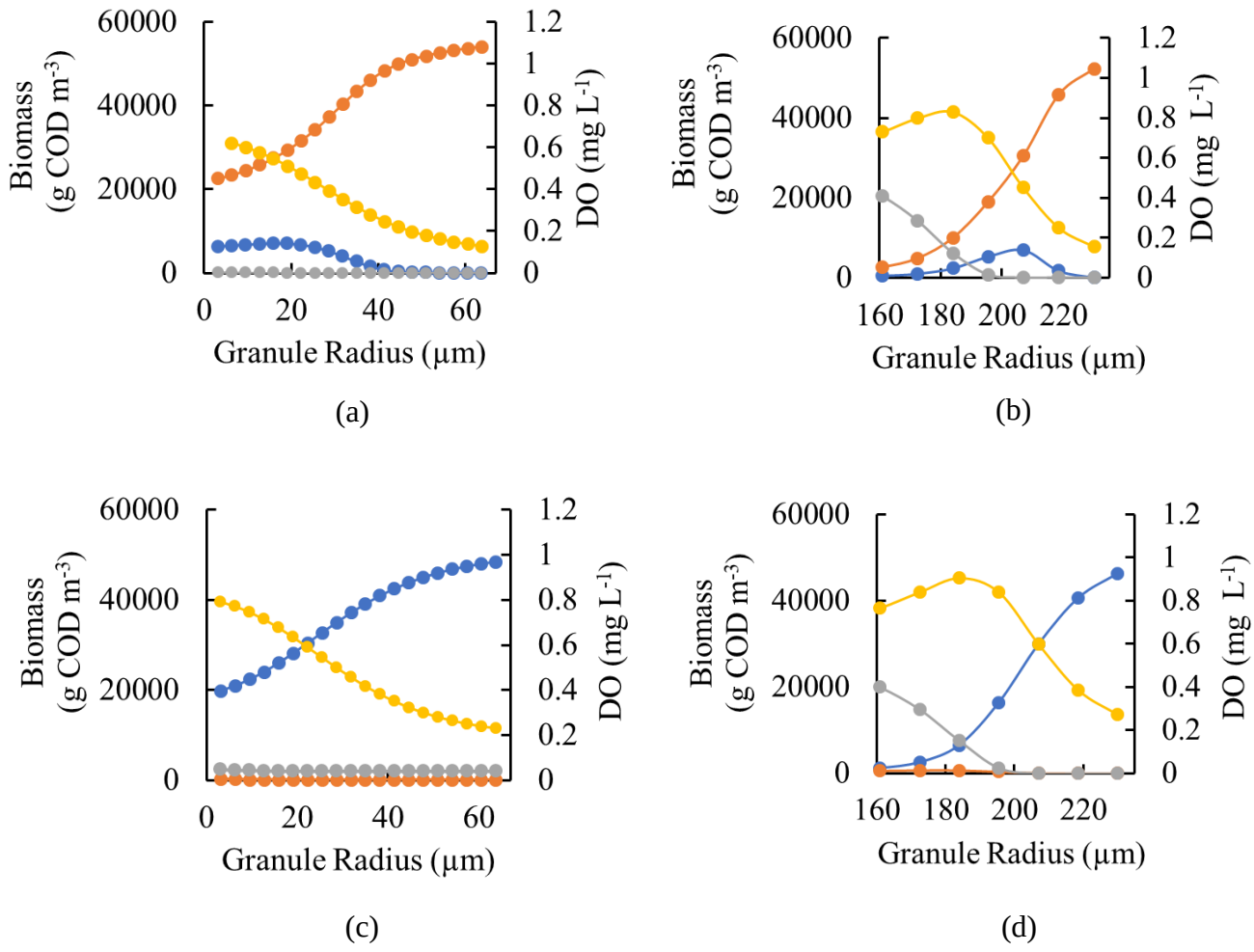

Figure 36. Model simulated biomass and DO distributions in the top layers of granules with radius of 63.75 (a,c) and 230 (b,d) µm and without (a,b) and with (c,d) FA inhibition *(blue – AOB, orange – NOB, grey – AMX, yellow – Inert)*

Chapter 5 – Discussion

5.1 Role of free ammonia inhibition in granules for mainstream wastewater treatment

5.1.1 Granulation mechanism in partial nitritation CFR

Three types of aerobic granules may form depending on the mechanism. The reactor in this study contained larger granules with AMX cores (**Figure 33**), e.g. ASAGs, and smaller granules in which oxygen penetration prevented AMX growth (**Figure 33**). These small granules likely follow the mechanism of CAGs. ASAGs may form without a selection pressure, whereas CAGs require selection based on either settling velocity or granule size (Kent et al., 2018). Selection pressure in the study was supplied by a three-phase separator which allowed heavier biomass, i.e. granular sludge to settle, and lighter biomass, i.e. individual cells and flocs, to flow out with the effluent (**Figure 22**). The stability of the granules after an eight-month operation in this study demonstrates the effectiveness of the separator at applying a settling velocity-based selection pressure (**Figures 27** and **28**).

5.1.2 FA inhibition at low TAN

In this study, NOB was successfully inhibited by FA in a CFR fed with synthetic wastewater containing 50 to 60 mg NH_4^+-N L^{-1} (**Table 5**). This represents the upper limit for domestic wastewater (Xu et al., 2015), showing that FA has the potential to be effective for NOB suppression under mainstream conditions. Although different influent TAN concentrations were not tested in this study, it is likely that lower influent TAN values may also provide inhibitory concentrations of FA. This is because even though a lower TAN means a lower FA, it also leads to a less AOB activity, and therefore smaller pH drop across the granule radius, which gives a relatively higher FA level according to Eq. (11). Since pH was the driving factor for the change in FA in this study (**Figure 34**), sufficiently high levels of FA might be expected at lower TAN. Maintaining a low DO, such as the 0.76 mg L^{-1} in this study, will also be important to implementing FA inhibition. This low DO will limit AOB activity, keeping FA at a sufficiently high level to inhibit NOB. However, more experimentation should be done to evaluate the limits for the application of FA inhibition to mainstream aerobic granular sludge.

5.1.3 Impact of granule size on the effectiveness of FA inhibition

FA effectively inhibited NOB in the partial nitritation-anammox reactor as indicated by the low NO_3^- and NOB concentrations predicted in **Figures 32** and **33**, respectively. This study demonstrated that FA can have a significant impact on the relative activities of AOB and NOB in granular sludge. Due to pH gradients within the granule structure (**Figure 34**), FA has a stronger inhibitory effect on NOB in smaller granules, as shown by larger AOB:NOB ratios (**Figure 29**)

and smaller $K_{I,FAapp}$ values (**Figure 35**). Hence, small granules should be selected over larger ones for effective NOB suppression, based on these results. Since the smallest granules evaluated in this study, i.e. those with diameters in the range of 106 to 149 µm, showed the least NOB growth, the performance of a partial nitritation reactor may be optimized by supplying a size-based selection pressure such that only smaller granules are retained. This is usually accomplished in the literature with sieves (Kent et al., 2018).

This is contrary to the strategy proposed by Winkler et al., 2011 and Morales et al., 2016, where discarding of smaller aggregates is supposed to favor nitrite accumulation. This is due to the approach used by these researchers in which diffusion-limited oxygen penetration was the only mechanism for suppressing NOB. NOB would be able to grow well in the smaller granules which were fully penetrated by DO, but not in the larger granules where diffusion resistance was significant. This is why some studies have observed increasing AOB:NOB ratios with increasing size (Zhu et al., 2018; Winkler et al., 2011). Effluent FA was likely below inhibitory levels in these cases. Analysis of **Figure 31** confirms the conclusion that the AOB:NOB ratio will increase with increasing granule size when FA is non-inhibitory and DO limitation is the only means of NOB suppression; however, AOB:NOB activity ratio will decrease as granules become larger when FA inhibition is present (**Figures 29** and **31**). The latter trend, i.e. decreasing AOB:NOB activity ratio with granule size, was also observed by Vlaeminck et al., 2010. Although FA was not considered in that paper and an effluent TAN concentration was not given to compute it, the high influent TAN, i.e. 250 to 350 mg N L^{-1} and pH of 8 suggest high FA may well have been present in the reactor. FA inhbition, then, is the most likely explanation for the decrease in AOB:NOB ratio, which is consistent with this study.

5.1.4 Application to the partial nitritation-anammox process

The prerequisite for AMX growth is that the DO must be depleted so that an anoxic core can form, which, as seen in this study, is typical of larger granules (**Figures 32** and **33**). This is the opposite trend to that for effective FA inhibition, i.e. nitrite accumulation. Since both nitrite accumulation and AMX activity are required for the partial nitritation-anammox process, it appears a compromise must be made for successful implementation in a single aerobic reactor. Another option is to separate the partial nitritation and AMX processes in two separate reactors as illustrated in **Figure 37**. As discussed by Kent et al., 2018, granule sizes in mainstream, continuous flow reactors tend to be on the smaller side of the size scale. It may, therefore, be easier for mainstream application to adopt the split system. An example of such a plant would allow the utilization of FA inhibition to accumulate nitrite in a first, aerobic reactor containing small granular sludge. AMX granules could be contained in a second, anoxic reactor to complete the nitrogen removal process. Besides taking advantage of the unique benefits of small and large granules, separation of AMX from the aerobic reactor will allow for prior depletion of COD, the presence of which is known to suppress AMX activity (Cao et al., 2017).

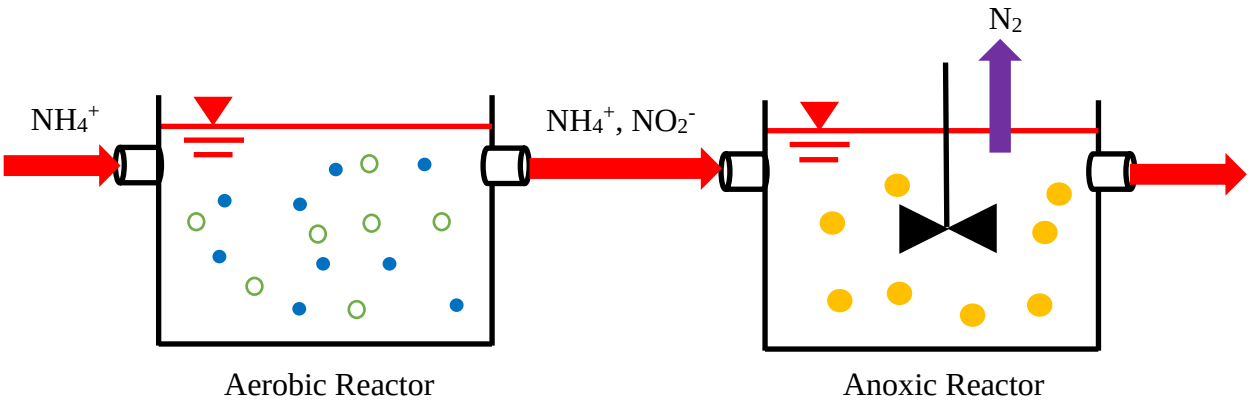

Figure 37. Illustration of a two-stage partial nitritation-anammox reactor system in which small granules with high AOB:NOB ratio like those in **Figure 33** are selectively retained to partially oxidize NH_4^+ to NO_2^- in an aerobic reactor, followed by conversion of NH_4^+ and NO_2^- to N_2 gas in an anoxic reactor with AMX granules. *(blue – AOB granules; yellow – AMX granules; green – air bubbles)*

5.2 Mechanism of AOB/NOB stratification in aerobic granules

When discussing the mechanism of the stratification of AOB and NOB, it is necessary to first define what is meant by "stratification." Stratification herein means that AOB dominates at the granule or biofilm surface with NOB being nearly absent from the surface layer as shown in **Figure 20a-c** reported in previous studies. Further, NOB becomes more prevalent as the distance from the surface increases. This means that suppression of NOB does not necessarily lead to stratification. For example, if NOB is present at low concentrations at the surface, but remains constant or decreases along the granule radius, this would not be considered stratification defined in this thesis.

The literature explanations for the formation of a coherent AOB layer over a layer of NOB are ultimately not satisfactory. Competition for low DO, although certainly essential for the suppression of NOB in aerobic granules, cannot itself explain why NOB would not grow at the granule surface because DO is always higher on granules surfaces (**Figure 32**). After all, higher levels of DO and NO_2^- at the surface should promote NOB growth. Picioreanu et al., 2016 has already demonstrated with their model that NOB suppression by means of relative oxygen affinities actually requires that the AOB and NOB already be stratified as a pre-condition (Section 2.12). Stratification would then not be caused by NOB suppression, but rather be a requirement for NOB suppression. Moreover, if AOB has a lower K_{O2}, as is generally accepted (Ma et al., 2016, Ge et al., 2015), one would anticipate the opposite order in stratification, i.e., AOB would dwell in the granule interior where diffusion results in low DO concentrations. The model used in this study only showed stratification of AOB over NOB when FA inhibition was included in the model (**Figures 33** and **36**). NOB was forced to inhabit the granule interior, where diffusion had reduced FA to a less inhibitory concentration (**Figure 34**) even though the DO is also very low (**Figure**

32). FA inhibition, then, was essential to the stratification of AOB and NOB defined in this study. Stratification, then, is not a requirement for but rather a consequence of NOB suppression.

Poot et al., 2016 attempts to explain stratification as the result of DO limitation brought about by increased AOB activity under conditions of low DO:TAN ratio (Section 2.12). However, this strategy has the same problem as before, i.e. it depends on the pre-existence of AOB-NOB segregation. Unless some other mechanism, such as FA inhibition, prevents NOB growth, the presence of nitrite and DO at the surface should be expected to eventually promote nitrite oxidation.

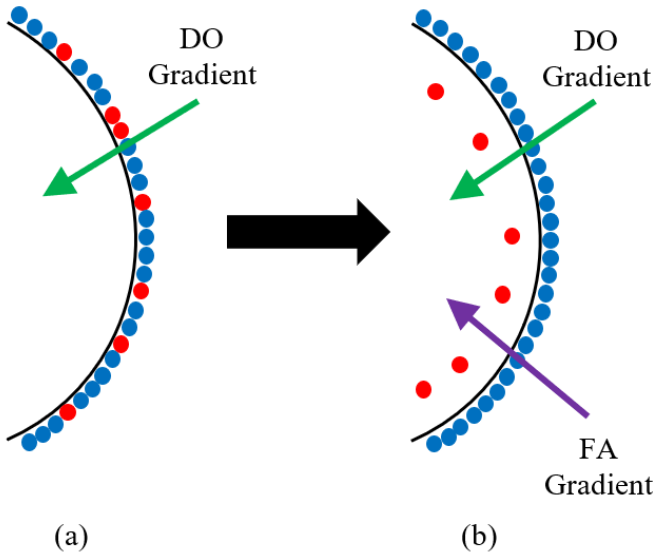

Figure 38. Illustration of biomass distribution at the granule surface for two NOB suppression mechanisms (*red dots – NOB, blue dots – AOB*): (a) DO limitation alone, (b) combined FA inhibition and DO limitation

The results of this and previous studies allow for formulation of a more complete mechanism for AOB-NOB stratification. It is likely that neither FA inhibition nor DO limitation is individually capable of completely suppressing nitrite oxidation, requiring the synergistic cooperation of the two. The need for this two-pronged approach to successful NOB suppression in biofilms is consistent with the results of two papers from one research group of Park et al. One of the studies concluded that long-term suppression of nitrite oxidation was not possible with either FA or low DO individually, but was only achieved under a combination of the two (Park et al., 2015). They acknowledged the role of FA, but credited DO as the most important factor for large, mature biofilms (Park et al., 2010). However, the data in this latter study shows that although low DO decreased the activity of NOB at the biofilm surface, it caused a similar decrease in the growth of AOB. Since the relative activities of AOB and NOB is what truly counts for nitrite accumulation, one would not actually expect this condition to favor nitrite accumulation. It was the other factors,

such as pH and FA, that provided significant differences in the activities of the two competing groups, showing the importance of FA inhibition at the surface. A complete mechanism for stratification, then, is that FA inhibits NOB at the surface, and DO limitation suppresses its activity in the granule interior (**Figure 38**). This would explain the success that has been observed in the literature from maintaining a low DO:TAN ratio.

Chapter 6 – Conclusions

Following concluding remarks can be drawn from this study:

1. In this study, granules performing partial nitritation-anammox were maintained stably for eight months in a CFR. This indicates that the three-phase separator was effective at providing a settling velocity-based selection pressure (Section 3.1.1). The median granule size cultivated in this reactor was 247 µm, which is on the lower end of the range typically observed in granular reactors. These results support the findings of other studies that small granules formed by slow growing, autotrophic bacteria may be stably maintained for extended periods in CFRs. This study, however, further demonstrates that both ASAGs and CAGs (Section 2.2) may coexist for an extended period of time in a CFR performing partial nitritation-anammox. This is significant given the different formation mechanisms for the two granule types, CAGs requiring selection pressure and ASAGs not requiring such selection.
2. The results of this study have several implications for the suppression of NOB by FA in aerobic granular sludge. Firstly, FA inhibition is possible for domestic wastewater with high nitrogen content (50 to 60 mg NH_4^+-N L^{-1}). However, the ability of FA to inhibit NOB is limited by diffusional resistance as it penetrates the granule core. Small granules, therefore, are preferred for partial nitritation-anammox processes relying on FA for NOB suppression.
3. Diffusion also results in a stratified distribution with AOB dominating in the outer layer, where FA is inhibitory, and NOB existing only in the granule interior, where FA is too low to suppress its growth. For effective NOB suppression, however, a low DO must be also maintained inside the granule to limit NOB activity. A model was developed which predicted that stratification would not occur without the influence of FA inhibition. This suggests that FA contributes to the stratification of granules by suppressing NOB at the surface.
4. This study is the first to quantify the impact of diffusion on the $K_{I,FAapp}$ of NOB in granular sludge. The influence of diffusion is further manifested by an increasing $K_{I,FAapp}$ as granule size increases. These measured values do not accurately reflect the intrinsic inhibition coefficient, $K_{I,FA}$, but are easy to use and helpful in gaining qualitative insight into the effectiveness of FA inhibition in granular sludge and biofilms.

Chapter 7 – Future Research

The following areas of research are suggested to further the current understanding of FA inhibition of NOB in granular sludge:

1. **The relative importance of FA inhibition and oxygen limitation**. Previous studies have demonstrated the importance of oxygen limitation to the inhibition of NOB and stratification of aerobic granules. On the other hand, this study has demonstrated that FA is also essential. Further research should be done to investigate how these two factors combine to form a complete mechanism.
2. **The impact of NOB speciation on NOB suppression and stratification.** Limited study has been devoted to the effect of the NOB community makeup on the success of FA inhibition. Ushiki et al., (2017) has reported 0.85 and 4.3 mg NH_3 L^{-1} as the minimum inhibitory levels for two strains of pure culture *Nitrospira*, and 14.8 mg NH_3 L^{-1} as the minimum value for *Nitrobacter Winogradskyi*. Blackburne et al., 2007 reported 0.04 to 0.08 and 50 mg NH_3-N L^{-1} as inhibitory to enriched *Nitrospira* and *Nitrobacter* cultures, respectively. This evidence indicates that *Nitrospira* is much more susceptible to the inhibitory effects of FA than *Nitrobacter*. Indeed, even different clades within *Nitrospira* differ in sensitivity to FA, e.g. lineage I is more prone to inhibition than lineage II (Ushiki et al., 2017). Clearly, the speciation of NOB is relevant to the impact of FA and should be considered when this approach to NOB suppression is desired.
3. **Stable granulation in mainstream CFRs**. Only four attempts have been made to achieve granulation in CFRs of mainstream WWTPs, but none of them were successful (Kent et al., 2018). The granules have been stable for eight months in the CFR used in this study, indicating it is possible to achieve continuous flow aerobic granulation. As pointed out in my previous study, nitrifier growth over a core of AMX bacteria (ASAG) might be a possible mechanism accounting for the success in this study (Kent et al., 2018). It was also pointed out that size-based selection pressure is preferred for NOB suppression by FA. Few studies have attempted this mechanism in CFRs. Therefore, it is desirable to better understand and further develop the mechanisms of continuous flow aerobic granulation.
4. **FA inhibition at low TAN in mainstream CFRs**. It is also unclear whether influent TAN concentrations significantly lower than 50 mg N L^{-1} will be able to provide inhibitory concentrations of FA. Further study needs to be done to determine the minimum TAN that may allow for inhibitory concentrations of FA.

References

Ali, M., Chai, L.Y., Min, X.B., Tang, C.J., Afrin, S., Liao, Q., Wang, H.Y., Peng, C., Song, Y.X., Zheng, P., 2016. Performance and characteristics of a nitritation air-lift reactor under long-term HRT shortening. Int. Biodeterior. Biodegrad. 111, 45-53.

Almstrand, R., Daims, H., Persson, F., Sörensson, F., Hermansson, M. 2013. New methods for analysis of spatial distribution and coaggregation of microbial populations in complex biofilms. Appl. Environ. Microbiol. 79(19), 5978–5987.

Anthonisen, A.C., Loehr, R.C., Prakasam, T.B.S., Srinath, E.G. 1976. Inhibition of nitrification by ammonia and nitrous-acid. J. Water Pollut. Control Fed. 48(5), 835-852.

APHA, 2012. Standard Methods for the Examination of Water and Wastewater, twenty second ed. American Water Works Association.

Azari, M., Lübken, M., Denecke, M. 2017. Simulation of simultaneous anammox and denitrification for kinetic and physiological characterization of microbial community in a granular biofilm system. Biochem. Eng. J. 127, 206–216.

Bartroli, A., Perez, J., Carrera, J. 2010. Applying ratio control in a continuous granular reactor to achieve full nitritation under stable operating conditions. Environ. Sci. Technol. 44(23), 8930-8935.

Blackburne, R., Vadivelu, V.M., Yuan, Z.G., Keller, J. 2007. Kinetic characterisation of an enriched Nitrospira culture with comparison to Nitrobacter. Water Res. 41(14), 3033-3042.

Bruce, S.C.R., Downing, L., Young, M., Nerenberg, R., 2014. Floc or granule? Evidence of granulation in a continuous flow system. Proceedings of WEFTEC 2014. New Orleans, Louisiana, USA: Water Environ. Fed. 2891-2897.

Bumbac, C., Ionescu, I.A., Tiron, O., Badescu, V.R., 2015. Continuous flow aerobic granular sludge reactor for dairy wastewater treatment. Water Sci. Technol. 71(3), 440-445.

Cao, Y. S., van Loosdrecht M.C.M., Daigger, G.T. 2017. Mainstream partial nitritation-anammox in municipal wastewater treatment: Status, bottlenecks, and further studies. Appl. Microbiol. Biotechnol. 101(4), 1365-83.

Carvajal-Arroyo, J.M., Puyol, D., Li, G.B., Swartwout, A., Sierra-Alvarez, R., Field, J.A., 2014. Starved anammox cells are less resistant to NO_2-inhibition. Water Res. 65, 170-176.

Celtic Anglian Water, n.d. Ringsend wastewater treatment works. http://www.caw.ie/docs/ringsend-wastewater-treatment-works.pdf (accessed 28 September 2017).

Chen, C.Q., Bin, L.Y., Tang, B., Huang, S.S., Fu, F.L., Chen, Q.Y., Wu, L.Y., Wu, C.M., 2017. Cultivating granular sludge directly in a continuous-flow membrane bioreactor with internal circulation. Chem. Eng. J. 309, 108-117.

Chen, F.Y., Liu, Y.Q., Tay, J.H., Ning, P., 2015a. Rapid formation of nitrifying granules treating high-strength ammonium wastewater in a sequencing batch reactor. Appl. Microbiol. Biotechnol. 99(10), 4445-4452.

Chen, X., Yuan, L.J., Lu, W.J., Li, Y.Y., Liu, P., Nie, K., 2015b. Cultivation of aerobic granular sludge in a conventional, continuous flow, completely mixed activated sludge system. Front. Environ. Sci. Eng. 9(2), 324-333.

Chen, Y.C., Lin, C.J., Chen, H.L., Fu, S.Y., Zhan, H.Y., 2009. Cultivation of biogranules in a continuous flow reactor at low dissolved oxygen. Water Air Soil Pollut. 9, 213-221.

Chen, Y.Y., Ju, S.P., Lee, D.J., 2016. Aerobic granulation of protein-rich granules from nitrogen-lean wastewaters. Bioresour. Technol. 218, 469-475.

Ciudad, G., Werner, A., Bornhardt, C., Munoz, C., Antileo, C. 2006. Differential kinetics of ammonia- and nitrite-oxidizing bacteria: A simple kinetic study based on oxygen affinity and proton release during nitrification. Process Biochem. 41, 1764–1772.

Cobb, T.J., Kincannon, D.F., Tiederman, W.G., 1973. The hydrocyclone for water clarification. American Water Works Association. 65(6), 409 - 413.

Corsino, S.F., Campo, R., Di Bella, G., Torregrossa, M., Viviani, G., 2016. Study of aerobic granular sludge stability in a continuous-flow membrane bioreactor. Bioresour. Technol. 200, 1055-1059.

Cui, F., Park, S., Mo, K., Lee, W., Lee, H., Kim, M. 2017. Experimentation and mathematical models for partial nitrification in aerobic granular sludge process. KSCE J. Civ. Eng. 21(1), 127-133.

Daims, H., Lebedeva, E.V., Pjevac, P., Han, P., Herbold, C., Albertsen, M., Jehmlich, N., Palatinszky, M., Vierheilig, J., Bulaev, A., Kirkegaard, R.H., von Bergen, M., Rattei, T., Bendinger, B., Nielsen, P.H., Wagner, M., 2015. Complete nitrification by Nitrospira bacteria. Nature. 528(7583), 504-509.

DC Water, n.d. The largest advanced wastewater treatment plant in the world. https://www.dcwater.com/blue-plains (accessed 28 September 2017).

de Bruin, L.M.M., de Kreuk, M.K., van de Roest, H.F.R., Uijterlinde, C., van Loosdrecht, M.C.M., 2004. Aerobic granular sludge technology: An alternative to activated sludge? Water Sci. Technol. 49(11-12), 1-7.

de Kreuk, M.K., Kishida, N., van Loosdrecht, M.C.M., 2007. Aerobic granular sludge - state of the art. Water Sci. Technol. 55(8-9), 75-81.

Deng, F., Zhang, R., 2012. Research on COD removal and SOUR of aerobic granule with intermittent aeration in continuous flow system. Adv. Mater. Res. 518-523, 478-484.

Devlin, T.R., di Biase, A., Kowalski, M., Oleszkiewicz, J.A., 2017. Granulation of activated sludge under low hydrodynamic shear and different wastewater characteristics. Bioresour. Technol. 224, 229-235.

Dionisi, H.M., Layton, A.C., Harms, G., Gregory, I.R., Robinson, K.G., Sayler, G.S. 2002. Quantification of Nitrosomonas oligotropha-like ammonia-oxidizing bacteria and Nitrospira spp. from full-scale wastewater treatment plants by competitive PCR. Appl. Environ. Microb. 68(1), 245-253.

Edzwald, J.K., 2011. Water Quality & Treatment: A Handbook on Drinking Water, sixth ed. McGraw-Hill, U.S.A.

Ekama, G.A. 2015. Recent developments in biological nutrient removal. Water SA. 41(4), 515-524.

Faraji, A., Asadollafardi, G., Shevidi, A., 2013. A pilot study for the application of one- and two-stage tube settlers as a secondary clarifier for wastewater treatment. Int. J. Civ. Eng. 11(4a), 272-280.

Flemming, H.C., Wingender, J., Szewzyk, U., Steinberg, P., Rice, S.A., Kjelleberg, S., 2016. Biofilms: An emergent form of bacterial life. Nat. Rev. Microbiol. 14(9), 563-575.

Flora, E.M.C.V., Suidan M.T., Flora, J.R.V., Kim, B.J. 1999. Speciation and chemical interactions in nitrifying biofilms. I: Model development. J. Environ. Eng. 125(9), 871-877.

Ford, A., Rutherford, B., Wett, B., Bott, C., 2016. Implementing hydrocyclones in mainstream process for enhancing biological phosphorus removal and increasing settleability through aerobic granulation. Proceedings of WEFTEC 2016. New Orleans, Louisiana, USA: Water Environ. Fed. 2809-2822.

Gao, D.W., Liu, L., Liang, H., Wu, W.M., 2011. Aerobic granular sludge: Characterization, mechanism of granulation and application to wastewater treatment. Crit. Rev. Biotechnol. 31(2), 137-152.

Gao, Y.N., Liu, Z.J., Liu, F.X., Furukawa, K., 2012. Mechanical shear contributes to granule formation resulting in quick start-up and stability of a hybrid anammox reactor. Biodegrad. 23(3), 363-372.

Ge, S., Wang, S., Yang, X., Qiu, S., Li, B., Peng, Y. 2015. Detection of nitrifiers and evaluation of partial nitrification for wastewater treatment: A review. Chemosphere. 140, 85-98.

Gee, C.S., Suidan, M.T., Pfeffer, J.T. 1990. Modeling of nitrification under substrate-inhibiting conditions. J. Environ. Eng-ASCE. 116(1), 18-31.

Gieseke, A., Bjerrum, L., Wagner, M., Amann, R. 2003. Structure and activity of multiple nitrifying bacterial populations co-existing in a biofilm. Environ. Microbiol. 5(5), 355-369.

Gil, K.I., Choi, E.S. 2001. Modelling of inhibition of nitrite oxidation in biological nitritation processes by free ammonia. Biotechnol. Lett. 23(24), 2021-2026.

Gonzalez-Martinez, A., Morillo, J.A., Garcia-Ruiz, M.J., Gonzalez-Lopez, J., Osorio, F., Martinez-Toledo, M.V., van Loosdrecht, M.C.M., 2015. Archaeal populations in full-scale autotrophic nitrogen removal bioreactors operated with different technologies: CANON, DEMON and partial nitritation/anammox. Chem. Eng. J. 277, 194-201.

Gonzalez-Martinez, A., Rodriguez-Sanchez, A., Garcia-Ruiz, M.J., Munoz-Palazon, B., Cortes-Lorenzo, C., Osorio, F., Vahala, R., 2016. Performance and bacterial community dynamics of a CANON bioreactor acclimated from high to low operational temperatures. Chem. Eng. J. 287, 557-567.

Gonzalez-Martinez, A., Rodriguez-Sanchez, A., Rivadeneyra, M.A., Rivadeneyra, A., Martin-Ramos, D., Vahala, R., Gonzalez-Lopez, J., 2017. 16S rRNA gene-based characterization of bacteria potentially associated with phosphate and carbonate precipitation from a granular autotrophic nitrogen removal bioreactor. Appl. Microbiol. Biotechnol. 101(2), 817-829.

Graham, D.W., Knapp, C.W., Van Vleck, E.S., Bloor, K., Lane, T.B., Graham, C.E. 2007. Experimental demonstration of chaotic instability in biological nitrification. ISME J. 1(5), 385-393.

Grunditz, C., Dalhammar, G. 2001. Development of nitrification inhibition assays using pure cultures of Nitrosomonas and Nitrobacter. Water Res. 35(2), 433-440.

Gu, A.Z., Pedros, P.B., Kristiansen, A., Onnis-Hayden, A., Schramm, A. 2007. Nitrifying community analysis in a single submerged attached-growth bioreactor for treatment of high-ammonia waste stream. Water Environ. Res. 79(13), 2510-2518.

Hao, X., Heijnen, J.J., van Loosdrecht, M.C.M. 2002. Model-based evaluation of temperature and inflow variations on a partial nitrification–ANAMMOX biofilm process. Water Res. 36, 4839–4849.

Hasebe, Y., Eguchi, M., Meguro, H., Tsuneda, S., 2011. Significance of reactor type for high-rate nitrification using aerobic granular sludge. J. Water Environ. Technol. 9(3), 289-296.

Hasebe, Y., Meguro, H., Kanai, Y., Eguchi, M., Osaka, T., Tsuneda, S., 2017. High-rate nitrification of electronic industry wastewater by using nitrifying granules. J. Water Environ. Technol. 76(11), 3171-3180.

Hiatt, W.C., Grady, C.P.L. 2008. An updated process model for carbon oxidation, nitrification, and denitrification. Water Environ. Res. 80(11), 2145-2156.

Hou, B.L., Han, H.J., Jia, S.Y., Zhuang, H.F., Zhao, Q., Xu, P. 2014. Effect of alkalinity on nitrite accumulation in treatment of coal chemical industry wastewater using moving bed biofilm reactor. J. Environ. Sci-China. 26(5), 1014-1022.

Hou, C., Shen, J.Y., Zhang, D.J., Han, Y., Ma, D.H., Sun, X.Y., Li, J.S., Han, W.Q., Wang, L.J., Liu, X.D., 2017. Bioaugmentation of a continuous-flow self-forming dynamic membrane bioreactor for the treatment of wastewater containing high-strength pyridine. Environ. Sci. Pollut. Res. 24(4), 3437-3447.

Huang, Z., Gedalanga, P.B., Olson, B.H. 2010. Distribution of Nitrobacter and Nitrospira communities in an aerobic activated sludge bioreactor and their contributions to nitrite oxidation. Proceedings of WEFTEC 2010. New Orleans, Louisiana, USA:Water Environ. Fed. 2390-2403.

Isanta, E., Reino, C., Carrera, J., Perez, J., 2015. Stable partial nitritation for low-strength wastewater at low temperature in an aerobic granular reactor. Water Res. 80, 149-158.

Jemaat, Z., Suarez-Ojeda, M.E., Perez, J., Carrera, J., 2014b. Sequentially alternating pollutant scenarios of phenolic compounds in a continuous aerobic granular sludge reactor performing simultaneous partial nitritation and o-cresol biodegradation. Bioresour. Technol. 161, 354-361.

Jemaat, Z., Tora, J.A., Bartroli, A., Carrera, J., Perez, J., 2015. Achievement of high rate nitritation with aerobic granular sludge reactors enhanced by sludge recirculation events. Front. Env. Sci. Eng. 9(3), 528-533.

Jensen, James N. 2003. A Problem-Solving Approach to Aquatic Chemistry. John Wiley & Sons, Hoboken, NJ.

Jin, R.C., Zheng, P., Mahmood, Q., Zhang, L., 2008a. Hydrodynamic characteristics of airlift nitrifying reactor using carrier-induced granular sludge. J. Hazard. Mater. 157(2-3), 367-373.

Jin, R.C., Zheng, P., Mahmood, Q., Zhang, L., 2008b. Performance of a nitrifying airlift reactor using granular sludge. Sep. Purif. Technol. 63(3), 670-675.

Juang, Y.C., Adav, S.S., Lee, D.J., Tay, J.H., 2010. Stable aerobic granules for continuous-flow reactors: Precipitating calcium and iron salts in granular interiors. Bioresour. Technol. 101(21), 8051-8057.

Jubany, I., Carrera, J., Lafuente, J., Baeza, J.A. 2008. Start-up of a nitrification system with automatic control to treat highly concentrated ammonium wastewater: Experimental results and modeling. Chem. Eng. J. 144(3), 407-419.

Kent, T.R., Bott, C.B., Wang, Z. 2018. State of the art of aerobic granulation in continuous flow bioreactors. Biotechnol Adv. 36(4), 1139-1166.

Kindaichi, T., Kawano, Y., Ito, T., Satoh, H., Okabe, S. 2006. Population dynamics and in situ kinetics of nitrifying bacteria in autotrophic nitrifying biofilms as determined by real-time quantitative PCR. Biotechnol. Bioeng. 94(6), 1111-1121.

Kishida, N., Kono, A., Yamashita, Y., Tsuneda, S., 2010. Formation of aerobic granular sludge in a continuous-flow reactor – control strategy for the selection of well-settling granular sludge. J. Water Environ. Technol. 8(3), 251 - 258.

Kishida, N., Totsuka, N., Tsuneda, S., 2012. Challenge for formation of aerobic granular sludge in a continuous-flow reactor. J. Water Environ. Technol. 10(2), 79 - 86.

Lackner, S., Gilbert, E.M., Vlaeminck, S.E., Joss, A., Horn, H., van Loosdrecht, M.C.M., 2014. Full-scale partial nitritation/anammox experiences - an application survey. Water Res. 55, 292-303.

Lee, D.J., Chen, Y.Y. 2015. Magnesium carbonate precipitate strengthened aerobic granules. Bioresour. Technol. 183, 136-140.

Lee, D.J., Chen, Y.Y., Show, K.Y., Whiteley, C.G., Tay, J.H., 2010. Advances in aerobic granule formation and granule stability in the course of storage and reactor operation. Biotechnol. Adv. 28(6), 919-934.

Li, D., Lv, Y.F., Cao, M.Z., Zeng, H.P., Zhang, J., 2016a. Optimized hydraulic retention time for phosphorus and COD removal from synthetic domestic sewage with granules in a continuous-flow reactor. Bioresour. Technol. 216, 1083-1087.

Li, D., Lv, Y.F., Zeng, H.P., Zhang, J., 2016b. Effect of sludge retention time on continuous-flow system with enhanced biological phosphorus removal granules at different COD loading. Bioresour. Technol. 219, 14-20.

Li, D., Lv, Y.F., Zeng, H.P., Zhang, J., 2016c. Enhanced biological phosphorus removal using granules in continuous-flow reactor. Chem. Eng. J. 298, 107-116.

Li, D., Lv, Y.F., Zeng, H.P., Zhang, J., 2016d. Long term operation of continuous-flow system with enhanced biological phosphorus removal granules at different COD loading. Bioresour. Technol. 216, 761-767.

Li, D., Lv, Y.F., Zeng, H.P., Zhang, J., 2016e. Startup and long term operation of enhanced biological phosphorus removal in continuous-flow reactor with granules. Bioresour. Technol. 212, 92-99.

Li, J., Cai, A., Ding, L.B., Sellamuthu, B., Perreault, J., 2015. Aerobic sludge granulation in a reverse flow baffled reactor (RFBR) operated in continuous-flow mode for wastewater treatment. Sep. Purif. Technol. 149, 437-444.

Li, J., Cai, A., Wang, M., Ding, L.B., Ni, Y.J., 2014. Aerobic granulation in a modified oxidation ditch with an adjustable volume intraclarifier. Bioresour. Technol. 157, 351-354.

Li, L.Y., Peng, Y.Z., Wang, S.Y., Wu, L., Ma, Y., Takigawa, A., Li, D. 2011a. Formation and characteristics of nitritation granules cultivated in sequencing batch reactor by stepwise increase of N/C ratio. Water Sci. Technol. 64(7), 1479-1487.

Li, X.J., Sun, S., Badgley, B.D., Sung, S.W., Zhang, H.S., He, Z., 2016f. Nitrogen removal by granular nitritation-anammox in an upflow membrane-aerated biofilm reactor. Water Res. 94, 23-31.

Li, Y., Liu, Y., Xu, H.L., 2008. Is sludge retention time a decisive factor for aerobic granulation in SBR? Bioresour. Technol. 99(16), 7672-7677.

Li, Z.R., Zhang, Z., Zhang, Z.J. 2011b. Inhibition of nitrification of ammonia-rich wastewater in immobilized nitrifiers system. Adv. Mater. Res-Switz. 183-185, 197-200.

Liu, G., Wang J. 2014. Role of solids retention time on complete nitrification: Mechanistic understanding and modeling. J. Environ. Eng. 140(1): 48-56

Liu, H.B., Li, Y.J., Yang, C.Z., Pu, W.H., He, L., Bo, F., 2012. Stable aerobic granules in continuous-flow bioreactor with self-forming dynamic membrane. Bioresour. Technol. 121, 111-118.

Liu, H.B., Xiao, H., Huang, S., Ma, H.J., Liu, H., 2014. Aerobic granules cultivated and operated in continuous-flow bioreactor under particle-size selective pressure. J. Environ. Sci. 26(11), 2215-2221.

Liu, J., Li, J., Tao, Y.Q., Sellamuthu, B., Walsh, R., 2017a. Analysis of bacterial, fungal and archaeal populations from a municipal wastewater treatment plant developing an innovative aerobic granular sludge process. World J. Microbiol. Biotech. 33(1), 1-8.

Liu, T., Ma, B., Chen, X., Ni, B., Peng, Y., Guo, J. 2017b. Evaluation of mainstream nitrogen removal by simultaneous partial nitrification, anammox and denitrification (SNAD) process in a granule-based reactor. Chem. Eng. J. 327, 973-981.

Liu, Y., Liu, Q.S., 2006. Causes and control of filamentous growth in aerobic granular sludge sequencing batch reactors. Biotechnol. Adv. 24(1), 115-127.

Liu, Y., Tay, J.H., 2002. The essential role of hydrodynamic shear force in the formation of biofilm and granular sludge. Water Res. 36(7), 1653-1665.

Liu, Y., Tay, J.H., 2004. State of the art of biogranulation technology for wastewater treatment. Biotechnol. Adv. 22(7), 533-563.

Liu, Y., Wang, Z.W., Qin, L., Liu, Y.Q., Tay, J.H., 2005. Selection pressure-driven aerobic granulation in a sequencing batch reactor. Appl. Microbiol. Biotechnol. 67(1), 26-32.

Liu, Y., Yang, S.F., Tay, J.H., 2004. Improved stability of aerobic granules by selecting slow-growing nitrifying bacteria. J. Biotechnol. 108(2), 161-169.

Liu, Y.Q., Lan, G.H., Zeng, P., 2015. Excessive precipitation of $CaCO_3$ as aragonite in a continuous aerobic granular sludge reactor. Appl. Microbiol. Biotechnol. 99(19), 8225-8234.

Liu, Y.W., Ngo, H.H., Guo, W.S., Peng, L., Pan, Y.T., Guo, J.H., Chen, X.M., Ni, B.J., 2016. Autotrophic nitrogen removal in membrane-aerated biofilms: Archaeal ammonia oxidation versus bacterial ammonia oxidation. Chem. Eng. J. 302, 535-544.

Long, B., Yang, C.Z., Pu, W.H., Yang, J.K., Liu, F.B., Zhang, L., Cheng, K., 2015a. Rapid cultivation of aerobic granular sludge in a continuous flow reactor. J. Environ. Chem. Eng. 3(4), 2966-2973.

Long, B., Yang, C.Z., Pu, W.H., Yang, J.K., Liu, F.B., Zhang, L., Zhang, J., Cheng, K., 2015b. Tolerance to organic loading rate by aerobic granular sludge in a cyclic aerobic granular reactor. Bioresour. Technol. 182, 314-322.

Luo, J., Chen, H., Han, X., Sun, Y., Yuan, Z., Guo, J. 2017. Microbial community structure and biodiversity of size-fractionated granules in a partial nitritation–anammox process. FEMS Microbiol. Ecol. 93(6), fix021.

Lydmark, P., Lind, M., Sörensson, F., Hermansson, M. 2006. Vertical distribution of nitrifying populations in bacterial biofilms from a full-scale nitrifying trickling filter. Environ. Microbiol. 8(11), 2036–2049.

Ma, B., Wang, S., Cao, S., Miao, Y., Jia, F., Du, R., Peng, Y. 2016. Biological nitrogen removal from sewage via anammox: Recent advances. Bioresour. Technol. 200, 981-990.

Manser, R., Gujer, W., Siegrist, H. 2005. Consequences of mass transfer effects on the kinetics of nitrifiers. Water Res. 39(19), 4633-4642.

Martin, K., A,S., de Clippeleir, H., Sturm, B., 2016. "Accidental granular sludge?": Understanding process design and operational conditions that lead to low SVI-30 values through a survey of full scale facilities in north america. Proceedings of WEFTEC 2016. New Orleans, Louisiana, USA: Water Environ. Fed. 3396-3405.

Matsumoto, S., Katoku, M., Saeki, G., Terada, A., Aoi, Y., Tsuneda, S., Picioreanu, C., van Loosdrecht, M.C.M., 2010. Microbial community structure in autotrophic nitrifying granules characterized by experimental and simulation analyses. Environ. Microbiol. 12(1), 192-206.

Metcalf & Eddy. 2014. Wastewater Engineering: Treatment and Resource Recovery, fifth ed. McGraw-Hill Education, New York, NY.

Morales, N., del Rio, A., Vazquez-Padin, J.R., Mendez, R., Campos, J.L., Mosquera-Corral, A. 2016. The Granular biomass properties and the acclimation period affect the partial nitritation/anammox process stability at a low temperature and ammonium concentration. Process Biochem. 51, 2134-2142.

Moussa, M.S., Lubberding, H.J., Hooijmans, C.M., van Loosdrecht M.C.M., Gijzen, H.J. 2003. Improved method for determination of ammonia and nitrite oxidation activities in mixed bacterial cultures. Appl. Microbiol. Biotechnol. 63(2), 217-221.

Mozumder, M.S.I., Picioreanu, C., van Loosdrecht, M.C.M., Volcke, E.I.P. 2014. Effect of heterotrophic growth on autotrophic nitrogen removal in a granular sludge reactor. Environ. Technol. 35(8), 1027-1037.

MWRD, n.d. Stickney WRP. http://www.mwrd.org/irj/portal/anonymous/stickney (accessed 28 September 2017).

Nguyen, P.T.T., Nguyen, P.V., Truong, H.T.B., Bui, H.M., 2016. The formation and stabilization of aerobic granular sludge in a sequencing batch airlift reactor for treating tapioca-processing wastewater. Pol. J. Environ. Stud. 25(5), 2077-2084.

Ni, B.J., Chen, Y.P., Liu, S.Y., Fang, F., Xie, W.M., Yu, H.Q. 2009. Modeling a granule-based anaerobic ammonium oxidizing (ANAMMOX) process. Biotechnol. & Bioeng. 103 (3), 490–499.

Nogaj, T. M., Randall, A.A., Jimenez, J.A., Takacs, I., Bott, C.B., Miller, M.W., Murthy, S., Wett, B. 2014. Mathematical modeling of the high rate activated sludge system: Optimizing the COD:N Ratio in the process effluent. Proceedings of WEFTEC 2014, Water Environ. Fed. 913-926.

Nyman, J., Lacintra, M.G., Westman, J.O., Berglin, M., Lundin, M., Lennartsson, P.R., Taherzadeh, M.J., 2013. Pellet formation of zygomycetes and immobilization of yeast. New Biotechnol. 30(5), 516-522.

Odegaard, H., 2016. A road-map for energy-neutral wastewater treatment plants of the future based on compact technologies (including MBBR). Front. Env. Sci. Eng. 10(4), 1-17.

Oueslati, A., Megriche, A., Hannachi, A., Elmaaoui, M., 2017. Performance study of humidification-dehumidification system operating on the principle of an airlift pump with tunable height. Process Saf. Environ. Prot. 111, 65-74.

Pambrun, V., Paul, E., Sprandio, M. 2006. Modeling the partial nitrification in sequencing batch reactor for biomass adapted to high ammonia concentrations. Biotechnol. Bioeng. 95(1), 120-131.

Paques a, n.d. Anammox®. http://en.paques.nl/products/featured/anammox (accessed 28 September 2017).

Paques b, n.d. Circox®. http://en.paques.nl/products/other/circox (accessed 28 September 2017).

Park, S., Bae, W. 2009. Modeling kinetics of ammonium oxidation and nitrite oxidation under simultaneous inhibition by free ammonia and free nitrous acid. Process Biochem. 44(6), 631-640.

Park, S., Bae, W., Rittmann, B.E. 2010. Multi-species nitrifying biofilm model (MSNBM) including free ammonia and free nitrous acid inhibition and oxygen limitation. Biotechnol. Bioeng. 105(6), 1115-1130.

Park, S., Chung, J., Rittmann, B.E., Bae, W. 2015. Nitrite accumulation from simultaneous free-ammonia and free-nitrous-acid inhibition and oxygen limitation in a continuous-flow biofilm reactor. Biotechnol. Bioeng. 112(1), 43-52.

Perez, J., Costa, E., Kreft, J.U. 2009. Conditions for partial nitrification in biofilm reactors and a kinetic explanation. Biotechnol. Bioeng. 103(2), 282-295.

Picioreanu, C., Perez, J., van Loosdrecht, M.C.M. 2016. Impact of cell cluster size on apparent half-saturation coefficients for oxygen in nitrifying sludge and biofilms. Water Res. 106, 371-382.

Picioreanu, C., van Loosdrecht, M.C.M., Heijnen, J.J. 1997. Modelling the effect of oxygen concentration on nitrite accumulation in a biofilm airlift suspension reactor. Water Sci. Technol. 36(1), 147-156.

Piculell, M., Suarez, C., Li, C., Christensson, M., Persson, F., Wagner, M., Hermansson, M., Jonsson, K., Welander, T. 2016. The inhibitory effects of reject water on nitrifying populations grown at different biofilm thickness. Water Res. 104, 292-302.

Poot, V., Hoekstra, M., Geleijnse, M.A.A., van Loosdrecht, M.C.M., Perez, J. 2016. Effects of the residual ammonium concentration on NOB repression during partial nitritation with granular sludge. Water Res. 106, 518-530.

Pronk, M., de Kreuk, M.K., de Bruin, B., Kamminga, P., Kleerebezem, R., van Loosdrecht, M.C.M., 2015. Full scale performance of the aerobic granular sludge process for sewage treatment. Water Res. 84, 207-217.

Qian, F.Y., Wang, J.F., Shen, Y.L., Wang, Y., Wang, S.Y., Chen, X., 2017. Achieving high performance completely autotrophic nitrogen removal in a continuous granular sludge reactor. Biochem. Eng. J. 118, 97-104.

Ramos, C., Suarez-Ojeda, M.E., Carrera, J., 2016. Biodegradation of a high-strength wastewater containing a mixture of ammonium, aromatic compounds and salts with simultaneous nitritation in an aerobic granular reactor. Process Biochem. 51(3), 399-407.

Reardon, J., Foreman, J.A., Searcy, R.L. 1966. New reactants for the colorimetric determination of ammonia: Clinical Chimica Acta. 14, 403-405.

Reino, C., Suarez-Ojeda, M.E., Perez, J., Carrera, J., 2016. Kinetic and microbiological characterization of aerobic granules performing partial nitritation of a low-strength wastewater at 10 degrees C. Water Res. 101, 147-156.

Ren, Y., Yan, L.L., Hao, G.X., Zhang, X.L., Wen, Y., Guo, Y.H., Chen, Z.L. 2016. Shortcut nitrification treatment of high strength ammonia nitrogen wastewater by aerobic granular sludge. J. Chem. Soc. Pakistan. 38(6), 1222-1229.

Rodriguez-Sanchez, A., Margareto, A., Robledo-Mahon, T., Aranda, E., Diaz-Cruz, S., Gonzalez-Lopez, J., Barcelo, D., Vahala, R., Gonzalez-Martinez, A., 2017. Performance and bacterial community structure of a granular autotrophic nitrogen removal bioreactor amended with high antibiotic concentrations. Chem. Eng. J. 325, 257-269.

Rosman, N.H., Anuar, A.N., Chelliapan, S., Din, M.F.M., Ujang, Z., 2014. Characteristics and performance of aerobic granular sludge treating rubber wastewater at different hydraulic retention time. Bioresour. Technol. 161, 155-161.

Rossetti, S., Tomei, M.C., Nielsen, P.H., Tandoi, V., 2005. "Microthrix Parvicella", a filamentous bacterium causing bulking and foaming in activated sludge systems: A review of current knowledge. FEMS Microbiol. Rev. 29(1), 49-64.

Sajjad, M., Kim, I.S., Kim, K.S., 2016. Development of a novel process to mitigate membrane fouling in a continuous sludge system by seeding aerobic granules at pilot plant. J. Membr. Sci. 497, 90-98.

Saleh, A.M., Hamoda, M.F., 1999. Upgrading of secondary clarifiers by inclined plate settlers. Water Sci. Technol. 40(7), 141-149.

Schramm, A., Larsen, L.H., Revsbech, N.P., Ramsing, N.B., Amann, R., Schleifer, K.H. 1996. Structure and function of a nitrifying biofilm as determined by in situ hybridization and the use of microelectrodes. Appl. Environ. Microb. 62(12), 4641–4647.

Schwarzenbeck, N., Erley, R., Mc Swain, B.S., Wilderer, P.A., Irvine, R.L., 2004a. Treatment of malting wastewater in a granular sludge sequencing batch reactor (SBR). Acta Hydrochim. Hydrobiol. 32(1), 16-24.

Schwarzenbeck, N., Erley, R., Wilderer, P.A., 2004b. Aerobic granular sludge in an SBR-system treating wastewater rich in particulate matter. Water Sci. Technol. 49(11-12), 41-46.

Sen, D., Randall, C.W. 2008. Improved computational model (AQUIFAS) for activated sludge, integrated fixed-film activated sludge, and moving-bed biofilm reactor systems, Part II: Multilayer biofilm diffusional model. Water Environ. Res. 80(7), 624-632.

Shanahan, J.W., Semmens, M.J. 2015. Alkalinity and pH effects on nitrification in a membrane aerated bioreactor: An experimental and model analysis. Water Res. 74, 10-22.

Shi, Y.J., Wells, G., Morgenroth, E., 2016. Microbial activity balance in size fractionated suspended growth biomass from full-scale sidestream combined nitritation-anammox reactors. Bioresour. Technol. 218, 38-45.

Strous, M., Heijnen, J.J., Kuenen, J.G., Jetten, M.S.M. 1998. The sequencing batch reactor as a powerful tool for the study of slowly growing anaerobic ammonium-oxidizing microorganisms. Appl. Microbiol. Biotechnol. 50(5), 589-596.

Sun, Y., Zhang, D., Wang, Z. 2017. The potential of using biological nitrogen removal technique for stormwater treatment. Ecol. Eng. 106, 482-495.

Tarpagkou, R., Pantokratoras, A., 2014. The influence of lamellar settler in sedimentation tanks for potable water treatment - a computational fluid dynamic study. Powder Technol. 268, 139-149.

Tay, S.T.L., Ivanov, V., Yi, S., Zhuang, W.Q., Tay, J.H., 2002. Presence of anaerobic bacteroides in aerobically grown microbial granules. Microb. Ecol. 44(3), 278-285.

Trigo, C., Campos, J.L., Garrido, J.M., Mendez, R., 2006. Start-up of the anammox process in a membrane bioreactor. J. Biotechnol. 126(4), 475-487.

Tsuneda, S., Nagano, T., Hoshino, T., Ejiri, Y., Noda, N., Hirata, A. 2003. Characterization of nitrifying granules produced in an aerobic upflow fluidized bed reactor. Water Res. 37, 4965–4973.

Tsuneda, S., Ogiwara, M., Ejiri, Y., Hirata, A., 2006. High-rate nitrification using aerobic granular sludge. Water Sci. Technol. 53(3), 147-154.

Underhill, S.E., Prosser, J.I., 1987. Surface attachment of nitrifying bacteria and their inhibition by potassium ethyl xanthate. Microb. Ecol. 14(2), 129-139.

US EPA. 1979. Federal Register. 44(85), 25505.

US EPA, 1999. Wastewater technology fact sheet: Sequencing batch reactors. EPA 932-F-99-073. US Environmental Protection Agency, Office of Water, Washington D.C.

US EPA. 2017. Federal Register. 40 CFR part 136.

Ushiki, N., Jinno, M., Fujitani, H., Suenaga, T., Terada, A., Tsuneda, S. 2017. Nitrite oxidation kinetics of two Nitrospira strains: The quest for competition and ecological niche differentiation. J. Biosci. Bioeng. 123(5), 581-589.

Val del Rio, A., Figueroa, M., Mosquera-Corral, A., Campos, J.L., Mendez, R., 2013. Stability of aerobic granular biomass treating the effluent from a seafood industry. Int. J. Environ. Res. 7(2), 265-276.

Van Hulle, S.W.H., Vandeweyer, H.J.P., Meesschaert, B.D., Vanrolleghem, P.A., Dejans, P., Dumoulin, A., 2010. Engineering aspects and practical application of autotrophic nitrogen removal from nitrogen rich streams. Chem. Eng. J. 162(1), 1-20.

van Kessel, M.A.H.J., Speth, D.R., Albertsen, M., Nielsen, P.H., Op den Camp, H.J.M., Kartal, B., Jetten, M.S.M., Lucker, S., 2015. Complete nitrification by a single microorganism. Nature. 528(7583), 555-559.

Van Winckel, T., De Clippeleir, H., Mancell-Egala, A., Rahman, A., Wett, B., Bott, C., Sturm, B., Vlaeminck, S.E., Al-Omari, A., Murthy, S., 2016. Balancing flocs and granules by external selectors to increase capacity in high-rate activated sludge systems. Proceedings of WEFTEC 2016. New Orleans, Louisiana, USA: Water Environ. Fed. 5628 - 5633.

Vannecke, T.P.W., Volcke. E.I.P. 2015. Modelling microbial competition in nitrifying biofilm reactors. Biotechnol. & Bioeng. 112(12), 2550-2561.

Vadivelu, V.M., Keller, J., Yuan, Z. 2007. Free ammonia and free nitrous acid inhibition on the anabolic and catabolic processes of Nitrosomonas and Nitrobacter. Water Sci. Technol. 56(7), 89-97.

Varas, R., Guzman-Fierro, V., Giustinianovich, E., Behar, J., Fernandez, K., Roeckel, M., 2015. Startup and oxygen concentration effects in a continuous granular mixed flow autotrophic nitrogen removal reactor. Bioresour. Technol. 190, 345-351.

Vazquez-Padin, J.R., Figueroa, M., Mosquera-Corral, A., Campos, J.L., Mendez, R. 2009. Population dynamics of nitrite oxidizers in nitrifying granules. Water Sci. & Technol. 60(10), 2529-2536.

Villaverde, S., Fdz-Polanco, F., Garcia, P.A. 2000. Nitrifying biofilm acclimation to free ammonia in submerged biofilters. Start-up influence. Water Res. 34(2), 602-610.

Vlaeminck, S.E., Terada, A., Smets, B.F., De Clippeleir, H., Schaubroeck, T., Bolca, S., Demeestere, L., Mast, J., Boon, N., Carballa, M., Verstraete, W. 2010. Aggregate size and architecture determine microbial activity balance for one-stage partial nitritation and anammox. Appl. Environ. Microbiol. 76(3), 900-909.

Volcke, E.I.P., Picioreanu, C., De Baets, B., van Loosdrecht, M.C.M. 2010. Effect of granule size on autotrophic nitrogen removal in a granular sludge reactor. Environ. Technol. 31(11), 1271-1280.

Volcke, E.I.P., Picioreanu, C., De Baets, B., van Loosdrecht, M.C.M. 2012. The granule size distribution in an anammox-based granular sludge reactor affects the conversion—Implications for modeling. Biotechnol. Bioeng. 109(7), 1629-1636.

Wagner, J., Weissbrodt, D.G., Manguin, V., da Costa, R.H.R., Morgenroth, E., Derlon, N., 2015. Effect of particulate organic substrate on aerobic granulation and operating conditions of sequencing batch reactors. Water Res. 85, 158-166.

Wan, C.L., Lee, D.J., Yang, X., Wang, Y.Y., Lin, L., 2014a. Saline storage of aerobic granules and subsequent reactivation. Bioresour. Technol. 172, 418-422.

Wan, C.L., Sun, S.P., Lee, D.J., Liu, X., Wang, L., Yang, X., Pan, X.L., 2013. Partial nitrification using aerobic granules in continuous-flow reactor: Rapid startup. Bioresour. Technol. 142, 517-522.

Wan, C.L., Yang, X., Lee, D.J., Liu, X., Sun, S.P., 2014b. Partial nitrification using aerobic granule continuous-flow reactor: Operations and microbial community. J. Taiwan Inst. Chem. Eng. 45(5), 2681-2687.

Wan, C.L., Yang, X., Lee, D.J., Liu, X., Sun, S.P., Chen, C., 2014c. Partial nitrification of wastewaters with high NaCl concentrations by aerobic granules in continuous-flow reactor. Bioresour. Technol. 152, 1-6.

Wan, C.L., Yang, X., Lee, D.J., Sun, S.P., Liu, X., Zhang, P., 2014d. Influence of hydraulic retention time on partial nitrification of continuous-flow aerobic granular-sludge reactor. Environ. Technol. 35(14), 1760-1765.

Wang, J.F., Wang, X., Zhao, Z.G., Li, J.W., 2008. Organics and nitrogen removal and sludge stability in aerobic granular sludge membrane bioreactor. Appl. Microbiol. Biotechnol. 79(4), 679-685.

Wang, L., Zheng, P., Xing, Y., Li, W., Yang, J., Abbas, G., Liu, S., He, Z., Zhang, J., Zhang, H., Lu, H. 2014. Effect of particle size on the performance of autotrophic nitrogen removal in the granular sludge bed reactor and microbiological mechanisms. Bioresour. Technol. 157, 240-246.

Wang, S., Shi, W.X., Tang, T., Wang, Y.Y., Zhi, L.L., Lv, J.Z., Li, J., 2017. Function of quorum sensing and cell signaling in the formation of aerobic granular sludge. Rev. Environ. Sci. Biol. 16(1), 1-13.

Wang, Y., Peng, D.C., 2008. Conditions of cultivating and characteristics of aerobic granular sludge in a completely mixed reactor. Proceedings of International Conference on Advances in Chemical Technologies for Water and Wastewater Treatment. Xian, China: Shaanxi Sci: 535-540.

Wang, Z.W., Li, Y., Zhou, J.Q., Liu, Y., 2006a. The influence of short-term starvation on aerobic granules. Process Biochem. 41, 2373-2378.

Wang, Z.W., Liu, Y., Tay, J.H., 2006b. The role of SBR mixed liquor volume exchange ratio in aerobic granulation. Chemosphere. 62(5), 767-771.

Wang, Z.W., Liu, Y., Tay, J.H., 2007. Biodegradability of extracellular polymeric substances produced by aerobic granules. Appl. Microbiol. Biotechnol. 74(2), 462-466.

Wett, B., Podmirseg, S.M., Gomez-Brandon, M., Hell, M., Nyhuis, G., Bott, C., Murthy, S., 2015. Expanding DEMON sidestream deammonification technology towards mainstream application. Water Environ. Res. 87(12), 2084-2089.

Wett, B., Rauch, W. 2003. The role of inorganic carbon limitation in biological nitrogen removal of extremely ammonia concentrated wastewater. Water Res. 37(5), 1100-1110.

Willoughby, A., Houweling, D., Constantine, T., Yin, H., Havsteen, L., Uri, N., Chandran, K., Li, Z., 2016. Protocols for researching the impact of sludge granulation on BNR processes. Proceedings of WEFTEC 2016. New Orleans, Louisiana, USA: Water Environ. Fed. 5876-5888.

Winkler, M.K.H., Boets, P., Hahne, B., Goethals, P., Volcke, E.I.P. 2017. Effect of the dilution rate on microbial competition: R-strategist can win over K-strategist at low substrate concentration. Plos One. 12(3).

Winkler, M.K.H., Kleerebezem, R., Kuenen, J.G., Yang, J.J., van Loosdrecht, M.C.M. 2011. Segregation of biomass in cyclic anaerobic/aerobic granular sludge allows the enrichment of anaerobic ammonium oxidizing bacteria at low temperatures. Environ. Sci. Technol. 45(17), 7330-7337.

World Water Works, n.d. Biocos. http://www.worldwaterworks.com/technologies/biocos (accessed 28 September 2017).

Wu, J., Li, Y., Zhang, M. 2017a. Activated sludge floc morphology and nitrifier enrichment can explain the conflicting reports on the oxygen half-saturation index for ammonium oxidizing bacteria (AOB) and nitrite oxidizing bacteria (NOB). J. Chem. Technol. Biotechnol. 92(10), 2673-2682.

Wu, J., Zhang, Y., Yan, G. 2016. Differentiating two partial nitrification mechanisms: Inhibiting nitrite oxidizing bacteria activity or promoting ammonium oxidizing bacteria activity. J. Environ. Chem. Eng. 4(3), 3260-3266.

Wu, J., Zhang, Y., Zhang, M., Li, Y.H. 2017b. Effect of nitrifiers enrichment and diffusion on their oxygen half-saturation value measurements. Biochem. Eng. J. 123, 110-116.

Xin, X., Lu, H., Yao, L., Leng, L., Guan, L., 2017. Rapid formation of aerobic granular sludge and its mechanism in a continuous-flow bioreactor. Appl. Biochem. Biotechnol. 181(1), 424-433.

Xu, G.J., Zhou, Y., Yang, Q., Lee, Z.M.P., Gu, J., Lay, W., Cao, Y.S., Liu, Y. 2015. The challenges of mainstream deammonification process for municipal used water treatment. Appl. Microbiol. Biotechnol. 99(6), 2485-2490.

Yang, S.F., Tay, J.H., Liu, Y. 2004. Inhibition of free ammonia to the formation of aerobic granules. Biochem. Eng. J. 17(1), 41-48.

Yang, Y., Zhou, D.D., Xu, Z.X., Li, A.J., Gao, H., Hou, D.X. 2014. Enhanced aerobic granulation, stabilization, and nitrification in a continuous-flow bioreactor by inoculating biofilms. Appl. Microbiol. Biotechnol. 98(12), 5737-5745.

Yu, S.J., Sun, P.D., Zheng, W., Chen, L.J., Zheng, X.L., Han, J.Y., Yan, T., 2014. The effect of COD loading on the granule-based enhanced biological phosphorus removal system and the recoverability. Bioresour. Technol. 171, 80-87.

Yulianto, A., Soewondo, P., Handajani, M., Ariesyady, H.D., 2017. Preliminary study on aerobic granular biomass formation with aerobic continuous flow reactor. Proceedings of IC3PE 2017. Yogyakarta, Indonesia: AIP Publishing, 020113-1–020113-5.

Zhang, D.J., Cai, Q., Cong, L.Y., 2010. Enhancing completely autotrophic nitrogen removal over nitrite by trace NO_2 addition to an AUSB reactor. J. Chem. Technol. Biotechnol. 85(2), 204-208.

Zhang, J.G., Hu, B., 2012. A novel method to harvest microalgae via co-culture of filamentous fungi to form cell pellets. Bioresour. Technol. 114, 529-535.

Zhang, L., Zheng, P., Tang, C.J., Jin, R.C., 2008. Anaerobic ammonium oxidation for treatment of ammonium-rich wastewaters. J. Zhejiang Univ. Sci. B. 9(5), 416-426.

Zhang, T.C., Bishop, P.L. 1996. Evaluation of substrate and pH effects in a nitrifying biofilm. Water Environ. Res. 68(7), 1107-1115.

Zhao, X., Chen, Z.L., Wang, X.C., Shen, J.M., Xu, H., 2014. PPCPs removal by aerobic granular sludge membrane bioreactor. Appl. Microbiol. Biotechnol. 98(23), 9843-9848.

Zheng, Y.M., Yu, H.Q., Liu, S.H., Liu, X.Z., 2006. Formation and instability of aerobic granules under high organic loading conditions. Chemosphere. 63(10), 1791-1800.

Zhou, D.D., Dong, S.S., Gao, L.L., Liu, M.Y., Niu, S., 2013a. Distribution characteristics of extracellular polymeric substances and cells of aerobic granules cultivated in a continuous-flow airlift reactor. J. Chem. Technol. Biotechnol. 88(5), 942-947.

Zhou, D.D., Liu, M.Y., Gao, L.L., Shao, C.Y., Yu, J., 2013b. Calcium accumulation characterization in the aerobic granules cultivated in a continuous-flow airlift bioreactor. Biotechnol. Lett. 35(6), 871-877.

Zhou, D.D., Liu, M.Y., Wang, J., Dong, S.S., Cui, N., Gao, L.L., 2013c. Granulation of activated sludge in a continuous flow airlift reactor by strong drag force. Biotechnol. Bioprocess Eng. 18(2), 289-299.

Zhou, D.D., Niu, S., Xiong, Y.J., Yang, Y., Dong, S.S., 2014. Microbial selection pressure is not a prerequisite for granulation: Dynamic granulation and microbial community study in a complete mixing bioreactor. Bioresour. Technol. 161, 102-108.

Zou, J., Tao, Y., Li, J., Wu, S., Ni, Y., 2018. Cultivating aerobic granular sludge in a developed continuous-flow reactor with two-zone sedimentation tank treating real and low-strength wastewater. Bioresour. Technol. 247, 776-783.

Zhu, T., Xu, B., Wu, J. 2018. Experimental and mathematical simulation study on the effect of granule particle size distribution on partial nitrification in aerobic granular reactor. Biochem Eng. J. 134, 22-29.